August 2023

ROLE OF FAT CONTENT ON THE STRUCTURE AND FUNCTION OF HUMAN SKELETAL MUSCLE

Joseph A. Gordon III
University of Massachusetts Amherst

ROLE OF FAT CONTENT ON THE STRUCTURE AND FUNCTION OF HUMAN SKELETAL MUSCLE

A Dissertation Presented

By

Joseph A. Gordon III

Submitted to the Graduate School of the University of Massachusetts Amherst in partial fulfillment of the requirements for the degree of

DOCTOR OF PHILOSOPHY

May 2023

Department of Kinesiology

ROLE OF FAT CONTENT ON THE STRUCTURE AND FUNCTION OF HUMAN SKELETAL MUSCLE

A Dissertation Presented

By

Joseph A. Gordon III

Approved as to style and content by:

_____

Jane A. Kent, Chair

_____

Mark S. Miller, Member

_____

Gwenael Layec, Member

_____

Bruce M. Damon, Outside Member

_____

Richard Van Emmerik, Chair
Department of Kinesiology

DEDICATION

This work is dedicated to the time, energy, and resources that my mother, Mary Gordon, and my father, Joseph A. Gordon Jr., committed to my life.

ACKNOWLEDGEMENTS

I wish I could say that the last 5+ years flew by. The reality is, I can recollect my time throughout this process with peculiar detail. The weight of unprecedented challenges that presented themselves (beyond the labor of this dissertation) seemed insurmountable. It has taken everything inside of me to draw the strength to reach this point.

Thank you to my advisor Jane Kent, for providing an opportunity to impact individuals and communities that have not traditionally been represented in academia or research. The skills I have acquired and resources I have been exposed to are invaluable, and I appreciate you being open to looking at topics through a different lens. I would also like to thank Drs. Mark Miller and Bruce Damon for approaching any type of problem with an engineer's mind, and being willing to offer me unscheduled moments of your time. Thank you to Dr. Gwenael Layec for your work on my committee, and challenging me to put my science into a larger perspective.

There are many graduate students that I could thank for their personal and professional support, but I would specifically like mention: Chris Hayden, Nick Remillard, Jules Miehm, Luke Arieta, Zoe Smith. Thank you to the Muscle Biology Lab for always being willing to engage with a question, and help me get some data together: Chad Straight, Phil Woods, Matt Limoges, Aurora Foster, Chris Lee. I would also like to acknowledge Dr. Rajakumar Nagarajan, Dr. Mike Busa, and Elena Bliss. Thanks to my friends: Hank, Matt, Adrian, Austin, Warner for being a light in the dark stretches. Finally, I will forever be indebted to my mother for her unwavering support in every conceivable way throughout this process. Thanks for doing all you have to make sure I had a chance.

ABSTRACT

ROLE OF FAT CONTENT ON THE STRUCTURE AND FUNCTION OF HUMAN SKELETAL MUSCLE

MAY 2023

JOSEPH A. GORDON III, B.S., UNIVERSITY OF CENTRAL FLORIDA

M.S., UNIVERSITY OF CENTRAL FLORIDA

Ph.D., UNIVERSITY OF MASSACHUSETTS AMHERST

Directed by: Professor Jane A. Kent

Muscle size does not fully explain variations in muscle strength. Fat content has been implicated in muscle weakness, though this relationship remains unclear. The relationship between fat and strength may vary between scales (e.g., cellular, organ, and organism). The goal of this dissertation was to clarify the role of fat in the structure and function of muscle using *in vitro* and *in vivo* techniques across multiple scales in adults 21-45 years old. Study 1 tested the agreement of intramyocellular lipid (IMCL) content between oil red o (ORO) and magnetic resonance spectroscopy (MRS) techniques. These measures of IMCL were also compared to measures of quadriceps fat content (fat fraction, FF) by magnetic resonance imaging (MRI). Results showed that fat by ORO, MRS, nor MRI were related. This suggests that extracellular lipid contributes to IMCL by MRS, and that fat is not a primarily storage location within muscle cells. Study 2 quantified the relationships between FF, architecture, and strength *in vivo* using MRI, diffusion tensor imaging (DTI), and isokinetic dynamometry. There was a relationship between FF and fascicle length. However, FF was not related to measures of muscle strength. This suggests that fat may be related to shorter fascicles, but does not impair maximal strength. Muscle curvature and pennation angle were related to muscle strength,

suggesting that they may be additional contributors to strength. Study 3 compared measures of single fiber function to whole muscle strength. The relationship between IMCL and single fiber function was also quantified. Measures of IMCL, FF, and BMI were not related, suggesting that IMCL does not contribute to fat t measured at the whole muscle or whole body levels. Measures of IMCL were also not related to single fiber function, indicating that greater levels of lipid accumulation may be necessary for fat-induced impairment of single fiber function. Collectively, the findings of this dissertation indicate that fat and mechanical function must be evaluated at the same anatomical scale for clear interpretations of their relationship. Additionally, this work suggests that fat may have a relationship with muscle structure, but not does have a direct effect on strength.

PREFACE

This dissertation is composed of three separate studies that address an overall objective. These studies used data from multiple grant-funded projects to this end. As such, Chapter 3 describes methods for all studies, and Chapters 4, 5, and 6 have been be formatted as three manuscripts to expedite their submission for peer review.

TABLE OF CONTENTS

LIST OF TABLES

Table Page

LIST OF FIGURES

Figure Page

CHAPTER 1

INTRODUCTION

Background

In many populations, the loss of muscle strength (i.e., the ability to generate maximal force) resulting from age, disuse, or infirmity is not proportional to decreases in muscle size (95, 104, 226). Muscle size, as represented by area, volume, mass, also becomes less predictive of muscle strength with advancing age in the knee extensor muscles, which are crucial for functional tasks (197). This disparity indicates that there are additional causes of muscle weakness aside from muscle atrophy. Therefore, it is important to determine these other factors that contribute to the reduced capacity of muscle to produce force. Fat content has been purported to be an independent predictor of physical function and disability across the lifespan (153, 229, 241); this is an area requiring further investigation. Rates of obesity in the U.S. have also increased to 42.4% in 2018 (186). Therefore, research that clarifies the relationship between fat content and muscle strength is critical. Compared to muscle strength, muscle power (defined as the product of the force and velocity of a muscular contraction) better predicts functional capacity in physical tasks such as a chair rise or 400-meter walk (200). Therefore, designing experiments where the muscle length is fixed (e.g., isometric) and changing length (e.g., isokinetic) is important to understand the potential modulators of force production. Including a dynamic muscle action in experimental design may also provide insight on some of the mechanisms for how fat may affect muscle strength under different conditions. Muscle torque, a variable used commonly in isokinetic dynamometry and is used in our investigations, is the result of force being exerted about an axis of rotation.

This dissertation will define muscle composition as the relative distribution of muscle contractile and fat content in skeletal muscle. The term muscle morphology describes components related to muscle size and shape, and muscle architecture will be defined as the macroscopic arrangement of fibers relative to the mechanical line of action of the muscle (147). Though the relationship between fat content and muscle strength is unclear, both morphology and architecture are known to play a critical role in the ability to generate and transmit force (147). Other factors such as fiber type distribution and neural activation patterns can also contribute to muscle strength; however, these factors will not be detailed in this work. Researchers have also investigated the molecular and cellular determinants of muscle performance by quantifying cross-bridge kinetics at the single fiber level (166, 169, 224). However, less is known about the role of fat content, and its effects on force production. A proposed mechanism for the fat-induced impairment of muscle strength is presented in the conceptual framework (Figure 1.1). At the single fiber level, lipid droplets may reduce myofilament stiffness or interfere with the cross-bridge cycle by delaying myosin attachment to actin. At the level of whole muscle, greater fat content may disorganize muscle structure, indicated by shorter fascicle length, greater curvatures, and fat-induced increases in pennation angle; this may decrease functional capacity. This dissertation will quantify the relative contributions of muscle size, fat content, architecture, and cross-bridge kinetics on measures of force output across multiple levels of organization (e.g., molecular, cellular, whole muscle) in human skeletal muscle. This research will clarify the distinct mechanisms by which force production is impaired by fat content in muscle.

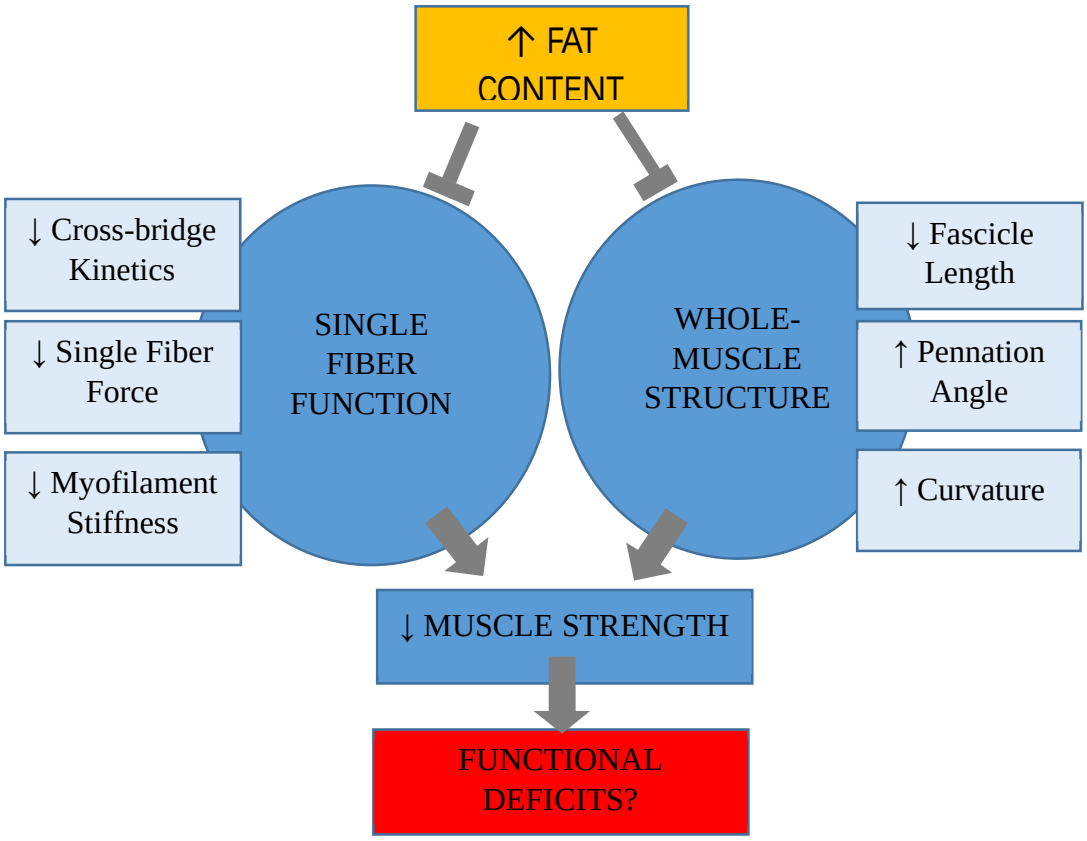

Figure 1.1. **Proposed mechanisms for how fat content may limit functional capacity.** Increased fat content in muscle may decrease strength at the level of the whole-muscle by impairing single fiber function (*left*), disorganization of muscle structure (*right*), or a combination of both. A decrease in whole-muscle strength would then lead to functional deficit in activities of daily living.

Myosin Heavy Chain & Cross-Bridge Function

Muscle fibers and are made up of many sarcomeres, which are the smallest contractile unit of the muscle cell. Sarcomeres are composed of two contractile proteins: actin and myosin. The number of cross-bridges that are formed by the interaction between actin and myosin at any given time will dictate the force output for a muscle at any anatomical level (i.e., cellular or organ). For *in vitro* methods, a group of acto-myosin crossbridges produce more force than is predicted from single crossbridge measurements (242). When moving from a group of acto-myosin crossbridges to a single fiber preparation, studies have shown that force output increases even further (169). This phenomenon is due in

part to the fact that a single bound myosin increases the attachment rates of neighboring myosin molecules (94, 162). Greater measured forces for myosin heads at higher organizational levels are also likely due in part to contributions from other regulatory proteins and structures affecting force output or transmission with increasing scale (e.g., tropomyosin, titin). When relating cross-bridge kinetics (i.e., efficiency of the cross-bridge cycle) to whole muscle force, faster myosin attachment rates and lower attachment times are related to greater force *in vivo* (167). This is because a faster attachment rate is indicative of more power strokes at the molecular and cellular levels, which produces more bound crossbridges in the muscle. There is also a hierarchy of fiber type, such that myosin heavy chain (MHC) IIX fibers produce more force per area than MHC IIA, and both types produce more force per area than MHC I fibers, or MHC IIX > MHC IIA > MHC I (214, 221). Even when adjusting for the cross-sectional area (CSA) of a fiber, this hierarchy remains due to faster attachment rates in MHC IIX fibers (214). It is easy to see then, how distinguishing between the different organizational scales of muscle is crucial to drawing conclusions related to the mechanisms of muscle weakness. Further, differences in cross-sectional area, cross-bridge kinetics, and MHC content of muscle fibers may change the force-producing characteristics of muscle (6, 191). Single fiber force (mN/mm^2) is affected by molecular cross-bridge kinetics and like whole-muscle, maximal isometric force of single fibers is also dictated by cross-sectional area (CSA).

Characteristics of Muscle Composition

The relative area that is made up of contractile (e.g., muscle) vs. non-contractile (e.g., fat, connective tissue) tissue will dictate force output. Though we are aware that fat deposition occurs within muscle, we do not know whether the amount or pattern of

accumulation disrupts its orderly structure or alters force output. A greater contractile content, or fat-free fiber CSA (mm^2) allows the potential for more cross-bridge connections to be made in a parallel arrangement, thereby producing greater force. Quantification of muscle CSA at the cellular level can be accomplished by manual measurement of top and side width of a single fiber using a compound microscope (170). In addition to muscle CSA, recent studies have reported that differences in lipid content may also play a role in mechanical force production, such that this process is impaired in skeletal muscle fibers with greater fat content (36, 224).There are limitations to these studies, however. Results in humans are scarce, and these findings are primarily limited to samples of older adults or clinical populations. Expanding these results to healthy younger adults would provide more definitive conclusions about the role of fat content in muscle force production without the confounding effects of old age, comorbidity, or clinical pathology. Cellular lipid content is commonly reported *in vitro* by oil red o (ORO) analyses (128) and *in vivo* by proton magnetic resonance spectroscopy (^{1}H-MRS), however the latter measure is known to be highly variable (133, 245).

When increasing the scale to the whole muscle level, cross-sectional area (CSA) and volume (cm^3) of muscle tissue have the greatest effect on muscle force(161). Magnetic resonance imaging (MRI) is a widely-used method for the measurement of muscle size *in vivo* (57). Specifically, fat-water (e.g., “Dixon”) imaging can be utilized for reliable and accurate measurement of muscle and fat tissue (50, 73, 150). Whereas cellular measures of fat content are primarily used to represent intracellular deposits, quantification of fat content by MRI primarily reflects extracellular fat (2). Compared with *in vitro* studies, there are more research articles implicating fat content in muscle weakness and functional

impairment of humans *in vivo* (109, 129, 136, 155, 156). This is in large part due to the invasive nature of single fiber investigations, and the difficulty of their analyses. In the absence of age or disease-related muscle atrophy, increases in fat content may disrupt orientation of the muscle architecture. Further, these potential changes in muscle architecture may or may not be significant enough to alter force output. By investigating the effects of morphology and composition at the molecular and cellular levels, we may be able to better understand the relationship between size and strength that is commonly observed *in vivo*.

Muscle Architecture and Diffusion

In addition to size, the orientation of muscle fibers can affect force output (147). Structural changes at the molecular, cellular, or whole muscle level can affect force production and overall physical function (84, 134, 168). The location and magnitude of these changes may potentially explain some of the differences in muscle strength between different muscle groups or populations (e.g., younger vs. older; males vs. females). Changes in muscle architecture, evaluated at the whole muscle level, have been shown to be a modulator of muscle force in populations such as older adults or those with musculoskeletal disease (58, 134). To quantify architecture in whole muscle, ultrasound imaging is the most prevalent method of acquisition *in vivo* due to its low cost and ease of use. There are limitations to this technique, however, such as its limited field of view, restriction to superficial muscle groups, and limitation to two dimensions. A novel component of this dissertation is the use of magnetic resonance diffusion tensor imaging (DTI), which addresses these limitations, and provides additional information related to the microstructural changes in muscle. Commonly used imaging modalities such as

ultrasound or T_1-weighted MRI cannot detect these microscopic changes (188), therefore subtle differences in muscle architecture due to training, atrophy, or disease progression may not be captured with these techniques.

Diffusion tensor imaging estimates muscle architecture by exploiting the diffusive properties of water in a medium (11). The magnitude of water diffusion in muscle can be quantified by mean diffusivity (MD), while the fractional anisotropy (FA) reflects the degree of difference between the eigenvalues, or how isotropic the water diffuses within the muscle; both will be explained later in more detail (43). These variables are used in DTI and have been used to characterize skeletal muscle following injury (252), exercise (64), and disease (193). Typical outcomes for muscle architecture, such as fascicle length and pennation angle, can be acquired with DTI, as well as variables that are less frequently reported such as muscle curvature and variability in fascicle orientation (43). While muscle curvature has been previously reported (53, 173), to our knowledge, variability in fascicle orientation has not yet been reported in the literature. Variability in fascicle orientation is the measure of the variation of fiber orientation within a given region of interest, and may provide another useful way to characterize a muscle or explain differences in muscular function.

Statement of the Problem

The primary contributor to muscle force production in humans is well known to be muscle size (161). However, our incomplete understanding of the additional factors that may affect force production (e.g., fat content) limits our knowledge of the mechanisms by which functional deficits occur as a result of aging, obesity, or neuromuscular disease. Adequate muscle strength is a critical factor for maintaining mobility, which is known to

increase quality of life and mitigate the risk of chronic disease (240). There are many organizational levels in the body (e.g., molecular, cellular, organ, organism; Figure 1.2), and disruptions may occur at any point of the force production pathway. This can limit the ability to perform functional tasks in both healthy younger (e.g., sprinting, jumping) and older adults (e.g., chair rise, stair climb). In aging, a greater physical capacity resulting from greater muscle strength improves numerous markers of metabolic health and allows older adults to maintain higher levels of independence (78). However, the potential role of fat in mechanical muscle dysfunction is unclear. This dissertation will address this problem by quantifying the contributions of fat content, architecture, and cross-bridge kinetics to muscle performance *in vivo*. Discerning the effects of these variables on muscle will allow researchers and clinicians to focus on developing effective diagnostic criteria and subsequent interventions to mitigate the loss of muscle force for activities of daily living, which is relevant to a various populations and conditions.

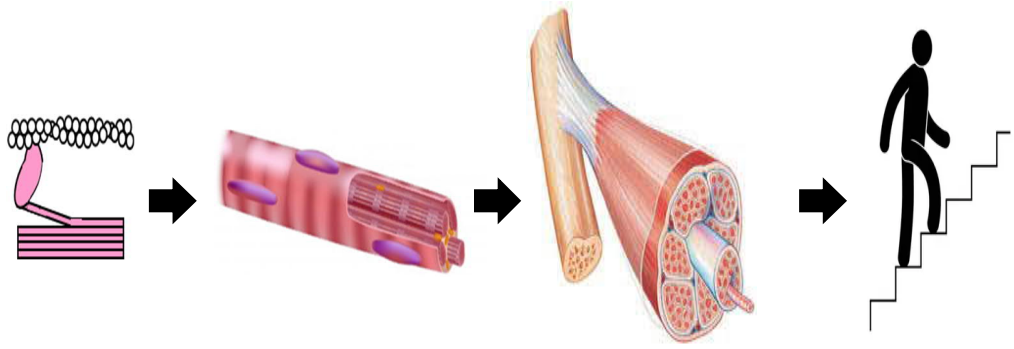

Figure 1.2. **Anatomical levels of muscle.** Myosin-actin interactions at the molecular level dictate single fiber function. These molecular and cellular interactions determine whole muscle function and, in turn, performance in whole-body tasks. [Adapted From Aurora Foster Thesis 2019.]

Dissertation Goals

Considering these issues, this dissertation encompasses three studies with the aim of elucidating the relationships between composition, architecture, and mechanical function in human skeletal muscle. This dissertation has evaluated the impact of fat content in the disorganization of muscle structure and impairment of mechanical function. These relationships were explored at various levels of organization (i.e., molecular, cellular, and organ). Successful completion of this dissertation has advanced the field by determining the likelihood of fat-induced muscle impairment in young adults. This work has also provided new information about additional factors that may contribute to mechanical muscle function, beyond muscle size.

Study 1: Comparisons of Human Skeletal Muscle Fat Content at Multiple Anatomical Scales

Despite the clinical and functional relevance of fat content, agreement has not been demonstrated between many of the commonly-used and highly sensitive methods in skeletal muscle (102). This problem makes it difficult to determine whether results are consistent across methods, scales, or populations. For our first study, the aim was to compare three *in vitro* and *in vivo* methods for fat measurement to determine whether these values were comparable at different scales and across modalities in the skeletal muscle of young adults. To that end, a sample of males and females aged 21-45 years with a body mass index (BMI) of 18.5-39.9 $kg \cdot m^{-2}$ were investigated to quantify fat content in the quadriceps using different modalities. Fat content is increasingly being used as a variable of interest in studies of aging (48, 157) and clinical populations (87,

182). Therefore, understanding the associations between these common measures is crucial.

Aim 1.1: Compare in vitro and in vivo intramyocellular lipid content (IMCL) using ORO and ^{1}H-MRS in the vastus lateralis muscle

Hypothesis 1.1: A positive linear relationship between *in vitro* IMCL (lipid area fraction, %; measured by ORO) and *in vivo* IMCL (IMCL/TCr; IMCL/Water, measured by ^{1}H-MRS). This hypothesis was tested with linear regression.

Aim 1.2: Compare intramyocellular lipid content (IMCL) by ORO and ^{1}H-MRS with fat content by MRI

Hypothesis 1.2a: A positive linear relationship between lipid area fraction (%) measured by ORO and fat fraction (%) measured by MRI. This was tested with linear regression.

Hypothesis 1.2b: A positive linear relationship between IMCL (IMCL/TCr; IMCL/Water) measured by ^{1}H-MRS and fat fraction (%) measured by MRI. This was tested with linear regression.

Support of the hypotheses in Aim 1 would indicate that IMCL acquired by *in vitro* and *in vivo* modalities represent the same quantity of fat within the muscle tissue, and determine whether fat content at the intramuscular and intracellular levels are in agreement.

Study 2: Mechanical Contributions of Fat Content to Muscle Structure and Function *in vivo*

Studies have suggested that fat content may affect muscle strength (13, 129). Still, evidence linking fat content to changes in strength is limited. Muscle architecture is generally estimated from a small percentage of the total muscle area in conventional ultrasound techniques (235). With DTI, we can evaluate the entire length of a muscle in three dimensions for a model of muscle structure that may provide more ecological validity. Despite this advantage, there are few studies that have investigated the relationship between fat content and muscle architecture using DTI. It has also been suggested that predicting muscle weakness in functional tasks is increased when force is measured at movement speeds which resemble day to day activities (52, 246). In the second study, the primary aim was to use DTI to determine the degree to which fat content may affect muscle architecture and muscle strength under static and dynamic conditions. Measures of diffusion (mean diffusivity, fractional anisotropy) have been identified as clinically significant variables in aging (217), injury (252), and disease (98). Therefore, we also evaluated whether diffusive variables were related to fat content or muscle strength in young adults.

Aim 2.1 Quantify the relationships between muscle fat content and architecture

Hypothesis 2.1a: A positive relationship between pennation angle (°) and fat fraction (%). This was tested with linear regression.

Hypothesis 2.1b: An inverse relationship between tract length (mm) and fat fraction (%). This was tested with linear regression.

Hypothesis 2.1c: A positive relationship between curvature (m^{-1}) and fat fraction (%). This was tested with linear regression.

Aim 2.2: Quantify the relationships between fat content and muscle strength and unloaded contraction velocity

Hypothesis 2.2: No relationship between fat fraction (%) maximal isometric torque (Nm), isokinetic torque (Nm), or peak contraction velocity ($deg \cdot s^{-2}$). This was tested with linear regression.

This study quantified the relationship between fat content and muscle structure as well as muscle function *in vivo*. Support of the hypotheses in Aim 2 would indicate that measures of fat content were related to architecture by DTI, but not muscle strength under both static and dynamic contraction conditions. Study 2 also provided new information about the relationship between intramuscular fat content and diffusivity *in vivo*.

Study 3: Intramyocellular Lipid Content Does Not Explain Variations in Whole Muscle Fat Fraction and is not Related to Single Fiber Function

Few studies have investigated whether variations in muscle composition and function observed *in vivo* are present at the cellular level. The third study evaluated fat content and muscle strength in whole muscle to determine if these variables reflected the lipid content and cross-bridge kinetics of single fibers, respectively. When the muscle is evaluated at larger anatomical levels, there are a greater number of factors that affect the transmission of force at its terminal point. Therefore, it is reasonable to infer that fat content may play differing roles at different levels of organization. Further, single fibers with different

MHC types also have different phenotypical and functional characteristics. It may be that fiber types with a greater potential to store and utilize fat (e.g., MHC I) may not be impaired by greater levels of fat content, relative to other fiber types (e.g., MHC II). This study evaluated the contribution of CSA, fat content, and cross-bridge kinetics at the cellular and whole muscle levels to delineate the contributions of each factor on *in vivo* muscle performance.

Aim 3.1: Compare fat content at the single fiber and in vivo levels

Hypothesis 3.1: No relationship between *in vitro* lipid area fraction (%) and *in vivo* fat fraction (%). These relationships were tested with linear regression.

Aim 3.2: Compare cross-bridge kinetics with in vivo muscle force across a range of velocities

Hypothesis 3.2a: Positive linear relationship between single fiber specific tension (mN/mm^2) in MHC IIA, but not MHC I fibers and maximal specific torque ($Nm \cdot cm^{-2}$) at all contraction velocities. This was tested with linear correlation.

Hypothesis 3.2b: Positive linear relationship between myosin attachment rate (s^{-1}) in MHC IIA, but not MHC I fibers and maximal specific torque ($Nm \cdot cm^{-2}$) at all contraction velocities. This was tested with linear correlation.

Hypothesis 3.2c: Positive linear relationship between myosin attachment time (ms) in MHC IIA, but not MHC I fibers and maximal specific torque ($Nm \cdot cm^{-2}$) at all contraction velocities. This was tested with linear correlation.

Aim 3.3: Quantify the relationship between intramyocellular lipid content and cross-bridge kinetics

Hypothesis 3.3a: Inverse relationship between lipid area fraction (%) will have and specific tension (mN/mm^2) in MHC IIA, but not MHC I fibers. These relationships were tested with a linear correlation.

Hypothesis 3.3b: Inverse relationship between lipid area fraction (%) and myosin attachment rate (s^{-1}) in MHC IIA, but not MHC I fibers. This was tested with a linear correlation.

Hypothesis 3.3c: Positive relationship between lipid area fraction (%) and myosin attachment time (ms) in MHC IIA, but not MHC I fibers. This was tested with a linear correlation.

The hypotheses in Aim 3 demonstrated whether whole muscle characteristics are also observed at the single fiber level in the absence of age-related changes or chronic disease. This study was also the first to quantify the relationship between IMCL and mechanical single fiber kinetics in healthy young adults.

This dissertation project has accomplished multiple goals. First, **Study 1** has provided new data comparing fat content measurements from commonly-used *in vitro* and *in vivo* methods. Individuals in clinical, research, and applied settings will be able to interpret these data in a way that allows them to determine the level of agreement in their measures and apply the findings to their hardware or subject population. For example, those working with obese populations now know that global or regional adiposity may not be

useful in answering questions about cellular fat content. **Study 2** has provided essential information about the relationships between fat content and muscle architecture in greater detail than previous studies. Despite the sensitivity and sophistication of DTI, it is still a rather new technique (11), and has not been frequently used in combination with other MR sequences. Our study has provided novel data about fat content and its relationship with the structure and function of skeletal muscle in a young, health cohort. Finally, **Study 3** has described the relationship between fat content and function between the whole muscle and single fiber levels. This study has also identified the role of IMCL in single fiber kinetics. In all, this dissertation has provided new information about how fat content is related to muscle structure and function, and how human skeletal muscle is affected by variables beyond its size. This was achieved by evaluating the relationships between fat content, architecture, and function across multiple scales. This work has identified specific variables to investigate to address the gap between the disproportionate changes in muscular size and strength. Because we have controlled for many factors in our studies, researchers may consider these findings when selecting methods for intramuscular fat quantification. Additionally, our findings will contribute to future research wishing to draw conclusions about how fat content affects muscle structure and mechanical function in a variety of populations.

CHAPTER 2

REVIEW OF LITERATURE

Relationships Between Muscle Size and Muscle Force

As previously mentioned, the size of muscle is the biggest determinant of its force output (161, 197, 207). Muscle "size" can refer to: mass (g), volume (cm^3), or cross-sectional area (cm^2). Biologically, mass refers to the amount of matter within muscle, whereas the CSA and volume refer to the space taken up by muscle in two and three dimensions, respectively. The literature has shown that CSA explains approximately two-thirds of the of amount of muscle force in various ambulatory muscles of healthy adults (4, 90, 121). These cross-sections of muscle size are commonly sampled at the middle of the tibia or femur. The femur is a reliable anatomical landmark, but does not represent the peak muscle CSA of the upper leg, which is between 60-65% of femur length (i.e., knee=0%, hip=100%) (97, 175). Still, these values do correlate well with maximal strength and are useful in evaluating the functional capacity of muscle.

Previous reports have generally shown that males have greater muscle mass than females (113), and obese individuals have greater muscle mass than normal weight adults (105), which leads to greater muscle force. When considering the subtleties and differences between sample populations, there are still deficits in the knee extensors of certain populations, even when muscle area is considered (116, 154). For example, older adults produce less force than their younger counterparts, even when adjusting for muscle size (111). This finding suggests that there are other factors that affect the ability of the muscle to produce greater maximal force between these groups. A necessary consideration is the fact that muscle area is commonly measured in two ways, fat-free

muscle cross-sectional area (mCSA) and physiological cross-sectional area (PCSA) (68, 195). The PCSA takes into consideration the architecture of a muscle by including the fascicle length (and sometimes pennation angle) in the calculations. By considering the fascicle length, PCSA has more physiological relevance due to the consideration of the excursion of the muscle fibers (force x distance); this is applicable for different muscle shapes and in functional tasks (159).

Pathway of Force Production

In order to produce force, there is a complex system of electrical, biochemical, and mechanical events that must occur. Impairment of function within any of these systems can lead to diminished force capacity. As the force production pathway increases in scale from single-molecule interactions to gross motor function, more components become involved in the production and transmission of force. Problems at any stage in this pathway can alter maximal force-producing capacity in skeletal muscle. This force production pathway is illustrated in Figure 2.1; a brief explanation will be given here. The force production process is initiated by electrical and chemical events. Neural impulses originating in the motor cortex are the principal factor in the activation of force. These systems that reside in the brain and spinal cord are referred to as central mechanisms of motor control. After moving down the spinal cord, neural impulses travel to a peripheral motor neuron, which ends at many neuromuscular junctions (NMJ) in skeletal muscle. When a neural signal propagates across the NMJ and along the muscle membrane, the signal then proceeds to what is referred to as the peripheral sites of force production. Excitation-contraction coupling (ECC) refers to the process by which muscle turns an electrical signal into a mechanical event. The ECC process begins with the

depolarization of the sarcolemma by an action potential; this action potential spreads down the transverse tubules and causes a release of Ca^{++} ions from the sarcoplasmic reticulum (SR) deep within the muscle cell. The action potential excites L-type, voltage-gated Ca^{++} channels on the sarcoplasmic reticulum which change shape, subsequently causing ryanodine receptors (RyR) to open. The opening of the RyR allows Ca^{++} ions to move down an electrochemical gradient from the SR to the cytosol; this sudden increase in Ca^{++} ion concentration facilitates cross bridge formation. Cross-bridge formation can be explained as the mechanical interaction of the thick and thin filaments. The thick filament is primarily made up of myosin, and the thin filament is primarily made up of actin, though there are other proteins which make up their structure and contribute to their function (e.g., nebulin, titin, etc.). After Ca^{++} moves into the cytosol, it binds to troponin which undergoes a conformational change on the thin filament. The change in troponin allows tropomyosin to move along the actin filament, which allows binding of myosin heads to actin; this is the first mechanical event in the process of force production. Thus, Ca^{++} concentrations and binding initiate the physical interaction of myosin heads to actin in the sarcomeres. Sarcomeres are the smallest functional unit of the cell, and multiple repeating sarcomeres make up myofibrils. The cooperative effect of multiple sarcomeres causes the production of force observed *in vivo*.

Thousands of sarcomeres that make up a muscle cell, and the more sarcomeres that are in parallel, the greater the force that can be produced. Identifying the distinct structures and mechanisms that limit maximal force in this process allows investigators more accurately track muscle quality changes that occur in humans. Muscle quality can be an ambiguous term but is generally defined as the amount of force produced per

available muscle tissue (60, 149). The latter definition is commonly measured in normalized force values (e.g., force/cm^2).

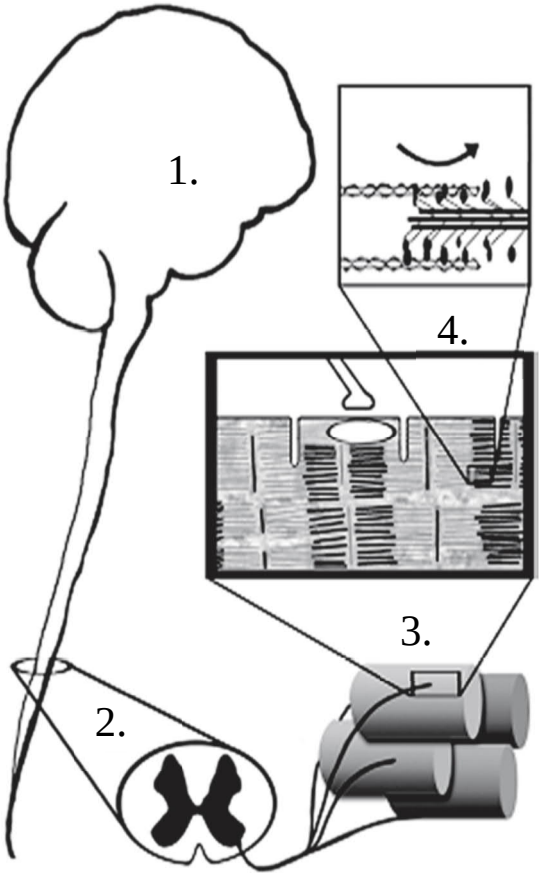

Figure 2.1**. Pathway of force production**. Schematic of the events leading to muscle activation. Beginning with: 1. Cortical excitation 2. Motor unit activation 3. Depolarization of the sarcolemma and subsequent calcium release 4. Actin-Myosin binding, dephosphorylation of ATP and force generation. [Damien M. Callahan, 2010.]

Additional Factors Affecting Muscle Force Production

The literature has shown that differences in central activation are not a primary factor for differences in muscle force between the sexes (122) or with age (126) among healthy adults. This supports the hypothesis that the mechanisms for muscle weakness in healthy adults lie downstream from the central factors, or in the peripheral components of force

production. Interestingly though, while CSA is the primary determinant of force production at the whole muscle level, myosin heavy chain (MHC) characteristics of MHC II fibers have been shown to better predict force when compared to CSA (166). We have a strong understanding of the relationship between muscle size and muscle force. This dissertation project will explain the effects of other structural and mechanical factors that may diminish skeletal muscle force. Specifically, this work will quantify the role of fat in structural disorganization or impairment of muscle function. Identifying additional factors which affect maximal force production will aid researchers, clinicians, and practitioners in quantifying the functional capacity of muscle among many populations.

Fat Content in the Body

Body fat, i.e., adipose tissue, is stored at multiple locations in the human body. At the whole-body level, fat is found in subcutaneous, visceral, or muscular depots (93). Beyond muscle and fat, there are other relevant components that also can affect the degree of whole muscle force, such as fibrosis. Although fibrotic tissues are also a consideration when evaluating muscle, muscle and fat content are the largest factors influencing muscle composition. Thus, connective tissues will not be measured in the scope of this dissertation. The metabolic effects of fat content on global systems like cardiovascular health and local factors such as insulin sensitivity have been extensively researched (79, 239). Though there is strong support for the hypothesis that fat location and fat content will affect metabolic (106, 125, 215) and inflammatory processes (34, 38) in muscle (particularly over time), there is far less information available about how fat may affect mechanical muscle functioning. This has likely contributed to interest in accurate and reliable fat quantification, evidenced by the substantial increase in the number of studies

related to the topic in recent years (24). Despite this, the role of fat content and its effect on muscle force output is still unclear. Further, researchers have failed to reach a consensus regarding the mechanisms that lead to fat-induced muscle dysfunction, and whether these mechanisms vary at different levels of organization. Fat redistribution is also known to occur with age, moving from subcutaneous to visceral locations and ectopic depots (211). This redistribution occurs despite a decrease or no change in total body fat (74, 211). Investigations have reported greater fat content in older adults compared to younger (78, 201). Considering that this finding is concurrent with the known decreases in muscle strength with age (48, 148), we must tease apart the independent effects of age and fat on muscle weakness. Some of the proposed mechanisms for fat-induced muscle dysfunction will be discussed later in this chapter.

Significant changes in diet and lifestyle have led to considerable increases in obesity rates over the last few decades (181, 186, 225). Lower levels of muscle quality have also been reported in obese adults (137, 154, 196), so determining the effect of fat accumulation on muscle is of great concern. At both the cellular and organ levels, differences in fat accumulation between muscle groups has been observed, with predominately slow-twitch muscle fibers having greater accumulation compared to fast-twitch fibers in animal models (7, 165) but the opposite effect in humans (233). Researchers have speculated that greater fat infiltration in fast-twitch muscle groups for humans may be due to maintenance of oxidative (e.g., postural) activities with a simultaneous decrease in power activities (233). Considering this, the mechanisms for decreases in force may vary between muscle types (i.e., slow vs. fast; weight bearing vs. non) and levels of organization (i.e., cellular vs. organ vs. organism).

Fat Content in Whole-Muscle

Even within the muscle organ, there are different locations of fat: between muscle groups (intermuscular), and within a muscle (intramuscular). Further, there are various locations for intramuscular fat depots within the cell (intramyocellular), and outside of the cell (extramyocellular) (85). Greater levels of intramuscular fat content have been purported to be a contributor to muscle dysfunction some populations (e.g., aging, chronic disease) (5, 178). These increases can be in addition to existing lean tissue (as is often the case in obesity), or "in place" of atrophied muscle tissue (in the case of aging or muscular dystrophies); the latter is more accurately termed fat infiltration. There have been studies in both animals (7, 56) and humans (48, 230) that have provided support for the hypothesis that fat directly impairs muscle function. What research has struggled to determine is whether increased fat content is an indicator of muscle weakness, or a direct modulator of force output. To this point, studies regarding the effects of fat content on muscle function have overwhelmingly investigated one organizational level at time, whether that be cellular, organ, or organism. There are relationships between fat content and muscle force (96, 157) as well as physical activity level (75). At this stage it is important to go a step further, with robust study designs that can elucidate the mechanisms underpinning the changes in muscle force by utilizing multiple techniques (e.g., *in vivo* and *in vitro*) across multiple levels of organization. In investigations such as those by Manini et al. 2007, marked reductions in physical activity for young adults were shown to increase fat content and decrease maximal strength in as little as 2 weeks (155). This provides evidence for the hypothesis that modest (albeit statistically significant) increases in fat content may directly impair force output in young, healthy, or physically

active individuals. In a counterargument, the decreased force outputs observed with fat content increases may be a result of exacerbations caused by other comorbidities such as obesity or sarcopenia. The ability to control for the observed differences in muscle force by organizational level can clarify the role of fat content in muscle strength at each level.

Changes in fat content resulting from aging (157), training (87) and neuromuscular disease (178) have been evaluated in the literature. What is not well known is whether the compositional changes that are observed at the whole muscle level are also present at the level of single fibers. Though this dissertation will not investigate fat content changes following training or neuromuscular disease, our findings will provide insight into the potential mechanisms for fat-induced muscle weakness by distinguishing the pattern of fat accumulation and its relationship with muscle functioning. The study design has allowed us to assess fat content along the length of the thigh across a range of body masses. Additionally, this research will not be confounded by the effects of sarcopenia or disease state.

Fat Content in Single Fibers

Fat is found within the cells of skeletal muscle, as muscle is a major site of lipid metabolism in the body (37). Investigation into intramyocellular lipids (IMCL) began primarily because of their role as a substrate during (endurance) exercise. Recently though, interest in IMCL has garnered more attention due to rising obesity rates, as well as the relationship between lipids and insulin resistance in skeletal muscle (37, 81, 160). Single fiber assessments of lipid content are extremely sensitive and have rigorous analyses. Indeed, effective acquisition of muscle tissue followed by careful storage techniques that will allow preservation of the tissue integrity is not a trivial procedure.

Despite this laborious process, muscle assessment at the cellular level allows researchers to resolve fat content and location to a greater extent than at the organ or organism level. These techniques are used in conjunction with *in vivo* measurements for holistic characterization of muscle composition at the level of whole muscle or whole body. This is essential, because of the differences in lipid distribution between muscle groups or individuals of varying age and biological sex. Assessment of lipid content and dynamics at the level of the single fiber provides invaluable information for delineating the effects of lipids on various muscle types (e.g., Type I vs. Type II; diseased vs. non).

There are a few commonly investigated variables in single fiber assessment of lipids: lipid droplet size, lipid droplet number, lipid location, and lipid area fraction, or the relative percentage of lipid area in each cross-sectional area (128, 224). Different techniques for cellular lipid quantification have been employed in the literature such as electron microscopy, histochemical staining (HCS), and ^{1}H-MRS; advantages and disadvantages of these techniques have been detailed elsewhere (210). This dissertation will utilize both HCS and spectroscopic (^{1}H-MRS) modalities to investigate the agreement between these commonly used methods. An advantage of this study design will also be the comparison of both invasive and non-invasive modalities in the same dataset. This will be useful for interpreting results between disparate study groups or under different conditions (e.g., maximal vs. submaximal exercise). For example, because of the invasive nature of muscle biopsies, ^{1}H-MRS measurement may be more appropriate for certain populations, or those undergoing multiple collections (e.g., training studies, longitudinal studies). On the other hand, a well-known limitation of spectroscopic imaging is the overlap of the much larger extramyocellular lipid (EMCL)

peak, which may affect quantification of IMCL (18). In studies involving clinical populations or simply those with greater amounts of fat tissue (e.g., obesity), HCS may be the more appropriate method for practical and reliable results. We are aware of two studies that sought to compare the agreement between biochemical assay, electron microscopy, ORO, and ^{1}H-MRS in order to quantify exercise-induced IMCL breakdown (46, 237). These studies had different study aims than what is being proposed in this dissertation, which requires consideration. For example, the investigation by de Bock et al. investigated a relatively small (n=9) and homogenous group of young, endurance trained men. Nonetheless, this study still found that the method of IMCL measurement had a significant effect on the quantification of IMCL utilization following exercise.

Fat Content Quantification in Skeletal Muscle

As multiple studies have proposed (46, 86, 102, 204, 218), one of the sources of discrepancy between interpretations may be the modality used to measure of fat content within muscle. Even though the importance of fat content is well accepted, the methods of measurement of these data can vary greatly between researchers, clinicians, or practitioners. Those in clinics or with less resources may use more accessible methods of measurement for ease of use (e.g., ultrasound, bioelectric impedance analysis), while those with more materials or specific research questions may use Computed Tomography (CT), MRI, or histological analyses. Inconsistencies in the interpretation of these data can cause confusion about their practical significance, particularly among disparate populations or in longitudinal study designs. This dissertation will employ *in vitro* and *in vivo* techniques to compare muscle fat content in healthy adults. This will help investigators further understand the strengths and limitations of three commonly used

modalities in fat content quantification: histochemical staining (HCS), magnetic resonance spectroscopy (^{1}H-MRS), and magnetic resonance imaging (MRI). These methods are detailed below.

Dixon Imaging. For nearly four decades, the measurement of non-contractile tissue or fat content was primarily accomplished via MRI with T1 Weighted Imaging (113, 123, 203). In 1984, Dixon proposed a chemical shift imaging method which exploited the resonance frequencies of water and fat in biological tissue (50). Unlike T1 Weighted Imaging, Dixon techniques modulate the phase of fat signals to represent the combined fat and water signal in complex numbers; these signals can then be calculated on a pixel-by-pixel basis (50, 73, 88, 150). With this acquisition technique, MRI scanners can produce four images: water only, fat only, water + fat, and water – fat (Figure 2.2). The water + fat images are referred to as "in-phase," as the water and fat protons are both contributing high signal intensity to the acquired image. Conversely, the water – fat images are referred to as "out-of-phase", where the water signal is the predominant signal in the acquired image. There are many advantages to Dixon imaging when compared to other clinical imaging techniques, such as fewer signal intensity artifacts, higher accuracy of fat quantification, and greater versatility across high field strengths ≥ 3.0 Tesla (73, 103, 150, 198). Over the next several years, this technique became the gold standard for fat quantification in MRI. The fat signal fraction (FF) is a commonly used marker of fat

content in Dixon techniques and represents a spatially resolved signal of fat tissue at the inter- and intramuscular levels.

^{1}H-MRS. For approximately 50 years, ^{1}H-MRS has been used to quantify metabolites in skeletal muscle (31, 101, 118, 119). In contrast to MRI techniques, which capture still images of the anatomical location of tissues, ^{1}H-MRS allows researchers to quantify the concentrations of metabolites within muscle (19, 110). Like Dixon imaging, proton spectroscopy allows noninvasive assessment of skeletal muscle, making it easier to support practical application of results. Even though fat content measured by ^{1}H-MRS can be reported at the intracellular level, these values are acquired and resolved from muscle at the intramuscular (i.e., organ) level (18). Aside from being able to quantify

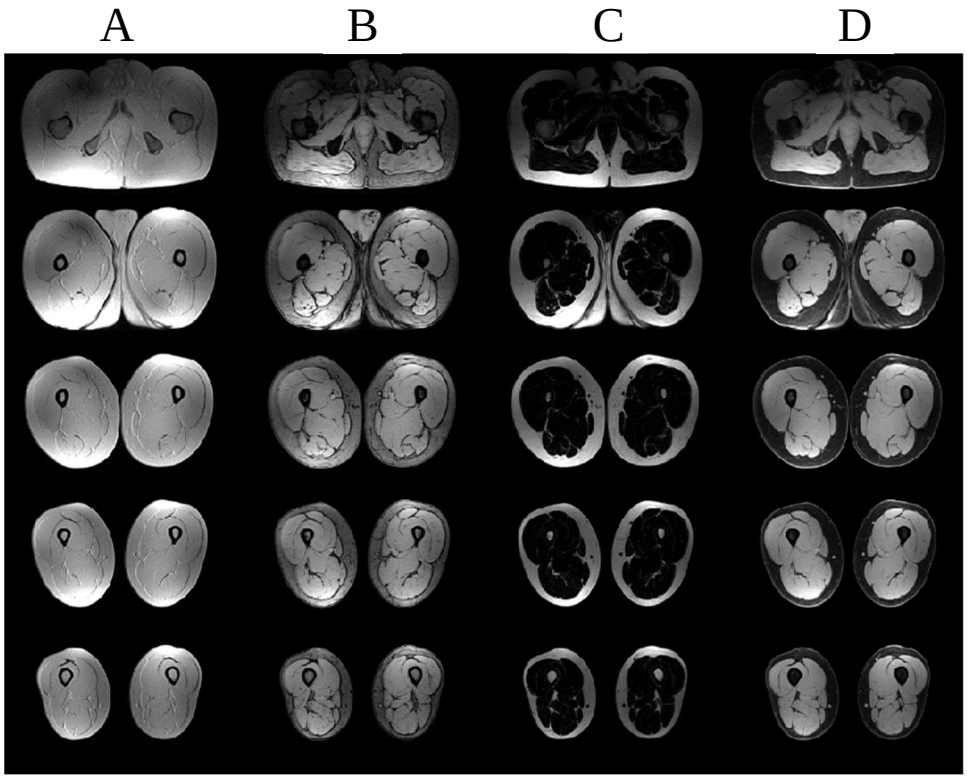

Figure 2.2. **In-phase and out-of-phase acquisition in Dixon imaging**. The figure depicts the four images produced from Dixon sequence. A: In-Phase, B: Out-of-Phase, C: Fat Only, and D: Water Only.

lipid concentrations within intracellular and extracellular (i.e., interstitial) compartments,

^{1}H-MRS allows concurrent acquisition of other sequences in an interleaved fashion, such as ^{31}P-MRS (238). This is a notable advantage for researchers performing studies with exercise protocols or those that would like to minimize acquisition time. Additionally, ^{1}H-MRS would likely be the preferred method of fat quantification for those who do not have access to *in vitro* techniques but would still like to quantify both IMCL and EMCL concentrations separately; concentrations of other metabolites (e.g., creatine) can also be acquired simultaneously. Notable limitations in fat quantification using this method are: 1. some of the proton spectra are highly sensitive to fiber orientation and 2. IMCL peaks may disappear due to high concentrations of EMCL (133, 245). Both issues can make sole reliance on ^{1}H-MRS for fat content a risk for study designs, such as those evaluating an intervention or disease progression.

Histochemical Staining. There are multiple modalities that could be described as histochemical staining. When evaluating *in vitro* fat content within skeletal muscle, oil red o (ORO) analyses are commonly used for quantification of cellular lipid content (164, 224, 236). Oil red o is a technique that allows lipid droplets to be quantified by labeling of proteins via staining (128). Staining by ORO can also be combined with immunofluorescent techniques for a more complete picture of cellular fat content and location. When compared to other fat quantification methods, ORO analysis has the advantage of being able to visualize the proximity of lipids to other organelles such as the mitochondria (212). Additionally, HCS can resolve fat content by fiber type (e.g., Type or Type II) (46), a notable advantage over *in vivo* techniques. This is why ORO is a method used for research studies interested in the role of lipid size and proximity in metabolism (46, 236).

Evaluation of Muscle Architecture

Our current work has brought attention to numerous investigations evaluating the role of fat content on muscle function. This dissertation proposes avenues for advancing the field in this area, including: 1. evaluating fat content along the entire length of the thigh, 2. using these data in conjunction with other modalities at the single fiber level, and 3. evaluating these data in young, healthy adults. Data will be presented from *in vitro* and *in vivo* methods at this single fiber level to compare potential differences in fat content by modality. We expand upon previous work seeking to delineate the mechanisms of impaired force by investigating the impact of muscle fat content on architecture and function. This will be accomplished with another sensitive modality, diffusion tensor imaging (DTI).

With reference to skeletal muscle, architecture can be defined as "the arrangement of muscle fibers within a muscle relative to the axis of force generation" (145). Unlike the relationship between force and CSA, which has a positive linear relationship, the relationship between force and muscle architecture (e.g., fascicle length, pennation angle) not consistent due to muscle shape and orientation. Early reports of muscle architecture values were conducted via manual measurement of human cadavers (40, 247). However *in vivo* methods have been used for more practical estimation of force output and more accurate inputs in modeling techniques (158).

The overwhelming majority of findings in the literature surrounding muscle architecture are measured by ultrasound B-mode sonography (1, 10, 17, 67, 82, 158). This hardware is commonly utilized due to its ease of use, low cost, and practicality (8, 235). However, certain populations and research questions require an imaging technique

to assess muscle architecture that can detect microstructural changes due to training, disease, or fiber re-organization (i.e., re-distribution of fat or muscle tissue). It also may be that investigators require a technique that can be combined with other data sets using the same equipment (e.g., MR scanner) or at the same timepoint.

Diffusion Tensor Imaging. Diffusion tensor imaging (DTI) allows quantification of tissue structure by exploiting the diffusive properties of water in a medium to quantify the magnitude and direction of diffusion in muscle (11, 12, 63, 140). Diffusion Tensor Imaging comprises a group of techniques where calculated eigenvalues ($\lambda1$, $\lambda2$, and $\lambda3$) and eigenvectors ($\varepsilon1$, $\varepsilon2$, and $\varepsilon3$) are used to create images reflecting various diffusion properties of a tissue. “Regular” Diffusion Weighted Imaging assigns a scalar value to represent the rate or directional preference of water within an area of interest using the sum or average of the eigenvalues (171, 176). The sum of the eigenvalues ($\lambda1+\lambda2+\lambda3$) is called the trace, while their average (i.e., trace/3) is referred to as mean diffusivity (MD) or apparent diffusion coefficient (ADC) (141, 171, 176). In this dissertation, the magnitude of diffusion will be reported as the MD. By repeating this process of diffusion weighting in multiple directions, a three-dimensional diffusion model (i.e., the tensor) can be estimated in muscle. This three-dimensional model can also be applied across the whole of the muscle length, unlike ultrasound acquisitions. Figure 2.3 illustrates a representative data set that can be acquired using this technique.

Using the MD and FA values acquired via DTI, a technique called fiber tractography can then be used to visualize and estimate the architecture of muscle (44, 63, 124, 193). In DTI, muscle fiber tracts largely represent the fascicles in a muscle group (22, 43). Like ultrasound imaging, architectural variables such as fiber tract length (mm), and pennation angle (°) can be acquired using DTI; these measures have been validated previously (22, 41). Apart from the MD and FA values, muscle tract curvature (m^{-1}) and variability in

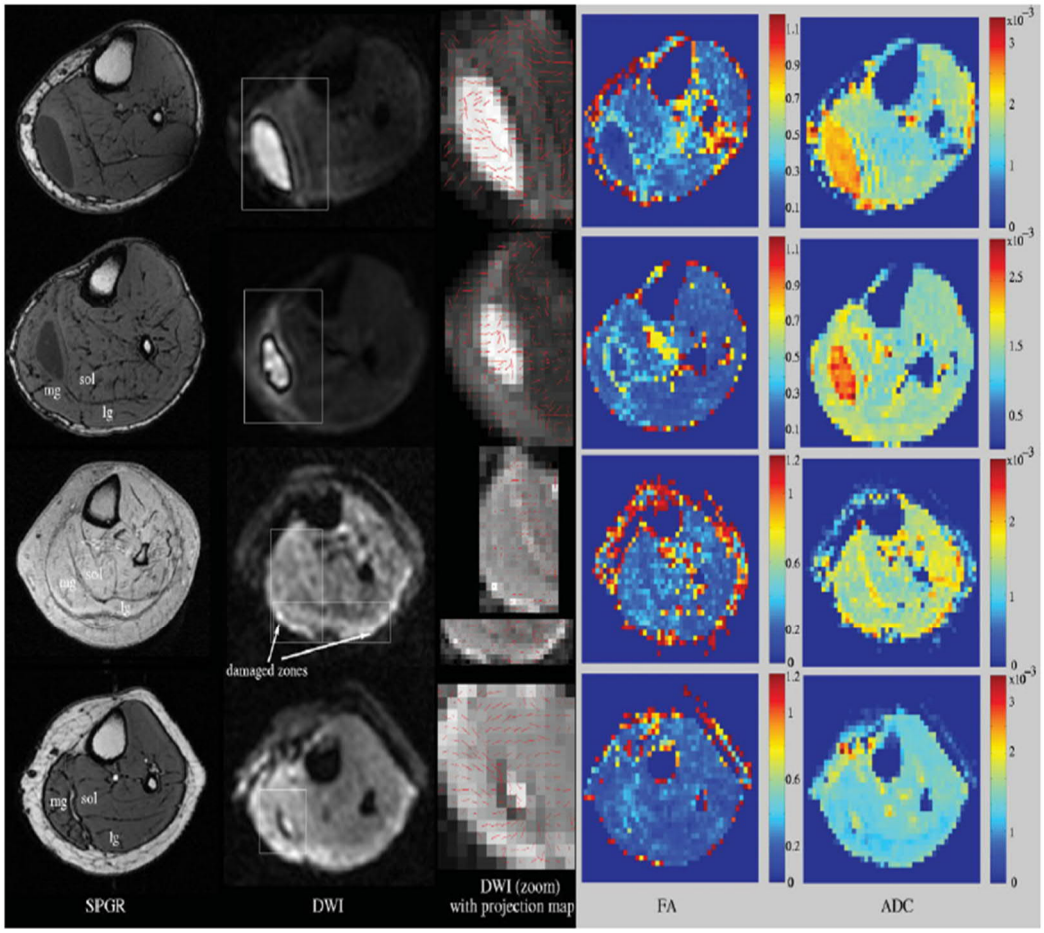

Figure 2.3. **Axial images of the human calf muscles with different types of injury**. First row: patient PS1 with 1-day-old acute gross intramuscular hematoma injury; second row: patient with five-day-old gross intramuscular hematoma injury; third row: patient with clinically apparent acute medial gastrocnemius tear injury; and fourth row: patient PS4 with clinically apparent chronic gastrocnemius tear injury. Within each row the images are shown in the following order: high contrast T1-weighted image obtained using the SPGR pulse sequence, DWI image, fragment of the DWI image showing the damaged area with 2D projection map (see text for details), the FA map, and the ADC map. The frames on DWI images outline the damaged areas of the calf muscles. The muscles studied are indicated on SPGR images, they are: sol, lg, and mg. FA is dimensionless and units for ADC are mm^2/second. [Zaraiskaya 2006.]

fascicle orientation (SD of ε1) can also be estimated. Other advantages of DTI over ultrasound or modeling techniques include: 1. the ability to reliably represent muscle in three dimensions, 2. the ability to acquire images over a larger area than ultrasound, 3. the ability to detect microstructural changes in muscle due to disease, injury, or training, and 4. the ability to acquire data in superficial and deep compartments.

Though DTI of skeletal muscle is a relatively new undertaking, there have already been attempts to characterize the diffusion and architecture of muscle tissue by age (70), gender (71), injury status (252), fiber type (208), and disease state (98). These investigations illustrate the immense potential for DTI in elucidating the subtle changes that precede the observed functional differences between distinct groups. Indeed, in an extensive review by Larsson and colleagues, it was suggested that the age-related changes in muscle power that have been reported to occur before the morphological and electrophysiological changes may be due to the lack of precision or sensitivity in the methods used (139). The authors went on to say that the application of more sophisticated techniques could allow for earlier detection of the molecular and cellular changes that precede the known impairments that occur with age (139). By combining DTI with methods such as ORO, Dixon, or ^{1}H-MRS, we can paint a more complete picture of how fat content and architecture may affect muscle function. Considering this, the present work could be used as a guide for future studies who wish to combine methods to answer specific research questions.

Potential Mechanisms of Mechanical Force Impairment

Given the information presented in this review of the current literature, there are several potential mechanisms for the mechanical impairment of maximal force in skeletal

muscle. Changing demographics and technological developments over the last 40 years have led to renewed interest and greater potential for answering a simple, but multi-layered question: what contributes to the variations in muscle strength among different populations? Structural and functional variables can provide specific areas to investigate the gap between muscle size and muscle strength. By combining data for fat content, muscle architecture, and function in the same cohort, across modalities, and at multiple levels, we can strengthen our understanding of how fat content may affect muscle structure and function.

Single Fiber Characteristics and Whole Muscle Strength

The force producing characteristics of single fibers play a key role in the force values recorded at the level of whole-muscle (166, 167). The size, proportion, and kinetics of Type II fibers have also explained differences in whole muscle performance between study groups (89, 167, 205). Type II muscle fibers are known to have a greater potential for hypertrophy and maximal force production when compared to Type I (151). Given the common finding of an inverse relationship between fat content and maximal force *in vivo*, fat infiltration at the cellular level may impair force production at the single fiber or whole muscle levels. A potential mechanism for this result could be the slowing of cross-bridge kinetics or reduction of myofilament stiffness by lipids, as suggested by Straight and colleagues (223).

Impairments in single fiber force production due to increased fat content have been observed in animal studies (56, 165, 184), but limited data has been shown for this relationship in humans. A study by de Sousa et al. demonstrated that muscle hypertrophy, but not muscle force was attenuated by diet-induced increases in fat content in mice (47).

Taken together, work in animal models has suggested that the increases in fat content may cause decreased potential for muscle tissue hypertrophy and/or direct impairment of force, the mechanisms by which are not clear. Though Type I fibers are expected to have greater levels of fat content than Type II due to their physiological role in muscle, previous work has suggested that larger lipid droplets may impair force production by inefficient mobilization (7). Similar fiber functioning between groups with differing fat contents would suggest that cross-bridge kinetics are not affected by greater levels of fat, but rather a result of differences in the intrinsic molecular characteristics of the fiber, such as cross-bridge number or stiffness.

Two studies have investigated the relationship between fat content and muscle function at both the single fiber and the whole muscle levels in humans (36, 224). The investigation by Choi and colleagues found that total area, lipid area fraction, and number of lipid droplets were greater in obese older adults compared to their normal weight counterparts at the level of the single fiber (36). This study also reported inverse relationships between lipids and shortening velocity, maximal velocity, and specific power. They also reported lower specific torque in the obese adults, consistent with the literature (62, 74, 154). The work by Straight et al. focused on the potential sex-differences in muscle function due to fat content. Myosin attachment time was the only measure associated with fat content at the single fiber or whole muscle levels in this cohort (224). When these measures were investigated by sex, females demonstrated an inverse relationship between intramuscular fat and specific force in both Type I and Type II fibers (224). This suggests that the slowing of fiber kinetics may be related to increased fat content in older women. Still, there were several limitations to these investigations.

The first is that the data presented are exclusively from an older adult population, therefore adding difficult in disentangling the potential effects of fat-induced force impairment from the known decreases in force production resulting from age or comorbidity. Additionally, the effect of fat deposition on muscle architecture was not explored, which could explain the differences in whole muscle strength between groups. This dissertation addresses these limitations and also uses more robust measurements of whole muscle fat quantification with Dixon analysis, compared to ultrasound or computed tomography (CT). Finally, evaluation of these variables with isometric as well as isokinetic contractions will clarify the role of single fiber fat content and kinetics on whole muscle force in static and dynamic conditions.

Potential Effects of Fat Content on Muscle Architecture

There have been few studies investigating the relationship of muscle fat content and muscle architecture (196). Though there have been reports that both elements will affect the function of muscle, nearly all conclusions related to their combined effect have been drawn independently. Even then, direct comparisons have relied on ultrasound analyses to quantify the relationship between these variables (i.e., echo intensity, fascicle length, and pennation angle) (189, 244). Fat content may indeed affect fascicle length or pennation angle by obstructing the organized arrangement of muscle. If fat does not directly act on muscle to acutely impair its function, it may be that fat indirectly affects force by disrupting the arrangement of its fascicles. Studies at both single fiber (166) and whole muscle level (189) have proposed that stiffness, perhaps influenced by fat content, may affect force; this is worthy of further investigation. Moreover, greater fat area fractions may decrease the number of sarcomeres in parallel and in series for a given

CSA. A relationship between tract length or pennation angle and fat content would suggest that differences in muscle strength are due to the premature termination of muscle fascicles or mechanical disruption of the displacement process in muscle. This would help explain the decreases in specific torque in obese or older adults compared to controls or younger adults, respectively.

Summary

The decreases in muscle strength far exceed the decreases in muscle mass. Muscle cross-sectional area explains most of the variation in muscle strength at the organ level of ambulatory muscles. However, the disproportionate changes in size and strength in aging or obese populations indicate other factors also diminish maximal muscle performance. Previous work has shown an association between fat content and force at the whole muscle and single fiber levels. By eliminating the confounding effects of age or chronic disease, we can better understand the relationship between muscle composition, architecture, and function. When considering the relationship between size and strength at the single fiber level, cross-bridge kinetics are potentially a greater contributor to force than CSA. Additionally, with increasing scale there are more structural components that contribute to the transmission of force. Therefore, it is reasonable to postulate differing roles for fat content, depending on the anatomical level being evaluated. This is a rational line of thought, as mechanical disruptions in the process of force production or transmission can occur at any step of the force production pathway. This underscores the importance of *in vitro* and *in vivo* assessment for practical application and interpretation. This review has outlined potential avenues to address the clear gaps in the current literature related to the possible role of fat content in the disorder of structure or

impairment of function in muscle. Considering this information, questions we may ask to address these gaps are:

1. Is there a discrepancy in fat measurement between commonly used modalities?
2. Is single fiber fat content related to whole muscle fat content in young, healthy adults without chronic conditions?
3. If there is a relationship in questions #2 or #3, are both MHC I and MHC II fibers related?
4. Is fat content related to muscle architecture in young, healthy adults?
5. Is lipid content related to single fiber function?
6. Is fat content related to whole muscle strength in static and dynamic tasks?

The answers to these questions will allow us to draw definitive conclusions about the relationship between muscle composition, muscle architecture, and muscle force in healthy young adults. By combining multiple variables that are known to affect muscle function, and using more sensitive tools of measurement than previous investigations, this dissertation will provide unique information about the mechanical means by which force is impaired, beyond decreases in muscle size. Further, we will be able to evaluate these results across multiple levels of organization, under static and dynamic conditions. This research will help investigators and practitioners identify specific variables that can mitigate the decreases in muscle weakness that occur due to age, obesity, or neuromuscular disorder. Identification of these variables can also serve as markers of training or disease progression, whether they be fat content, fascicle length, or fiber function. Surely there are immunological and biochemical mechanisms at play in the observed differences in muscle force, however, these considerations are beyond the scope

of this dissertation. Still, by pairing this information with what we know about the biochemical causes of muscle weakness, we can help resolve the contributions of different factors (e.g., neurological, biochemical, mechanical) on muscle impairment.

CHAPTER 3

METHODS

This dissertation seeks to identify several of the variables that may contribute to the impairment of maximal force in human skeletal muscle. Specifically, we would like to elucidate the role of fat in the structure and function of muscle. To this end, we evaluated the relationships between muscle composition, architecture, and function. In pursuit of the overall objective, three studies were performed to address distinct parts of these relationships. The next section will provide information on the sample sizes and participant characteristics for all three studies. The subsequent sections will detail all methods used in this dissertation project.

Participants

For all three studies, male and female participants between 21-45 years of age were recruited to be relatively sedentary and free of cardiovascular, musculoskeletal, neurological, or metabolic disease. All participants had a body mass index (BMI) between 18.5-39.9 $kg \cdot m^{-2}$ and were not taking any medications known to affect physical or muscular function. Study procedures were approved by the Institutional Review Board at the University of Massachusetts Amherst (Appendices A-C). After determining eligibility and MR safety via telephone screening (Appendix D), all participants were scheduled for a visit to the Life Science Laboratories at the University of Massachusetts Amherst where they completed an informed consent, medical history (Appendix E), and MR safety questionnaire (Appendix F). Measures of height and body mass were also obtained.

Physical Activity Assessment

To account for potential influences of habitual physical activity (PA) on our outcomes (Studies 1-3), PA was measured for each participant using uniaxial GT1M accelerometers (ActiGraph, Pensacola, FL). A trained researcher initialized the accelerometer to record at 80 Hz and with 60-s epochs. Participants were given the accelerometer in conjunction with an activity diary to record bouts of PA. Participants were then instructed to wear the accelerometer on their right hip for at least 7 days from the time that they wake up until they go to sleep. Participants removed the accelerometer during any water-related activities, such as showering and swimming. Standard cutpoints (232) were used to determine daily counts, minutes of moderate-to-vigorous physical activity (MVPA), and wear time, as reported in Choi et al. (35). Daily activity counts (arb. units), MVPA (min) and wear time were determined using ActiLife software (ActiGraph, Pensacola, FL). The first 6 valid ($\geq$10 hr wear time) days (i.e., 4 weekdays and 2 weekend days) were analyzed for each participant. Wear time was also confirmed by cross-referencing to the participant activity log (Appendix H).

Muscle Strength Measurements: Acquisition

Measures of maximal knee extensor muscle torque (Nm) and peak velocity ($deg \cdot s^{-1}$) were collected as indices of muscle performance *in vivo* using a Biodex System 4 dynamometer (Biodex Medical Systems, Inc., Shirley, NY, USA) (Study 2 and 3). Prior to muscle performance testing, participants performed a 5-minute, unloaded warm up on a stationary bicycle. Participants were then seated on the dynamometer in an upright position with a 110° hip angle. The Biodex lever arm was attached to the dominant leg using a Velcro strap approximately 2-3 cm above the lateral malleolus. Chair and

dynamometer settings were adjusted for each participant to correctly align the axis of rotation with the femoral condyle to ensure participant safety and accurate torque measurements. A representative image of these procedures can be found in Figure 3.1. To quantify knee extensor torque, unilateral maximum voluntary isometric contractions (MVIC) and maximal voluntary dynamic contractions (MVDC) were performed.

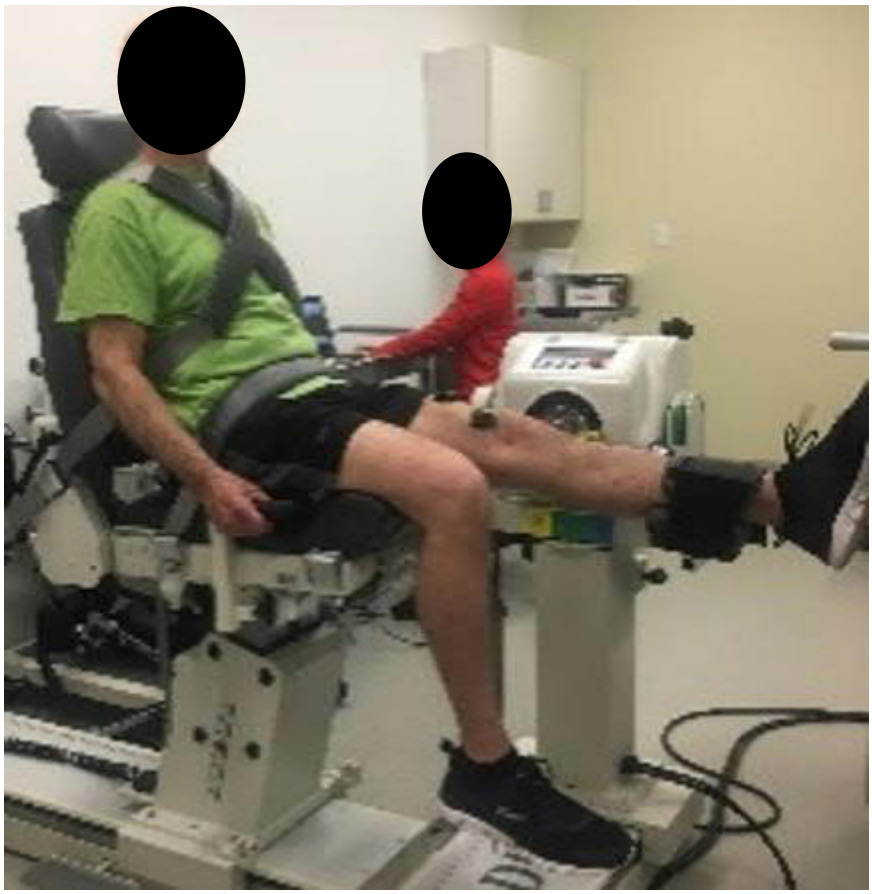

Figure 3.1. **Participant performing biodex protocol**. The image depicts the procedures for isometric and isokinetic muscle strength testing on the Biodex System 4 Dynamometer. [Photo from Muscle Biology Laboratory with permission of Mark Miller].

The experimental protocol consisted of 2 MVICs followed by 6 randomized sets of 3 repetitions of isokinetic MVDC's at 60, 120, 180, 240, 300, and 500 $deg \cdot s^{-1}$. Each MVDC

set consisted of 3 consecutive repetitions, with two minutes of rest between each set of contractions. Participants were instructed to “kick as hard and fast as possible” for each concentric contraction, and then “relax” when this phase was completed for a passive return to the starting position. After the MVDC’s, participants performed a third MVIC to evaluate potential fatigue that may have occurred during the MVDC protocol. The MVICs were performed at 100° of knee flexion and lasted 3-4 s. The MVDCs were performed over an 80° range of motion, from a starting point at 90° of knee flexion to 10° of knee flexion (almost fully extended). Peak contraction velocity was estimated using isokinetic contraction speeds of 500 $deg \cdot s^{-1}$, which were essentially unloaded contractions (torque was not recorded for these contractions). Visual feedback and verbal encouragement from the researcher will be provided throughout the protocol to ensure maximal effort.

Muscle Strength Measurements: Analysis

Dynamometer data was analyzed using a custom-written MATLAB program (Mathworks, Natick, Massachusetts). For MVICs, a trained researcher manually selected the beginning and the end of the contraction. For each MVDC, a trained researcher manually selected multiple points: the start of contraction, the start of the isovelocity phase, the end of the dynamometer artifact, the end of the isovelocity phase, and the end of contraction. Outcome variables included: peak isometric torque (Nm), peak isokinetic torque (Nm), specific torque ($Nm \cdot cm^{-2}$), and peak velocity ($deg \cdot s^{-1}$). Peak isometric and isokinetic torque were defined as the greatest torque value acquired from one of the three total contractions. Specific torque was calculated by using peak isometric torque and normalizing to the peak muscle cross-sectional area (mCSA).

In vivo Muscle Size and Composition: Magnetic Resonance Imaging

Figure 3.2 depicts a schematic of the order of the sequences for all MR data in this dissertation. The total scan time does not include repeat shims, acquisition, or positioning of participants between scans.

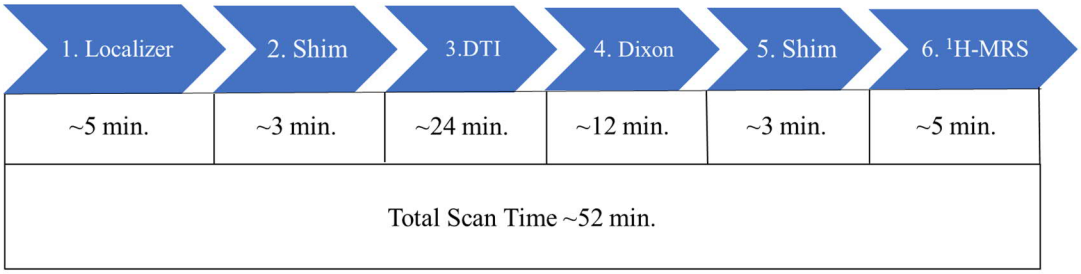

Figure 3.2. **Order of MR sequences**. The image depicts the order of each imaging technique in the MR scanner and approximate time for each scan.

Six-point Dixon Acquisition

Scans for all three studies were performed on a Siemens Skyra 3T scanner, 70-cm bore MR system (Siemens Healthcare, Erlangen, Germany) running on VE11C platform. Participants were positioned supine on the exam table with feet oriented towards the scanner. Gradient-echo scout images were used to confirm optimal leg positioning in the isocenter and correct coil positioning over the muscle. Serial images of the dominant thigh were acquired in all participants from the lateral epicondyle of the femur to the greater trochanter of the hip (Figure 3.3a). Images were acquired using an 18-channel phased array coil combined with a spine coil built into the exam table. To limit movement, the coil was secured to the thigh using inelastic straps. A six-point Dixon technique was applied to generate water- (W) and fat- (F) only images using a 2D gradient echo sequence (73). Parameters will be as follows: image resolution (1.25 x

1.25 x 5 mm^3), repetition time = 35 ms; slice thickness = 5 mm; 24 slices, field of view = 240 x 240 mm^2; echo times =2.46, 6.15; 3.69, 7.38; 4.92, 8.61 ms; matrix = 192×192 mm^2; GRAPPA factor = 2; flip angle = 15°, bandwidth = 1090 Hz/pixel, 1 average, and acquisition time = 12 min.

Six-point Dixon Analysis

Water and fat images were reconstructed offline using the MATLAB Fatty Riot algorithm (219). Figure 3.3 illustrates the analysis procedures explained next. First, the anatomical landmarks for the femur (lateral epicondyle and greater trochanter) were identified and recorded (Figure 3.3a). Then, all slices in which all four quadricep muscles are visible will be identified; this portion of the thigh is referred to in this document as the "4-to-4 region." This is represented by the green bars in Figure 3.3a. Regions of interest (ROI) were drawn around the quadriceps on contiguous out-of-phase images in each slice.

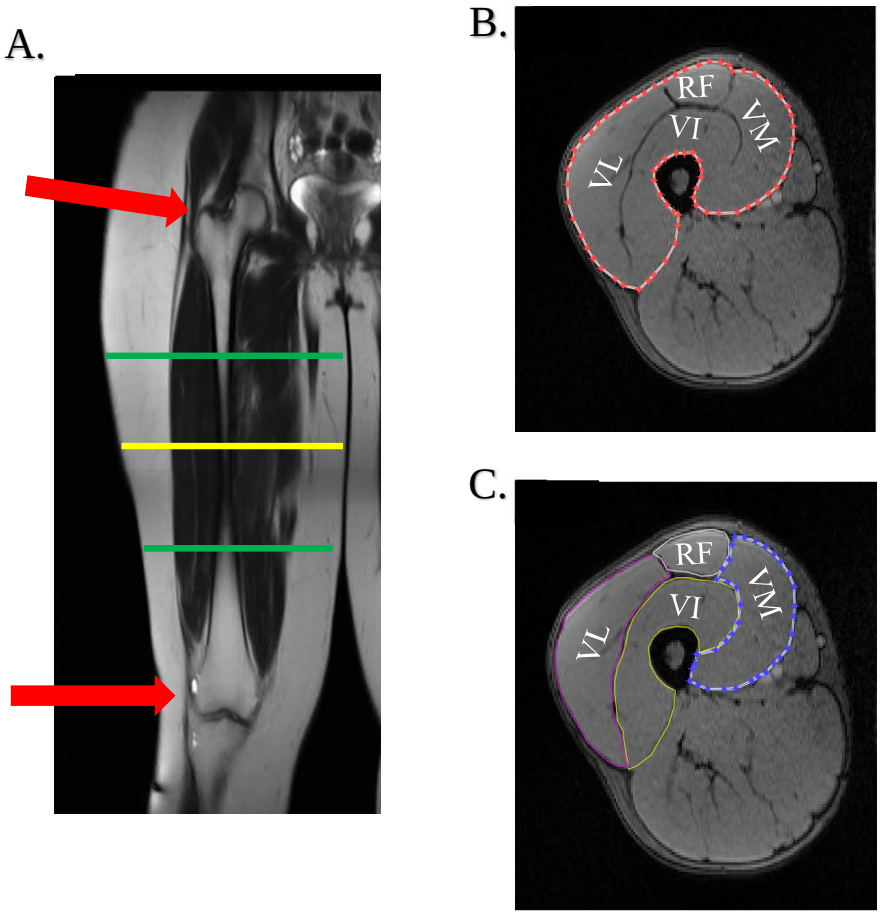

Figure 3.3. **MRI acquisition area and 1-ROI vs. 4-ROI analyses**. Panel A. Represents the coronal image of the right upper leg of a participant. The red arrows indicate the anatomical landmarks for the length of the femur; the greater trochanter (upper) and the lateral epicondyle (lower). The yellow line represents the location of a mid-femur slice, while the green lines represent the region in which all four quadriceps muscles are visible from axial images (4-to-4 region). Panel B. Represents an axial image of a participant with 1-ROI (red). Panel C. Represents an axial image of the same participant with 4-ROI (magenta= vastus lateralis, white= rectus femoris, yellow= vastus intermedius, blue= vastus medialis).

Subcutaneous fat, bone and regions of intermuscular fat or connective tissue were excluded as much as possible when drawing each ROI. Mean FF was calculated on a pixel-by-pixel basis as:

$$FF = 100\% * F/(W + F) \qquad \textit{Equation 1}$$

Where W is the water signal intensity and F is the fat signal intensity. Fat signal fraction, referred to as fat fraction was calculated as an average of the values for each

ROI. Fat-free muscle CSA (cm^2) for each ROI was calculated as total area for the ROI minus the fat area. Muscle volume (cm^3) of the quadriceps was calculated as the sum of all mCSAs multiplied by the slice thickness. Peak mCSA (cm^2) was determined from the slice having the largest muscle CSA; its location along the length of the femur was also recorded.

^{1}H-Magnetic Resonance Spectroscopy: Acquisition

Proton magnetic resonance spectroscopy (^{1}H-MRS) was used to provide a noninvasive measure of intramyocellular lipid (IMCL) content (19) (Study 1). For all spectroscopic measures, participants were positioned as previously described for MRI acquisition. All ^{1}H-MRS data were acquired in a Siemens 3TSkyra MRI scanner from the vastus lateralis muscle of participants. All ^{1}H-MRS spectra were acquired using a dual-tuned 31P/1H circular surface coil (8 X 10.5 cm; Stark Contrast, Erlangen, Germany). Gradient-echo scout images were used to confirm optimal leg positioning in the isocenter and correct coil positioning over the muscle. A Point-Resolved Spectroscopy (PRESS) sequence was used with a single voxel and the following parameters: TR/TE=2000/30 ms, 128 averages for water suppression and one average for non-water suppression, voxel size = 8 cm^3, complex points = 2048, bandwidth = 2000 Hz, and acquisition time = 4:34 minutes. A representative sample of the voxel placement can be seen in Figure 3.4.

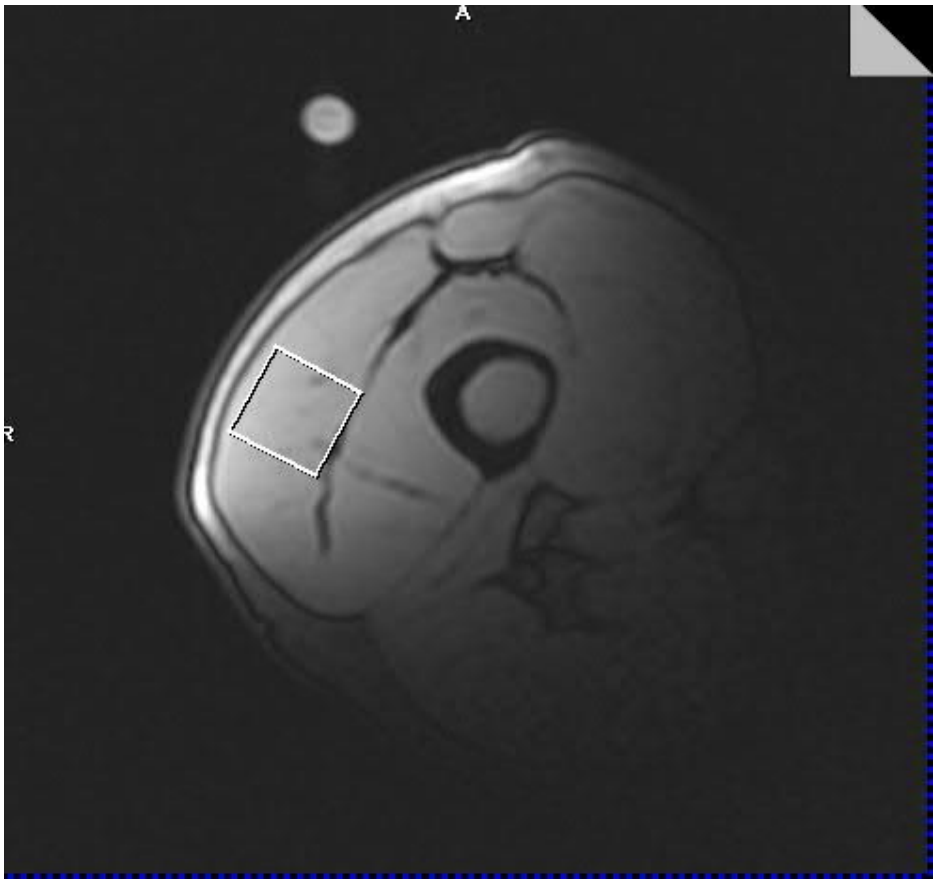

Figure 3.4. **^{1}H-MRS voxel placement**. The white box depicts the area of acquisition for 1H proton spectroscopy on the vastus lateralis.

Magnetic Resonance Spectroscopy: Analysis

To calculate the relative concentrations of muscle metabolites, spectral analysis was completed using jMRUI v6.0beta (Leuven, Belgium) (179). Water suppressed free induction decays were individually zero filled (2,048 points), apodized (1 Hz Lorentzian filter), and converted into the frequency domain via Fourier transform. The zero-order phase was manually adjusted to create a level baseline throughout the spectra. Visual identification of the creatine peak was then used to set the reference frequency at 3.02 parts per million (ppm). Prior knowledge files were also applied for peak identification. The AMARES algorithm was used to line-fit and quantify the area under the curve for the following peaks of interest: intramyocellular lipid CH_3 (IMCL) at 1.28 ppm,

extramyocellular lipid CH_2 (EMCL) at 1.49 ppm, and creatine CH_3 (Cr) at 3.02 ppm. Other visible peaks, along with a baseline correction, were also fit to ensure accuracy in the results. Non-water suppressed data were analyzed in the same manner for the quantification of water concentration, with the only differences being that the water peak at 4.65 ppm was used to set the reference frequency and was the lone peak fit using separate prior knowledge files. The area of each peak represents the relative concentration of the individual metabolites, in arbitrary units. Ratios between relative concentrations of IMCL and creatine as well as water (i.e., IMCL/TCr; IMCL/W) were calculated (245); these measures rely on the assumption that both creatine and water concentrations are similar amongst the study participants. These procedures are represented in Figure 3.5.

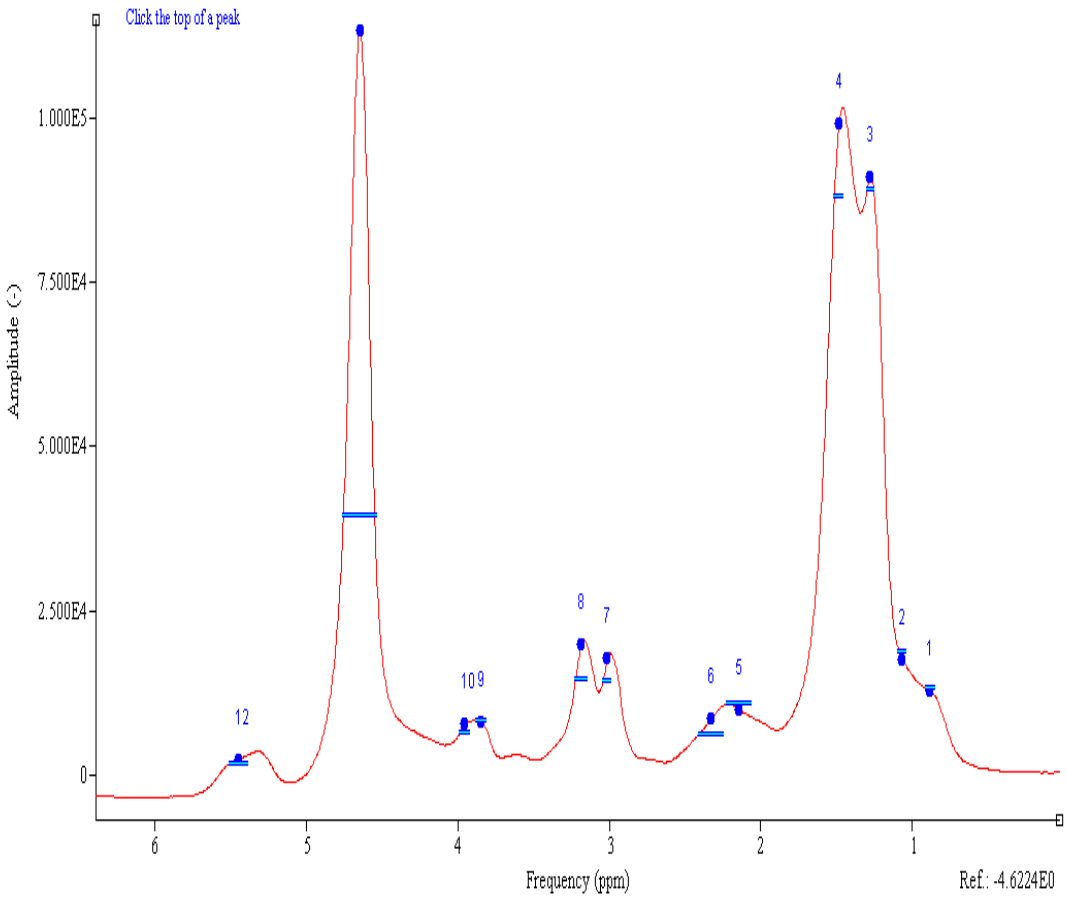

Figure 3.5. **^{1}H-MRS analysis using jMRUI**. The image depicts a representative spectrum for identifying the methyl and methylene peaks of IMCL (point 1 and 2, respectively) and EMCL (points 3 and 4, respectively).

In vivo Muscle Architecture Assessment

Diffusion Tensor Imaging Acquisition

All DTI scans (Study 2) were performed on a Siemens Skyra 3T scanner, 70-cm bore MR system (Siemens Healthcare, Erlangen, Germany) running on VE11C platform. The subjects were examined in supine position and feet first using an 18-channel phased array coil (Body 18, Siemens Healthcare, Erlangen, Germany) combined with the spine coil built into the exam table. Diffusion tensor images were acquired using a spin-echo echo-planar imaging (EPI) sequence with 12 gradient directions following the six-point Dixon acquisition. Four stacks were acquired from the lateral epicondyle of the femur to the

greater trochanter of the hip, as previously described. The acquisition parameters for DTI were: b-value=450 mm·s^{-2}; TR = 4400 ms, TE = 58ms; FOV = 240 × 240 mm^2; number of excitations = 6; slice thickness = 5 mm; 24 slices, matrix, 192 × 192, and acquisition time 24 min. Also, parallel imaging and SPAIR (spectral attenuated inversion recovery) fat suppression was used.

Diffusion Tensor Imaging Analysis

All DTI data were analyzed using a custom-written MATLAB program via the MuscleDTI_Toolbox github; all DTI processing steps are detailed in Damon 2021 (42). Images were pre-processed by inputting the raw images to accomplish multiple functions, including: image geometry adjustments between structural and DT images, image registration, image denoising, and DT calculations.

For post-processing analyses, several MATLAB scripts were used to produce outcome variables for measures of diffusivity: mean diffusivity (MD; mm·s^{-2}) and fractional anisotropy (FA; arbitrary units). The MD was calculated using the equation:

$$MD = \frac{\lambda 1 + \lambda 2 + \lambda 3}{3} \qquad \textit{Equation 2}$$

While the FA value was calculated with the equation:

$$\sqrt{\frac{3}{2}} \sqrt{\frac{(\lambda 1 - \langle MD \rangle)^2 + (\lambda 2 - \langle MD \rangle)^2 + (\lambda 3 - \langle MD \rangle)^2}{\lambda 1^2 + \lambda 2^2 + \lambda 3^2}} \qquad \textit{Equation 3}$$

where MD = mean diffusivity; λ1, λ2, and λ3 are eigenvalues representing diffusion in each the x, y, and z directions; and the principal eigenvalue (λ1) represents the direction of greatest diffusion, which in muscle is the z direction (12). The secondary and tertiary

eigenvalues represent diffusion in whichever direction has the second and third most diffusion, respectively. Eigenvectors (ε) were produced in the diagonalization of the diffusion tensor matrix, and indicate the directions associated with λ1, λ2, and λ3 (43). Measures of muscle architecture were also calculated with fiber tractography, the outcome variables for these measures are: mean tract length (mm), mean curvature (m^{-1}), and mean pennation angle (degrees). As an exploratory analysis, variability in fascicle orientation (SD ε1) was also quantified using DTI to determine whether this measure provided any useful information about the muscle not captured by the other variables.

For all analyses, an ROI was drawn around the outside of the vastus lateralis of the dominant leg to form a mask for creating the muscle's border. Then, seed points were placed to define the aponeurosis of insertion, and to create a mesh from which the estimated fiber tracts can propagate. Fiber tracking was then performed using the 4^{th} order Runge-Kutta integration of the principal eigenvector (λ1) at a step size of ½ of a voxel width (0.5 mm). Fibers were tracked with the principal stopping criterion of exiting the drawn image mask. Additional criteria included an FA value between 0.05 and 0.4 and an inter-point angle of >25°.

The above criteria needed to fail to be met in order to terminate a tract. Fiber tracts were terminated using the two binary (BIN2) criteria. The "2" in BIN2 represents the two successive points for which the criteria muscle fail to be met with the determined step size (0.5 mm). Following the fiber tract, fibers were then smoothed so that the row, column and slice positions of the originally propagated fiber tracts could be fitted to 4th, 4th, and 3rd order polynomial functions as functions of fiber tract distance, respectively. Measurements of fiber tract length, curvature, and pennation angle for all tracts

containing more than five fiber-tracking points were then quantified. Finally, a last quality assurance check was performed on the data set by excluding fibers of <10 mm in length, greater than 40° in pennation angle, and greater than 40 m^{-1} in curvature. These thresholds were set manually by the investigators to ensure accuracy of fiber tract estimation. Fiber tracts were also excluded that differ from those of their 24 neighboring points by > 2 standard deviations. Figure 3.6 shows a completed analysis of fiber tract estimation.

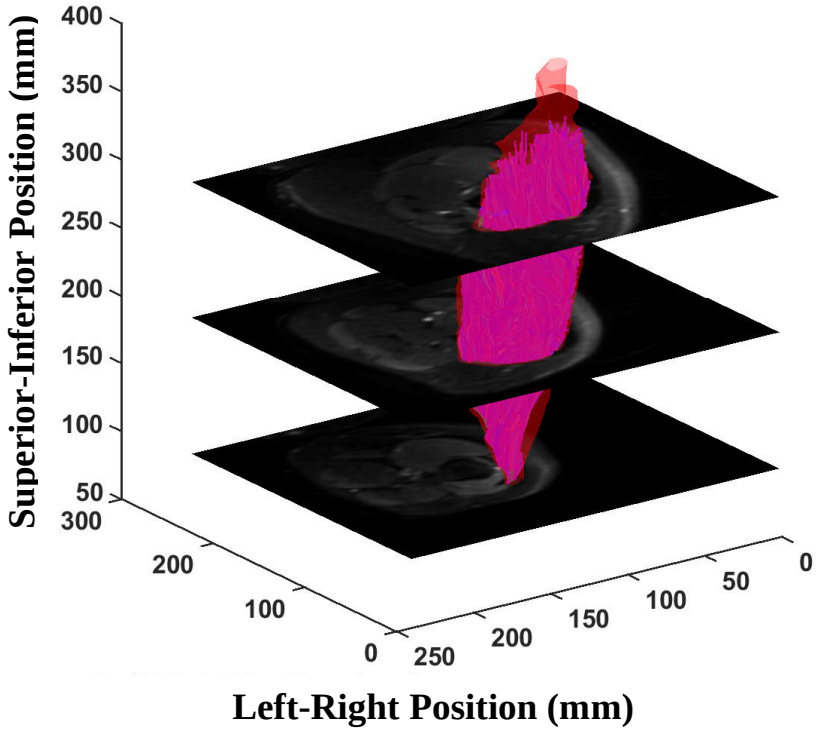

Figure 3.6. **DTI tractography of vastus lateralis**. The image depicts a representative image of fiber tracts for the vastus lateralis. These tracts are also utilized in for muscle architecture quantification.

in vitro Muscle Size and Composition: Single Fiber Measurements

Solutions

Dissection, skinning and storage solutions for muscle biopsy acquisition and storage as well as relaxing, pre-activating and activating solutions for mechanical analysis were as previously described (170). All solutions that were used for mechanical experiments had phosphate (P_i) levels set to 5 mM, which corresponds with resting Pi levels in human skeletal muscle (190), and were adjusted to an ionic strength of 175 mEq with sodium methane sulfate.

Muscle Biopsy & Storage Procedures

Percutaneous needle biopsies of the vastus lateralis muscle were performed in a subset of the participants (Study 1 and 3) under local lidocaine anesthesia and in the fasted state, as previously described (170). Muscle tissue was partitioned into samples for (1) single fiber mechanical and morphological analysis of chemically skinned fibers as well as for (2) fluorescent immunohistochemistry (IHC) and oil red o (ORO) staining on intact fibers. For chemically skinned fibers, tissue was immediately placed into a dissecting solution (4°C) for isolation of single muscle fiber bundles. Tissue was dissected into bundles of ~50 fibers, tied to glass rods at slightly stretched lengths, and placed in skinning solution for 24 hours (4°C). After skinning, bundles were placed into storage solution with increasing concentration of glycerol (10% v/v glycerol for 2 h, 25% glycerol for 2 h, 50% glycerol for 2 h) and then stored at -20°C until isolation of fibers for mechanical measurements within 4 wk of the biopsy procedure. For IHC and ORO analyses, muscle bundles were frozen in embedding medium (OCT; Sakura, Torrance, CA) in isopentane cooled with liquid N_2 and stored at -80°C until analyzed.

Single Muscle Fiber Composition Assessments

Fiber Type and Size Determination: Immunohistochemistry

Muscle fiber bundles were examined for determination of myosin heavy chain (MHC) composition with fluorescent immunohistochemistry (Study 3), as previously described (177) with slight modifications. Briefly, 6 μm thick cross-sections were incubated with primary and secondary antibodies, which fluoresced at different wavelengths for MHC I, IIA and IIX isoforms. These antibodies were then measured using a Keyence BZ-X800 microscope (Osaka, Japan) to produce blue, red, and green images that corresponded to the various MHC isoforms. The composite image was analyzed for each MHC isoform (I, I/IIA, IIA, IIAX and IIX) and fiber size using Image J software (NIH, Bethesda, MD, USA). A representative sample of these analyses is depicted in Figure 3.7.

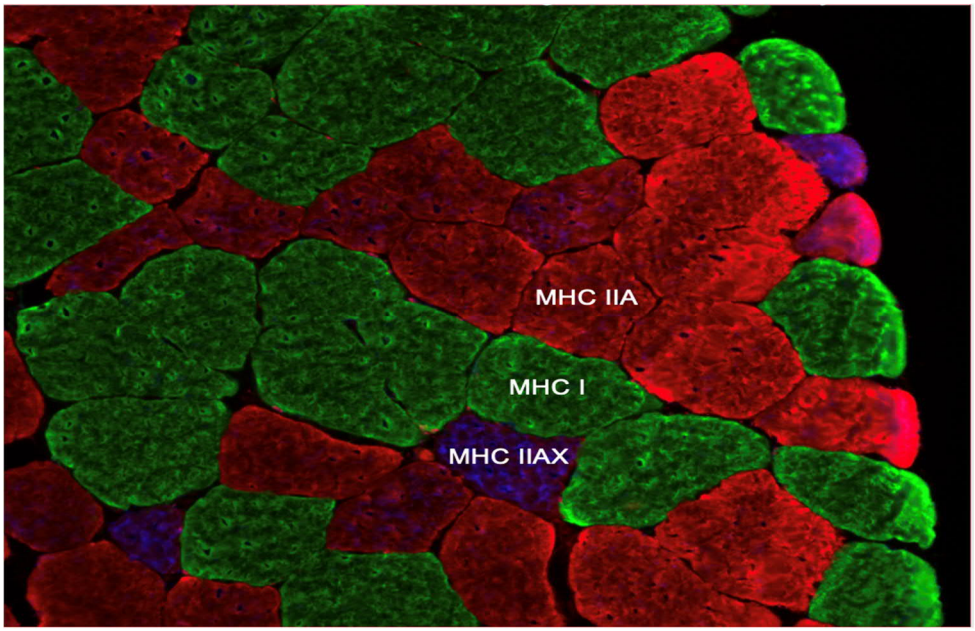

Figure 3.7. **Cross-section of single fiber bundle sample by immunohistochemistry**. Green areas depict MHC I fibers, red areas depict MHC IIA fibers, and the purple or red and blue overlay represents MHC IIAX fibers as labeled above. [Photo from Muscle Biology Laboratory with permission of Mark Miller]

Cellular Lipid Content Determination: Oil Red O (ORO) Staining

Muscle fiber bundles were examined for intramyocellular lipid (IMCL) content using ORO staining (Study 1 and 3), as previously described (128). After staining, 6 μm thick cross-sections were imaged using a Keyence BZ-X800 microscope and images for each fiber were analyzed for lipid droplet size (mm), area fraction occupied by lipid droplets (%), and number of droplets per area (#) using Fiji/ImageJ software (NIH, Bethesda, MD, USA). All collection and analyses of single muscle fiber compositional assessments will be conducted by trained individuals in the Muscle Biology Laboratory at the University of Massachusetts Amherst. These analyses are depicted in Figure 3.8

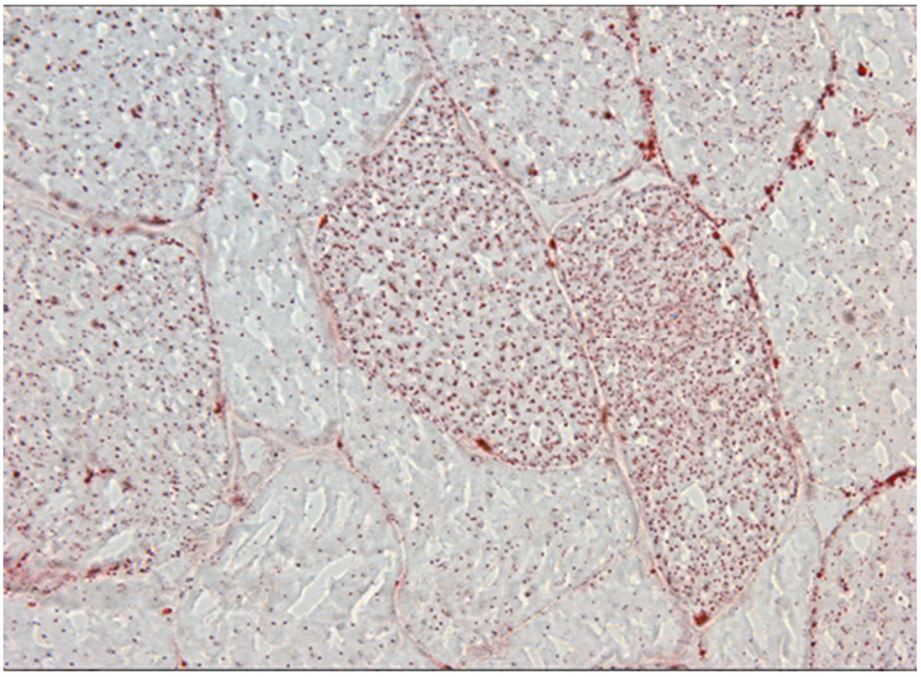

Figure 3.8. **Oil red o Staining of fiber bundle cross-section**. Red dots depict lipid droplets stained with red dye. [Photo from Muscle Biology Laboratory with permission of Mark Miller]

in vitro Single Fiber Function Assessment

Single Fiber Specific Tension Measurement

Single fibers were prepared for mechanical measurements and mounted on the experimental apparatus as previous described (170), except that bromophenol blue was used as an indicator dye instead of toluidine blue during the fixing of the ends of the fiber. Briefly, single fibers were placed in relaxing solution (15°C), and manually stretched to a sarcomere length of 2.65 μm as this resembles *in vivo* sarcomere length in human skeletal muscle (33). Sarcomere length was determined with a camera (Point Grey, FLIR Integrated Imaging Solutions, Inc., Richmond, BC, Canada) which was integrated with ImageJ software (NIH, Bethesda, MD, USA). Fibers were placed in pre-activating solution, moved to activating solution with force measured at its plateau, and placed back into relaxing solution. Initial activation was performed at 15°C, which improves fiber stability versus initial activation at 25°C. Temperature was then increased to 25°C, sarcomere length reset to 2.65 μm and cross-sectional area (CSA) determined by measuring fiber width on the apparatus' compound microscope. The height of fibers was estimated based upon the height-to-width ratio measured via microscope prior to mounting and presuming fiber CSA is elliptical. Fibers were placed in pre-activating solution, moved to activating solution with specific tension (mN/mm^2) measured at its plateau, sinusoidal analysis performed, and moved back into relaxing solution.

Molecular Kinetics Measurement

Myosin-actin cross-bridge kinetics and myofilament properties were derived using sinusoidal analysis, as previously described (170). Briefly, sinusoidal analysis was performed in activation solution at 25°C at the specific tension plateau by applying small-

amplitude, sinusoidal strain (normalized length, or length per change in length) to one end of the fiber at 48 frequencies from 0.125 to 200 Hz, while sinusoidal stress output (normalized force, or force per cross-sectional area) were measured at the other end of the fiber. The stress output was divided into its elastic and viscous components, then fit with a six-parameter equation to determine specific steps in the cross-bridge cycle, including myosin attachment time (t_{on}) and myosin attachment rate (s^{-1}). Other outcome variables were also be quantified that will not be included in this dissertation.

Myosin Heavy Chain Isoform Identification

After mechanical assessment, chemically skinned fibers were placed in gel loading buffer for determination of MHC isoform composition by SDS-PAGE to identify fiber type, as previously described (170).

All collection and analyses of *in vitro* single muscle fiber mechanics were conducted by trained individuals in the Muscle Biology Laboratory at the University of Massachusetts Amherst.

Statistical Analyses

For all analyses, data were tested for normality using the Shapiro-Wilk test prior to further analysis. All data are reported as mean ± standard deviation (SD) with the significance level set to $\alpha \leq 0.05$. Data was analyzed using SPSS software (SPSS, Inc., Chicago, IL, USA). For all data, precise p values and 95% confidence intervals for differences between means are given, as appropriate. Greater detail of statistical analyses are provided for each respective study (Chapters 4-6).

CHAPTER 4

STUDY 1: COMPARISONS OF HUMAN SKELETAL MUSCLE FAT CONTENT AT MULTIPLE ANATOMICAL SCALES

ABSTRACT

Fat content is widely used as a variable of interest in the assessment of skeletal muscle. However, agreement between many of the commonly-used and sensitive methods for intramuscular fat quantification has not been demonstrated. Therefore, it is not well known whether measures of intramuscular fat content are consistent across methods, scales, or populations. The purpose of this study was to test the agreement between *in vitro* and *in vivo* measures of intramyocellular lipid (IMCL) commonly used in the literature. Nineteen adults (31 ± 8 years; 11 female) were evaluated. IMCL was measured *in vitro* by oil red o (ORO) and *in vivo* by magnetic resonance spectroscopy (MRS) in the vastus lateralis, and FF of the entire quadriceps was measured with magnetic resonance imaging (MRI). IMCL/TCr was not associated with ORO lipid area fraction ($r=0.10$, $p=0.69$). Neither IMCL/TCr ($r=0.29$; $p=0.23$) nor ORO ($r=0.34$, $p=0.23$) had a relationship with quadriceps FF measured by MRI. However, both analysis methods by MRS were in strong agreement ($r=0.96$; $p<0.001$). Measures by MRS were more variable than ORO and FF, and the relative area of fat accumulation (i.e., area/fat signal fraction) was greater by MRI compared to ORO. Our findings indicate that measures of fat in the body or quadriceps muscle group do not reflect IMCL content. This supports previous findings that MRI represents fat from extracellular locations, and that younger adults do not store excess fat in intramyocellular locations.

INTRODUCTION

Biological fat or lipids have many forms and are known to affect many of the body's systems. The term "body fat" describes adipose tissue, which is composed of adipocytes, or fat cells. Triacylglycerols are located within these adipocytes, and they contain three fatty acids affixed to a glycerol backbone. There are fat depots in subcutaneous, visceral, cardiac, and intramuscular locations, therefore fat accumulation in these tissues has been of critical interest (29). Even in skeletal muscle there are different locations for fat storage: between muscles (intermuscular), within a single muscle (intramuscular), within a muscle cell (intramyocellular), and outside of a muscle cell (extramyocellular) (Figures 4.1-4.3). Particularly in research related to aging, obesity, and neuromuscular disease, fat content has been implicated as a contributor to muscle dysfunction (28, 154, 157). Over time, investigators have sought to elucidate the interplay between fat and metabolism, inflammation, and muscle force production; these studies have been undertaken in both humans (26, 36, 83) and animal models (7, 23, 206).

Despite the clinical and functional relevance of evaluating fat content in skeletal muscle, few comparisons have been made between some of the commonly-used methods (e.g., histochemical staining, magnetic resonance imaging, spectroscopy). These methods are sophisticated and sensitive with regard to data acquisition and processing. Fat content is also variable of interest in studies of aging (48, 157) and clinical populations (99, 202), such as in the assessment specific strength (strength per unit contractile area or volume). Values reported for fat content in ambulatory muscles have ranged from <10% percent in healthy adults to > 50% for individuals

with clinical pathology (69, 97). Both *in vitro* and *in vivo* techniques will continue to be employed for fat quantification due to differences in subject group, resource availability, and practical application. We do not know if results are consistent across methods, scales, or populations, therefore it is important to determine agreement between commonly used methods.

Histochemical staining (HCS) is used in research for *in vitro* quantification of fat for many reasons, including the precise location of intramyocellular (IMCL) and extramyocellular (EMCL) lipids, differentiation of fat content between muscle fiber types, and evaluation of lipid droplet number, area, and area occupied by lipids in the region of interest (e.g., lipid area fraction). Oil red o (ORO) is a well-known staining technique that uses a lysochrome solution to stain lipids on a biopsied section of muscle tissue (80). These cross-sections of stained tissue are then observed with a fluorescent microscope for identification of lipid size, number, and location, then quantified with computer software. While ORO is a robust measurement of IMCL, this technique has clear limitations. Muscle biopsy is an invasive procedure that may be contraindicated at any given time due to age, injury, or disease state, particularly if multiple biopsies are required for evaluation. The amount of tissue that is obtained is generally limited (on the order of μm), and the processing this muscle tissue is generally standardized to a particular area. Therefore, variations in fiber size may not be considered in analysis. Additionally, the results of one biopsy cannot be extended to all muscles involved in a particular function *in vivo* (e.g., metabolism, signaling, or force production).

To address some of these limitations, *in vivo* methods of fat quantification can be useful tools; one such method is proton magnetic resonance spectroscopy (^{1}H-MRS). Magnetic resonance spectroscopy exploits the differences in resonance frequencies of metabolites in various biochemical environments to quantify the relative concentrations of these metabolites in a tissue. Like HCS, this technique allows delineation of IMCL and EMCL, though these compounds cannot be distinguished between fiber type, and absolute quantification is challenging. Further, there is a noted inaccuracy of IMCL concentration in MRS quantification due to overlap between IMCL and EMCL in the spectra, and this method is susceptible fiber orientation (133, 245). Nonetheless, the noninvasive nature of MRS data collection compared with HCS is a great advantage, as is the relative ease of follow-up studies, and the ability to scan across multiple muscle groups.

Magnetic resonance imaging (MRI), and specifically fat-water Dixon techniques, can provide consistency and accuracy when quantifying fat content within muscle (86, 130). Investigators must consider that fat content values acquired by MRI represent the combined signals of all fat protons within the region of interest (ROI), and therefore cannot distinguish intracellular and extracellular compartments (25). That is, the fat fraction (FF) that is commonly used in Dixon imaging techniques to represent fat content is on the order of mm or cm in an MR image and primarily a result of EMCL signals that cannot be differentiated from IMCL (2). Additionally, measures of fat content by MRI are commonly acquired for a whole muscle, which may yield a different value than when evaluating fat in a smaller area such as when using *in vitro* techniques. Despite the differences in acquisition and

analysis, ORO, MRS, MRI, and other quantification methods are frequently used to characterize muscle quality and track progression, without careful consideration of the method type or scale being evaluated (222, 250). Measures of fat made by MRI have been compared to MRS and HCS, but notable gaps include lack of comparisons in skeletal muscle and for healthy adults (27, 135, 182, 218). Strengths and weaknesses of HCS, MRS, and MRI and other fat quantification methods in skeletal muscle have been reviewed previously (210).

Given this information, determining the agreement between these commonly used (but characteristically dissimilar) modalities is crucial. In principle, we presume both HCS and MRS estimate lipid content at the same scale, i.e., intracellular, and extracellular locations. Therefore, the first aim of this study was to determine the agreement between *in vitro* and *in vivo* measures of fat in the vastus lateralis muscle of healthy adults. Our first hypothesis was that there would be a positive relationship between IMCL by ORO (lipid area fraction, %) and IMCL by ^{1}H MRS (ratio of IMCL/TCr and IMCL/Water), due to the sampling location in the muscle belly for adults with modest levels of fat content. The second aim was to compare the IMCL measured by HCS and MRS with the FF of the quadriceps muscle group to determine the agreement about fat content on different scales. Our second hypothesis was that there would be a positive relationship between *in vitro* IMCL (lipid area fraction, %) and *in vivo* FF (%). Our third hypothesis was that there would be a positive relationship between *in vivo* IMCL (IMCL/TCr) and *in vivo* FF (%). This research will allow researchers to determine whether IMCL agrees

between *in vitro* and *in vivo* methods, and whether fat at the organ level reflects intracellular lipid content in young adults.

METHODS

Participants

Participants between 21-45 years of age were recruited to be relatively sedentary and free of cardiovascular, musculoskeletal, neurological, or metabolic disease. All participants had a body mass index (BMI) between 18.5-39.9 $kg \cdot m^{-2}$ and were not taking any medications known to affect physical or muscular function. Study procedures were approved by the Institutional Review Board at the University of Massachusetts Amherst (Appendices A-C). After determining eligibility and MR safety via telephone screening (Appendix D), all participants were scheduled for a visit to the Life Science Laboratories at the University of Massachusetts Amherst where they completed an informed consent, medical history (Appendix E), and MR safety questionnaire (Appendix F). Descriptive characteristics were recorded for all participants. Height and body mass were collected with a scale (SECA Model 769, Hamburg, Germany). The timeline of these events is listed in Figure 4.1.

Physical Activity Assessment

To account for potential influences of habitual physical activity (PA) on our outcomes, PA was measured for each participant using uniaxial GT1M accelerometers (ActiGraph, Pensacola, FL). Participants wore accelerometers on their right hip for at least 7 days prior to study selection, and maintained an activity diary during that period. Data were collected at 80 Hz and averaged over 60-s epochs. Daily activity counts (arb. units), MVPA (min) and wear time (hours) were

determined using ActiLife software (ActiGraph, Pensacola, FL). The first 7 valid (>10 hr wear time) days were analyzed for each participant. Standard cutpoints (232) were used to determine minutes of moderate-to-vigorous physical activity (MVPA), and wear time was calculated as described by Choi et al. (35). Physical activity logs were used to validate wear time, and exclude atypical days due to travel illness, etc. (Appendix H).

Muscle Biopsy Acquisition and Storage

Percutaneous needle biopsies of the vastus lateralis muscle were performed in a under local lidocaine anesthesia and in the fasted state, as previously described (170). Muscle tissue was partitioned into samples for oil red o (ORO) staining on intact fibers. For ORO analyses, muscle bundles were frozen in embedding medium (OCT; Sakura, Torrance, CA) in isopentane cooled with liquid N_2 and stored at -80°C until analyzed.

In vitro Cellular Lipid Content Determination: ORO

Muscle fiber bundles were examined for IMCL content using ORO staining, as previously described (128). After staining, 6 µm thick cross-sections were imaged using a Keyence BZ-X800 microscope, and images for each fiber were analyzed for lipid area fraction occupied by lipid droplets (%) using Fiji/ImageJ software (NIH, Bethesda, MD, USA). Figure 4.2 depicts a representative sample of ORO staining.

In vivo Cellular Lipid Content Determination: ^{1}H-MRS

Proton magnetic resonance spectroscopy (MRS) was used to provide a noninvasive measure of intramyocellular lipid (IMCL) content (19). Scans were

performed using a Skyra 3T scanner, 70-cm bore MR system (Siemens Healthcare, Erlangen, Germany) running on VE11C platform. The same MR system was used for all MRS and MRI measures. Participants were positioned supine on the exam table with feet oriented towards the scanner. Gradient-echo scout images were used to confirm optimal leg positioning in the isocenter and correct coil positioning over the muscle belly at a location similar to that of the muscle biopsy. Serial images of the dominant thigh were acquired in all participants from the lateral epicondyle of the femur to the greater trochanter of the hip. Localized spectra were acquired from the vastus lateralis using a dual-tuned $^{31}P/^{1}H$ circular surface coils (8cm/10.5 cm; Stark Contrast, Erlangen, Germany) placed over the belly of the muscle. Gradient-echo scout images were used to confirm optimal leg positioning in the isocenter and correct coil positioning over the muscle. A point-resolved spectroscopy sequence (PRESS) was used to acquire a single voxel positioned in the vastus lateralis muscle (Figure 4.3). and the following parameters: Repetition time/echo time = 2000/30 ms, 128 averages for water suppression and one average for non-water suppression, voxel size = 8 cm^3, complex points = 2048, bandwidth = 2000Hz, and acquisition time = 4:34 min. The coil was secured to the thigh using inelastic straps.

To calculate the relative concentration of muscle metabolites in the region of IMCL, spectral analysis was completed using jMRUI v6.0beta (Leuven, Belgium) (179). Water-suppressed free induction decays were individually zero-filled (2,048 points), apodized (1 Hz Lorentzian filter), and converted into the frequency domain via Fourier transform. The zero-order phase was manually adjusted to create a level baseline throughout each spectrum. Visual identification of the creatine peak was

then used to set the reference frequency at 3.02 parts per million (ppm). Prior knowledge files were also applied for peak identification. The AMARES algorithm was used to line-fit following peaks using a Lorentzian line shape: IMCL CH_3 (IMCL) at 1.28 ppm, extramyocellular lipid CH_2 (EMCL) at 1.49 ppm, and creatine CH_3 (Cr) at 3.02 ppm (Figure 4.4). Other visible peaks, along with a baseline correction, were also fit to ensure accuracy in the fitting of adjacent peaks. Non-water suppressed data were analyzed in the same manner for the quantification of water concentration, with the only differences being that the water peak at 4.65 ppm was used to set the reference frequency and was the lone peak fit using separate prior knowledge files. The area of each peak represents the relative concentration of that metabolite. Ratios between relative concentrations of IMCL and total creatine (TCr) as well as water (i.e., IMCL/TCr; IMCL/W) were calculated (245); these measures rely on the assumption that both creatine and water concentrations are similar among the study participants. The average full width at half maximum for the water peak was reported to provide a quantitative measure of the resolution or precision of each acquisition. The full width at half maximum for all MRS data was reported, and a value under 30 was considered a valid acquisition for our data.

In vivo Intramuscular Fat Content Determination: 6-point Dixon MRI

Next, images of the dominant thigh were acquired using an 18-channel phased array coil combined with a spine coil built into the exam table, with participants positioned as described above for MRS acquisition. A six-point Dixon technique was applied to generate water- (W) and fat- (F) only images using a 2D gradient echo sequence (73). Parameters were as follows: image resolution (1.25 x 1.25 x 5

mm^3), TR = 35 ms; slice thickness = 5 mm; 24 slices, FOV = 240 x 240 mm^2; TE =2.46, 6.15; 3.69, 7.38; 4.92, 8.61 ms; matrix = 192×192 mm^2; GRAPPA factor = 2; flip angle = 15°, bandwidth = 1090 Hz/pixel, 1 average, and acquisition time = 12 min.

Water and fat images were reconstructed offline using the MATLAB Fatty Riot algorithm (219). Methods for calculation of muscle fat-free cross-sectional area (mCSA), muscle volume, and FF (%) began with identifying and recording the slice in which the anatomical landmarks for the femur (first appearance of lateral epicondyle and greater trochanter) were located. Then, all slices in which all four quadriceps muscles were visible were identified, and a single region of interest (ROI) was drawn around the entire quadriceps muscle group in each of these slices. Subcutaneous fat, bone, and regions of intermuscular fat or connective tissue were excluded as much as possible when drawing each ROI. Mean FF was calculated on a pixel-by-pixel basis as:

$$FF = 100\% * F/(W + F) \qquad \textit{Equation 4}$$

where W is the water signal intensity and F is the fat signal intensity. Fat signal fraction, referred to as fat fraction was calculated as an average of the values for each ROI. Additionally, coefficients of variation were calculated for these variables with the equation:

$$\text{CoV} = (\text{SD}/\text{mean}) * 100 \qquad \textit{Equation 5}$$

where CoV is the coefficient of variation, SD is the standard deviation of all values.

Statistical Analyses

All data were tested for normality using the Shapiro-Wilk test prior to further analysis. All data are reported as mean ± standard deviation (SD) with the significance level set to $\alpha \leq 0.05$. All hypotheses were tested using Pearson correlations.

RESULTS

Descriptive data for the 19 participants are displayed in Table 4.1. Fat content by ORO, MRS, and MRI analyses are summarized in Figure 4.6. Values for lipid area fraction by ORO were 2.16 ± 0.69%, for IMCL/TCr by MRS were 4.63 ± 3.95, for IMCL/W by MRS were 0.017 ± 0.019, and for FF by Dixon were 7.77 ± 1.06%. Single fiber lipid content (%) by ORO was lower than FF (%) by MRI ($p<0.001$) (Figure 4.6). Associations between measures of fat content by ORO, MRS, and MRI are shown in Figure 4.7. The coefficient of variation for lipid area fraction by ORO was 32.04%, for IMCL/TCr by MRS as 85%, for IMCL/W by MRS was 114%, and for FF by Dixon was 14%. The full width at half maximum for all MRS data was 14.1 ± 2.1.

DISCUSSION

In this study we evaluated fat content in the quadriceps femoris to determine the agreement between three distinct and sophisticated acquisition methods: histochemical staining, proton magnetic resonance spectroscopy, and magnetic resonance fat-water imaging. In our sample of young adults with moderate physical activity levels and modest amounts of intramuscular fat, there was no association between fat content measured by ORO, MRS, and MRI. These results were

acquired across a large range of BMI's, suggesting that fat content at the whole body or whole muscle level does not reflect lipid content within muscle. These results also indicate that accumulation of IMCL and EMCL are under separate control for utilization, since lipid levels within the cell remain relatively low when compared to organ and organism level.

Relationships Between in vitro and in vivo Lipid Content

In contrast to our hypothesis, measures of IMCL by MRS showed no association with measures of IMCL by ORO. The ORO and MRS procedures are characteristically dissimilar in how they achieve their values, however both modalities are routinely utilized to determine IMCL concentrations. One method is *in vitro* while the other is *in vivo*, but the presence of EMCL can bias the results for MRS acquisitions as well.

Notably, the two normalization methods for IMCL measured by MRS had strong agreement (Table 4.2). This result suggests that investigators may choose to normalize to TCr or water depending on their sample. For example, normalizing to TCr may be useful in subjects with edema, because the greater water concentrations may artificially skew the IMCL to water ratios. So, knowing both methods are in strong agreement is useful so either method can be used when appropriate. Many investigations have compared MRI and histological methods of hepatic lipid quantification (51, 117, 135, 183), however, there are less studies comparing the agreement of lipid content in muscle. Our findings highlight the need for comparison of different methods for IMCL quantification in multiple study groups, because distribution can be different among populations (e.g., younger adults,

elderly, musculoskeletal disorders). Unlike the liver, skeletal muscle has greater variation in lipid content between locations (i.e., muscles) in healthy adults due to factors such as differences in fiber type (108, 253). We are aware of three investigations that have compared the IMCL in human skeletal muscle between *in vitro* and *in vivo* techniques, all of which included trained endurance athletes (46, 102, 237). Two of these studies evaluated the breakdown of IMCL before and after a 2- or 3-hour cycling bout (46, 237). These studies illustrate how acquisition and analysis methods may change the interpretation of results, even among a limited number of homogenous subjects. Still, these two studies suggested that variations in biopsies, sampling area, and analysis procedures are some of the factors that would affect the interpretation of the role of IMCL pools during a bout of aerobic exercise. In contrast to our findings, studies found modest associations between ORO and MRS in the vastus lateralis ($r = \sim 0.48$) and biochemical assay was acknowledged as the method with the lowest agreement when compared to all other methods evaluated (e.g., electron microscopy, biochemical assay, ORO, MRS). It was also noted that the agreement should have been greater than what was reported between *in vitro* and *in vivo* assessments, because both methods should ostensibly measure the same molecule at the same level in the same subjects.

Relationship between Lipid content in vitro and in vivo Compared to Fat Fraction

In contrast to our hypothesis, measures of IMCL by MRS and ORO were not associated with measures of FF by MRI. This is a considerable finding, with work by Gaeta and colleagues specifically noting that the lack of comparison between MRI techniques and MRS or muscle biopsy is a limitation to clarifying the

relationship between fat accumulation and disease severity (69). Our results show that one must compare measures of fat content and function at the same anatomical scale (e.g., organ, organism level) to increase the chance of drawing the most accurate conclusions about their relationship.

The IMCL lipid area fraction by ORO was almost 4 times greater than FF analyzed by MRI in our study (Figure 4.4). This is to be expected, as the MRI values include fat content that is both inside of and outside of the muscle cell. Studies reporting muscular measures of fat content by MRI are more common than those by HCS or MRS, however it is important to consider that MRI values primarily represent EMCL signals at the fascicular level (2). Regardless of the imaging sequence employed (e.g., T1-weighted, Dixon), fat quantification by MRI occurs on a larger scale than that of HCS or MRS, and cannot presently resolve lipids between intracellular and extracellular compartments. There have also been more comparisons of muscle fat content between *in vivo* techniques than there has been between *in vivo* to *in vitro* methods (57, 172, 185, 231) . This is due in large part to the invasive nature of the latter. Previous studies from our lab have evaluated the fat content in each quadriceps muscle and determined the vastus lateralis to have the lowest level of fat in the muscle group, with a mean FF of 6.5% (unpublished observations). Taken together, it is not surprising that relative fat content measured by MRI was greater than single fiber IMCL analyses, due to the greater amount of EMCL compared to IMCL in the MR signal (Figure 4.4).

Role of Physical Activity in Fat Assessment

Past investigations have suggested that physical activity may play a role in accumulation of intramuscular fat in some groups (123). Notably, the fat content of the quadriceps muscles was 2 to 3-fold greater in our study than young adults in other studies, (49, 97). The absence of physical activity reporting in the literature and the greater BMI of our study group may be two additional factors which contributed to our findings. In studies with heterogeneous groups or those with known levels of high fat infiltration, physical activity should be measured to explain variations between methods, as in the case of high IMCL content in well trained endurance runners (76). In otherwise healthy but obese groups, subjects may have relatively low levels of IMCL when assessed by *in vitro* methods and relatively high levels of FF when assessed by MRI due to the fact that MRI measures primarily represent fat from extracellular deposits, namely intra- and inter-muscular fat. The larger range in BMI but relatively low IMCL values by ORO in our sample also suggests that younger adults do not store excess fat within intramyocellular locations.

Limitations

There were some limitations in our study, including the assessment of both fiber types in the evaluation of IMCL by ORO. Figure 4.2 clearly depicts the known difference in fat infiltration between fiber types, and the analysis of the entire cross-section may have washed out similarities or differences between methods in this muscle group. Subjects with greater amounts of EMCL may also have erroneously conflated both IMCL and EMCL lipid pools. Low agreement between the studied

methods could have occurred due to introduced biases from any of these limitations. Another limitation was the comparison of two IMCL measures in the vastus lateralis to a measures of fat content in the quadriceps muscle group (FF). A measure of FF in just the VL would have been more appropriate, however this comparison was included as all three methods used in this study are frequently used to characterized muscle fat content.

Conclusion

In summary, there was no agreement of fat content measurement by ORO, MRS, and MRI. Based on these results, investigators can expect less variability in IMCL measurement via ORO analyses when compared to MRS. Additionally, MRS showed more variability when compared to ORO and MRI, though both MRS methods agreed with one another. Previous studies that have reviewed lipid quantification in MRS have not made recommendations on whether to normalize to TCr or water content. Our results suggest that future research can to normalize to TCr or water content, provided there are not large differences in water content as a result of edema within the sample. These data, in conjunction with previous reviews of different quantification methods (210) can be used to ensure proper method use for subject group and accurate interpretation of data between modality or muscle group.

Acknowledgements

The authors thank Nicholas Remillard, M.S., Luke Arieta, M.A., Christopher Hayden, M.S., Phillip Woods, M.S., Brent Momb, M.S., Shayelia Stanley B.S., Aurora Foster, M.S., Stuart Chipkin, M.D., and Elena Bliss, MRT, for their help on various parts of this study. We also thank all of the individuals who volunteered to participate in this research.

Funding

This research was funded by NIH: NIAMS R21 AR073511 and NIH/NIAMS R01 AR073831

Table 4.1. Participant characteristics

Variable	n=19 (11 female)
Age (years)	31 ± 8 (21 – 45)
Height (cm)	172 ± 10 (158 – 191)
Body Mass Index ($kg \cdot m^{-2}$)	29.2 ± 5.3 (18.9 – 39.9)
Physical Activity ($counts \cdot day^{-1}/1000$)	287 ± 121 (42 - 549)
Daily Moderate-Vigorous Physical Activity (min)	42 ± 22 (4 – 96)

Data are mean ± SD. Range noted in parentheses.

Table 4.2. Comparisons of fat content between modalities

		^{1}H-MRS, IMCL/TCr	^{1}H-MRS, IMCL/Water	MRI, Fat Fraction (%)
vs. Lipid Area Fraction		r=0.10, p=0.69	r=0.10, p=0.68	r=0.34, p=0.23
vs. IMCL/TCr			r=0.96, p<0.001	r=0.29, p=0.23
vs. IMCL/Water				r=0.27, p=0.26

Pearson correlation coefficients and p values for each comparison. Lipid area fraction= relative area occupied by fat droplets in single fiber cross-section (%). ORO= Oil Red O; ^{1}H-MRS= proton magnetic resonance spectroscopy; IMCL= intramyocellular lipid; TCr= total creatine; MRI= magnetic resonance imaging

Figure 4.1. Timeline of study events. Chronological timeline of events between study days and data collection order.

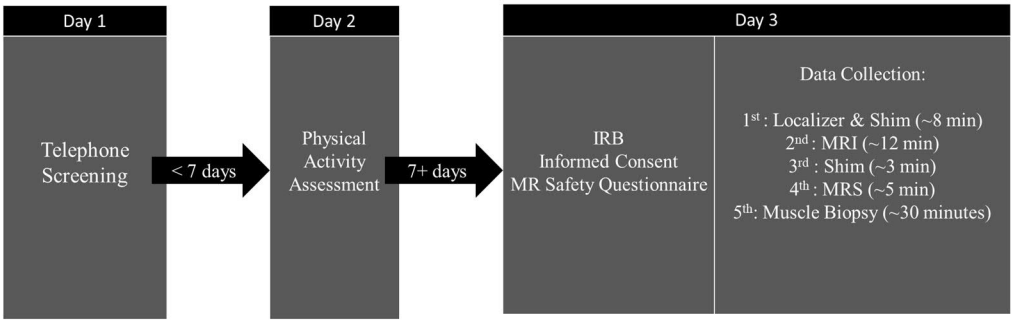

Figure 4.2. Oil red o staining of fiber bundle cross-section. Red dots depict lipid droplets stained with red dye.

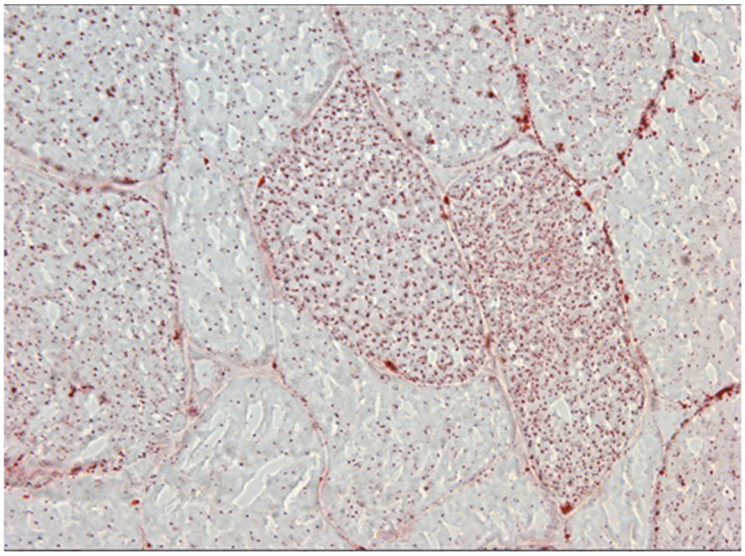

Figure 4.3. ^{1}H-MRS voxel placement. The top panel depicts the area of acquisition for ^{1}H-MRS in the vastus lateralis. The bottom panel depicts a representative spectrum for identifying the methyl and methylene peaks of IMCL (point 1 and 2, respectively) and EMCL (points 3 and 4, respectively)

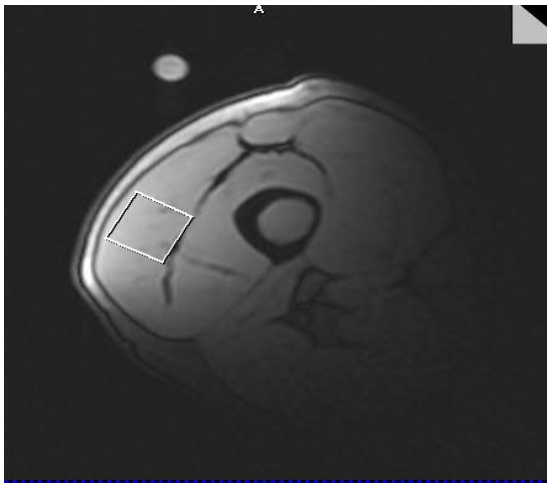

Figure 4.4.^{1}H-MRS analysis using jMRUI. The top panel depicts a representative spectrum for identifying the methyl and methylene peaks of IMCL (point 1 and 3, respectively) and EMCL (points 2 and 4, respectively). The bottom panel depicts a fit of the IMCL and EMCL peaks.

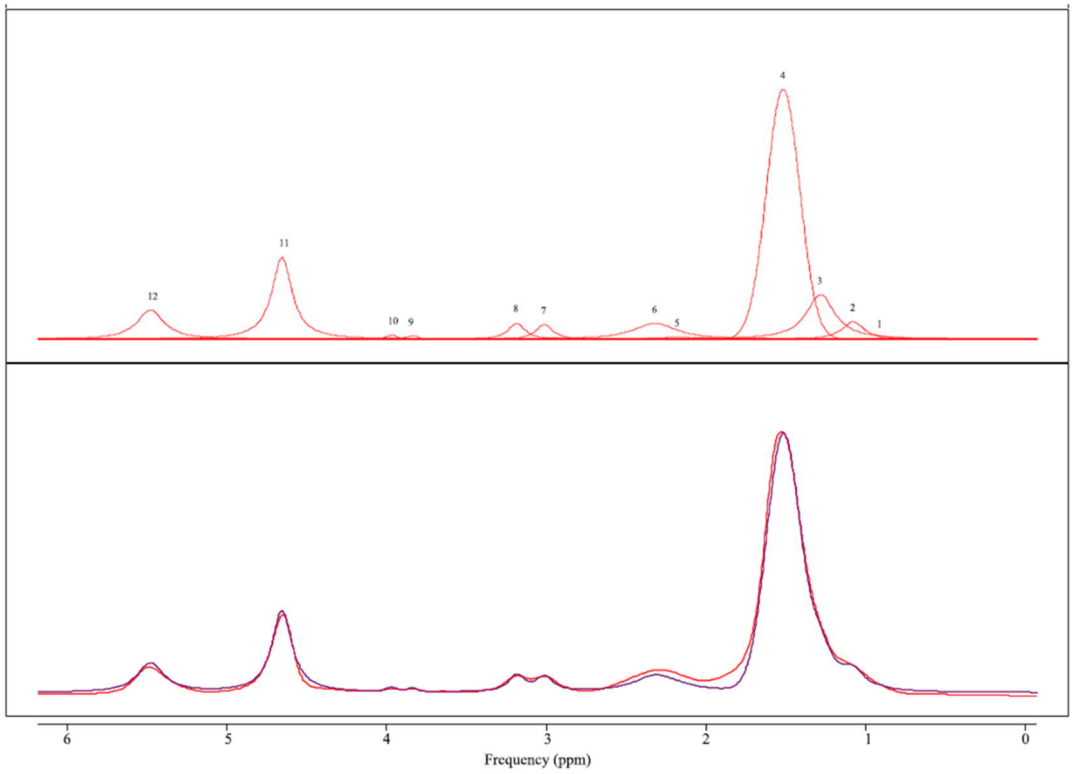

Figure 4.5. MRI region of interest for fat fraction analysis. Represents a single axial image of a participant with region of interest (red).

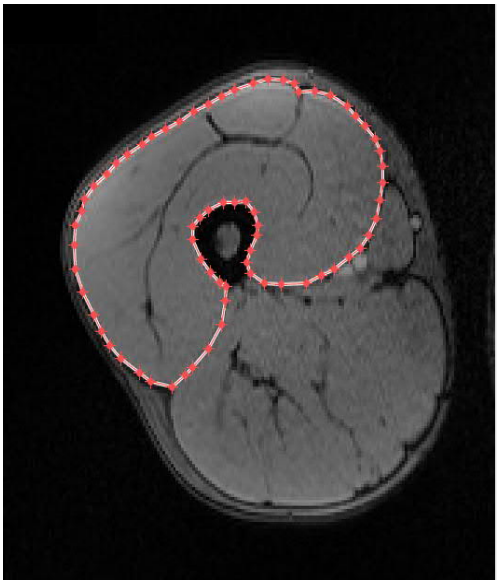

Figure 4.6. **Individual measures of fat content by various methods.** Lipid area fraction= % area occupied by fat droplets in single fiber cross-sections; fat fraction= % fat in quadriceps muscles; IMCL/TCr= Ratio of intramyocellular lipid to total creatine; Left axis for ORO and MRI columns; right axis for ^{1}H-MRS column. Red lines and data points represent the mean of all data.

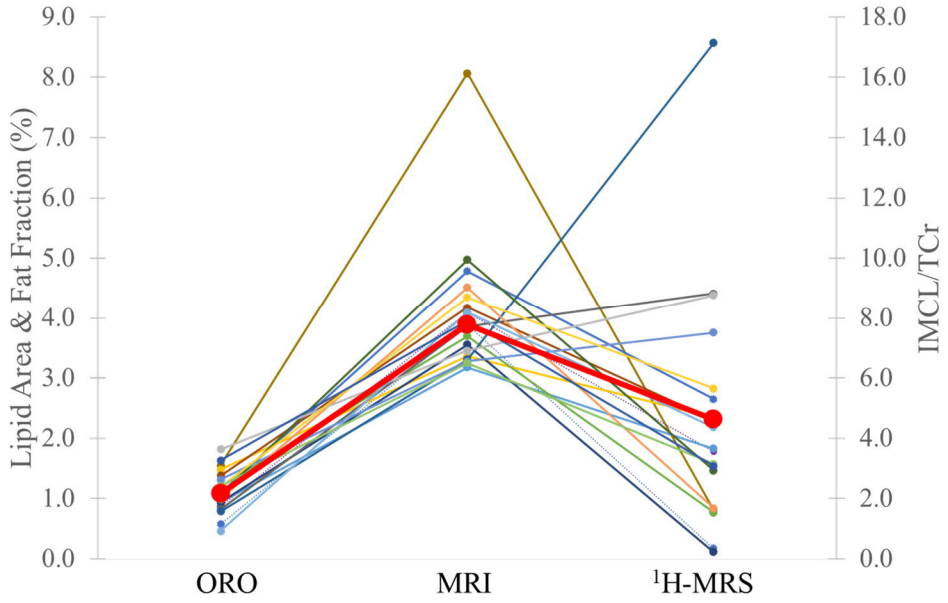

Figure 4.7. Associations between methods of fat content measurement. Lipid area fraction= relative area occupied by fat droplets in cross-section; IMCL/TCr= Ratio of intramyocellular lipid to total creatine; IMCL/W= Ratio of intramyocellular lipid to Water; Fat fraction= relative fat to water signal in quadriceps region of interest.

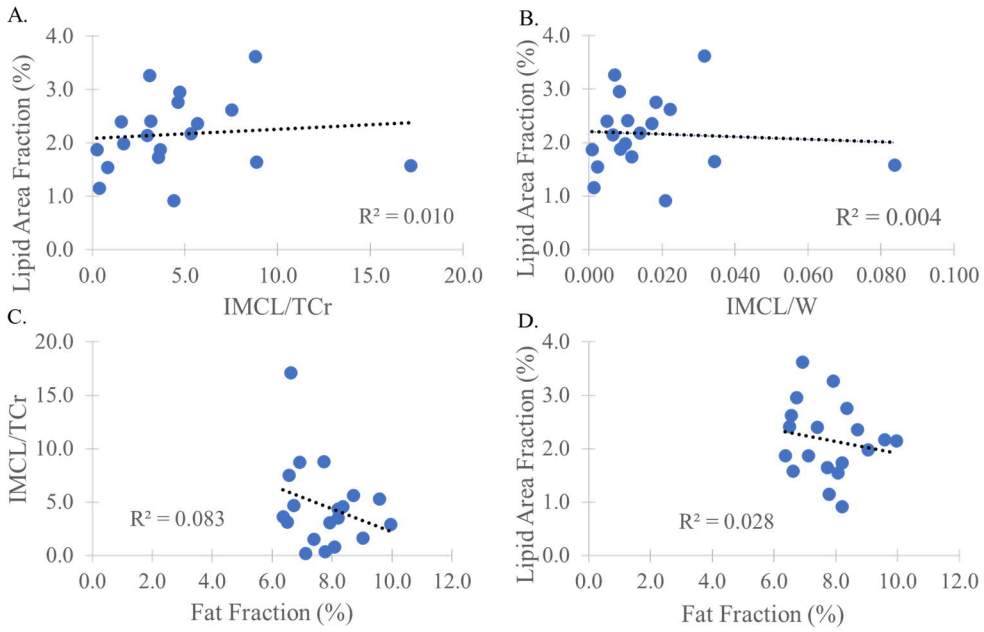

CHAPTER 5

STUDY 2: MECHANICAL CONTRIBUTIONS OF FAT CONTENT TO MUSCLE STRUCTURE AND FUNCTION IN VIVO

ABSTRACT

Muscle size does not fully explain variations in muscle strength (i.e., the ability to generate maximal force). Muscle size, fat content, and architecture have all been independently associated with muscle function. However, there have been few studies that have evaluated these components in the same study cohort. Diffusion tensor imaging (DTI) allows three-dimensional evaluation of whole muscle, and provides data for architectural assessment that is not provided by conventional imaging techniques. The purpose of this study was to determine the relationships between muscle fat fraction (FF), architecture and function. Due to the limited data in the literature, diffusive variables and the effect of sex were also investigated. Forty healthy adults (30 ± 7 years; 21 female) were evaluated by Dixon imaging, DTI, and isokinetic dynamometry to determine the relationships between FF and measures of architecture (tract length, curvature, pennation angle), function (maximal isometric and isokinetic torque, peak contraction velocity) and diffusion (mean diffusivity, MD; fractional anisotropy, FA) of the quadriceps femoris muscles. Fat fraction was related to tract length (r^2=0.11 p=0.05), but not to any measures of diffusion or muscle function (r^2<0.03, p>0.32). mCSA was associated with isometric (r^2=0.86 p<0.001) and isokinetic torque (r^2=0.86 p<0.001). Muscle volume was also associated with isometric (r^2=0.75 p<0.001) and isokinetic torque (r^2=0.72 p<0.001). When used as a base model in multiple regression analyses, and Males had greater fat-free muscle cross sectional area (mCSA) (82.8 ± 12.7 vs. 53.1 ± 9.6 cm^2), muscle volume (1393 ± 336 vs. 795 ± 158 cm^3), tract length (74.2 ± 11.9 vs. 65.1 ± 12.8 mm), isometric torque (275 ± 66 vs. 157 ± 32 Nm) and isokinetic

torque (163 ± 36 vs. 94 ± 21 Nm) than females. Our findings suggest that fat content is related to fascicle length, but does not impair muscle function in young adults.

INTRODUCTION

The etiology of skeletal muscle weakness is multifaceted. Muscle size (i.e., mass, cross-sectional area, volume) is the primary predictor of strength at the organ level (161, 207). Muscle strength is the ability to generate maximal force, and is a critical component in completion of physical tasks. However, differences in muscle size are not proportional to the differences in muscle strength due to aging, training, or neuromuscular disease (91, 104, 112, 201); this indicates that there are additional contributors to muscle weaknesses other than size. It is well known that composition (i.e., proportion of contractile and non-contractile components) and architecture play significant roles in the force production capabilities of muscle (39, 147). Muscle architecture is defined as the arrangement of muscle fibers relative to the axis of force generation (145). Both composition and architecture are two integral components that make up the highly organized structure of skeletal muscle, however nearly all estimations of their combined effect on muscle function have been drawn through independent investigations of either component. Neural factors will also influence voluntary strength, namely through recruitment and rate coding (15, 174). However, this relationship is outside the scope of our study, the focus of which is the contribution of composition and architecture to mechanical muscle function.

Non-contractile components can be defined as any structures in muscle that do not actively produce force, such as fat or connective tissue (123). Fat content has been researched extensively for its metabolic and immunological effects on muscle (38, 106). Additionally, fat has been implicated in the impairment of force production, and studies have indicated that fat may directly affect muscle strength (13, 48).

More research is needed to clarify the potential effects of fat content on the disorganization of muscle structure or disruption of muscle force, separate from the effects of aging or pathology. Elucidating the relationships between fat content, architecture, and strength can provide researchers, physicians, and practitioners with more information about the factors other than size that contribute to muscle strength.

There are several ways to measure skeletal muscle composition *in vivo*, including ultrasound, bioelectrical impedance, computed tomography, and dual x-ray absorptiometry. However, magnetic resonance imaging (MRI) is commonly referred to as the gold standard for assessment of soft tissues, due to the absence of ionizing radiation, high resolution of tissue compartments, and large field of view, among other advantages (55, 152, 194). Fat-water imaging, specifically Dixon techniques, give investigators the ability to reliably quantify tissues on a pixel-by-pixel basis, allowing for accurate evaluation of muscle and fat content in skeletal muscle (50, 73, 85). Additionally, Dixon imaging can be combined with other MR techniques and sequences such as magnetic resonance spectroscopy (MRS) or diffusion tensor imaging (DTI) to provide a more complete appraisal of muscle. Muscle architecture is commonly measured by B-mode ultrasound due to its low cost and ease of use (61, 147, 180). Still, DTI remains the only technique capable of 3D assessment of architecture along the length of a muscle *in vivo*, as noted by Franchi and colleagues (61). Diffusion tensor imaging exploits the diffusive properties of water to quantify the magnitude and the isotropic properties of water within the muscle via the apparent diffusion coefficient, also known as mean diffusivity (MD), and fractional anisotropy (FA), respectively (12). The MD and FA can then be used to estimate

the orientation of muscle fascicles and determine architectural properties of muscle in a method called fiber tractography (41). Comprehensive reviews of DTI applications can be found elsewhere (43, 115, 188, 220).

Studies have suggested that there may be subtle changes that occur in muscle that precede the atrophy of contractile tissue or impairment of functional performance, (127, 139). In addition to the advantage of measuring muscle architecture in superficial and deep compartments, DTI also quantifies variables that other techniques are not able to produce, such as diffusion, muscle curvature, and variability in fascicle orientation. These variables may provide novel insight into the structure-function relationship that is not understood from studies using standard imaging techniques.

Given these gaps in the literature, the first aim of this study was to use Dixon and DTI to determine the degree to which fat content may affect muscle architecture. It has been suggested that accuracy in detection of muscle weakness for functional tasks is increased when strength is measured at movement speeds that resemble day-to-day activities (52, 246). Therefore, we will evaluate the relationship between fat content and muscle torque using both isometric and dynamic contractions. We quantified the relationships between fat fraction (FF, %) and pennation angle (°), tract length (mm), and muscle curvature (m^{-1}). Our first hypothesis was that FF would have a relationship with pennation angle (°), tract length (mm), and muscle curvature (m^{-1}), potentially due to a fat-induced disorganization of muscle structures. We also quantified the relationship between FF and maximal isometric (Nm) as well as isokinetic torque (Nm). Our second hypothesis was that FF would have no

relationship with maximal isometric or isokinetic muscle strength (Nm), due to the modest levels of fat content in the sample of young adults. The effects of biological sex were evaluated in all analyses. The results of this study extend our knowledge regarding the relationship between fat content and muscle architecture as well as muscle strength *in vivo* by combining techniques and providing new information about muscle structure. This information can then be used to interpret the findings of studies which have reported differences in muscle quality (force/cm^2) (60, 149), by identifying the key determinants of force production, and the role of fat content in this process.

METHODS

Participants

Participants between 21-45 years of age were recruited to be relatively sedentary and free of cardiovascular, musculoskeletal, neurological, or metabolic disease. All participants had a body mass index (BMI) between 18.5-39.9 $kg \cdot m^{-2}$ and were not taking any medications known to affect physical or muscular function. Study procedures were approved by the Institutional Review Board at the University of Massachusetts Amherst (Appendices A-C). After determining eligibility and MR safety via telephone screening (Appendix D), all participants were scheduled for a visit to the Life Science Laboratories at the University of Massachusetts Amherst where they completed an informed consent, medical history (Appendix E), and MR safety questionnaire (Appendix F). Descriptive characteristics were recorded for all participants. Height and body mass were collected with a scale (SECA Model 769, Hamburg, Germany). Data from thirteen of the participants from Study 1 were

integrated into this data set with the addition of their architecture, diffusion, and muscle strength data. The timeline of these events is listed in Figure 5.1.

Physical Activity Assessment

To account for potential influences of habitual physical activity (PA) on our outcomes, PA was measured for each participant using uniaxial GT1M accelerometers (ActiGraph, Pensacola, FL). Participants wore accelerometers on their right hip for at least 7 days prior to study selection, and maintained an activity diary during that period. Data were collected at 80 Hz and averaged over 60-s epochs. Daily activity counts (arb. units), MVPA (min) and wear time (hours) were determined using ActiLife software (ActiGraph, Pensacola, FL). The first 7 valid (>10 hr wear time) days were analyzed for each participant. Standard cutpoints (232) were used to determine minutes of moderate-to-vigorous physical activity (MVPA), and wear time was calculated as described by Choi et al. (35). Physical activity logs were used to validate wear time, and exclude atypical days due to travel illness, etc. (Appendix H).

Muscle Composition Measurement: 6-point Dixon MRI

Scans for all participants were performed using a Skyra 3T scanner, 70-cm bore MR system (Siemens Healthcare, Erlangen, Germany) running on VE11C platform. Participants were positioned supine on the exam table with feet oriented towards the scanner. Gradient-echo scout images were used to confirm optimal leg positioning in the isocenter and correct coil positioning over the muscle. Serial images of the dominant thigh were acquired in all participants from the lateral epicondyle of the

femur to the greater trochanter of the hip. Images were acquired using an 18-channel phased array coil combined with a spine coil built into the exam table. To limit movement, the coil was secured to the thigh using inelastic straps. A 6-point Dixon technique was applied to generate water- (W) and fat- (F) only images using a 2D gradient echo sequence (73). Parameters were as follows: image resolution (1.25 x 1.25 x 5 mm^3), TR = 35 ms; slice thickness = 5 mm; 24 slices, FOV = 240 x 240 mm^2; TE = 2.46, 6.15; 3.69, 7.38; 4.92, 8.61 ms; matrix = 192×192 mm^2; GRAPPA factor = 2; flip angle = 15°, bandwidth = 1090 Hz/pixel, 1 average, and acquisition time = ~12 min.

Water and fat images were reconstructed offline using the MATLAB Fatty Riot algorithm (219). Methods for calculation of muscle fat-free cross-sectional area (mCSA), muscle volume, and fat fraction (FF, %) began with identifying and recording the anatomical landmarks for the femur (lateral epicondyle and greater trochanter). Then, all slices in which all four quadriceps muscles are visible were identified, and a single region of interest (ROI) was drawn around the entire quadriceps muscle group in each slice. Subcutaneous fat, bone, and regions of intermuscular fat or connective tissue were excluded as much as possible when drawing each ROI. Mean FF was calculated on a pixel-by-pixel basis as:

$$FF = 100\% * F/(W + F) \qquad \textit{Equation 6}$$

Where W is the water signal intensity and F is the fat signal intensity. Fat signal fraction, referred to as fat fraction was calculated as an average of the values for

each ROI. Fat-free muscle CSA (cm^2) for each ROI was calculated as total area for the ROI minus the fat area. The mCSA reported in this study represents the peak mCSA from all axial images for each participant. Muscle volume (cm^3) of the quadriceps was calculated as the sum of all mCSAs from the analyzed slices multiplied by the slice thickness.

Muscle Diffusion & Architecture Measurements: DTI

Following the 6-point Dixon imagine sequence, DTIs were acquired using a spin-echo echo-planar imaging (EPI) sequence with 12 gradient directions. Four stacks were acquired from the lateral epicondyle of the femur to the greater trochanter of the hip, as previously described. The acquisition parameters for DTI were: b-value = 450 $mm \cdot s^{-2}$; TR = 4400 ms, TE = 58 ms; FOV = 240 × 240 mm^2; excitations = 6; slice thickness = 5 mm; 24 slices, matrix = 192 × 192, and acquisition time 24 min. Also, parallel imaging and SPAIR (spectral attenuated inversion recovery) fat suppression were used. All DTI data were analyzed using a custom-written MATLAB program via the MuscleDTI_Toolbox github; all DTI processing steps are detailed in Damon 2021 (42). Images were pre-processed by inputting the raw images to accomplish multiple functions, including: image geometry adjustments between structural and DT images, image registration, image denoising, and DT calculations.

For post-processing, several MATLAB scripts were used to produce outcome variables for measures of diffusivity: MD ($mm \cdot s^{-2}$) and FA (dimensionless). The MD was calculated using the equation:

$$MD = \frac{\lambda 1 + \lambda 2 + \lambda 3}{3} \qquad \textit{Equation 7}$$

and FA was calculated with the equation:

$$\sqrt{\frac{3}{2}} \sqrt{\frac{(\lambda 1 - \langle MD \rangle)^2 + (\lambda 2 - \langle MD \rangle)^2 + (\lambda 3 - \langle MD \rangle)^2}{\lambda 1^2 + \lambda 2^2 + \lambda 3^2}} \qquad \textit{Equation 8}$$

where MD = mean diffusivity; λ1, λ2, and λ3 are eigenvalues representing diffusion in each the x, y, and z directions; and the principal eigenvalue (λ1) represents the direction of greatest diffusion, which in muscle is the z direction (12). The secondary and tertiary eigenvalues represent diffusion in whichever direction has the second and third most diffusion, respectively. Eigenvectors (ε) were produced in the diagonalization of the diffusion tensor matrix, and indicate the directions associated with λ1, λ2, and λ3 (43). The ε permits fiber tractography, and the standard deviation of ε1 provides information about the heterogeneity of fiber orientation within a slice. Measures of muscle architecture were then calculated with fiber tractography. The outcome variables for these measures were: tract length (mm), curvature (m^{-1}), pennation angle (°), and variability in fascicle orientation (SD ε1). All DTI variables represent the mean of all fibers tracked with the criteria outlined below.

For all analyses, an ROI was drawn around the outside of the vastus lateralis of the dominant leg to form a mask for creating the muscle's border (Figure 5.2). Then, seed points were placed to define the proximal and distal aponeuroses of the muscle, and to create a mesh from which the estimated fiber tracts would propagate. Fiber tracking was then performed using the 4^{th} order Runge-Kutta integration of $\lambda 1$ using a step size of ½ of the voxel width (0.5 mm). Fibers were tracked with the principal stopping criterion of exiting the drawn image mask. Additional criteria included an FA value between 0.05 and 0.4 (a.u.), and an inter-point angle of >25°.

The above criteria needed to fail to be met in order to terminate a tract. Fiber tracts were terminated using the two binary (BIN2) criteria. The "2" in BIN2 represents the two successive points for which the criteria muscle fail to be met with the determined step size (0.5 mm). Following the fiber tract, fibers will then be smoothed so that the row, column, and slice positions of the originally propagated fiber tracts could be fitted to 4th, 4th, and 3rd order polynomial functions as functions of fiber tract distance, respectively. Measurements of fiber tract length, curvature, and pennation angle for all tracts containing more than five fiber-tracking points were then quantified. Finally, a last quality assurance check was performed on the data set by excluding fibers of <10 mm in length, greater than 40° in pennation angle, and greater than 40 m^{-1} in curvature. These thresholds were set manually by the investigators to ensure accuracy of fiber tract estimation. Fiber tracts will also be excluded that differ from those of their 24 neighboring points by > 2 standard deviations. Figure 5.2 shows a completed analysis of fiber tract estimation.

Muscle Strength Measurement: Isokinetic Dynamometry

Measures of maximal knee extensor muscle torque (Nm) and peak unloaded velocity ($deg \cdot s^{-1}$) were collected as indices of muscle performance *in vivo* using a System 4 dynamometer (Biodex Medical Systems, Inc., Shirley, NY, USA). Prior to testing, participants performed a 5-min, unloaded warm-up on a stationary bicycle. Participants were then seated on the dynamometer in an upright position with a 110° hip angle. Chair and dynamometer settings were adjusted for each participant to correctly align the axis of rotation with the femoral condyle to ensure participant safety and accurate torque measurements. The experimental protocol consisted of 2 maximal voluntary isometric contractions (MVICs) followed by 6 randomized sets of 3 repetitions of isokinetic maximal voluntary dynamic contractions (MVDCs), including a set at 180 $deg \cdot s^{-1}$. Each MVDC set consisted of 3 consecutive contractions, with two minutes of rest between each set of contractions. Participants were instructed to "kick as hard and fast as possible" for each concentric contraction, and then "relax" when this phase was completed for a passive return to the starting position. After the MVDCs, participants performed a third MVIC to evaluate potential fatigue that may have occurred during the MVDC protocol. The MVICs were performed at 100° of knee flexion (180° being a straight leg) and lasted 3-4 s. The MVDCs were performed over an 80° range of motion, from a starting point at 90° of knee flexion to 10° of knee flexion (almost fully extended). Peak contraction velocity was estimated using isokinetic contraction speeds of 500 $deg \cdot s^{-1}$, which were essentially unloaded contractions (torque was not recorded for

these contractions). Visual feedback and verbal encouragement from the researcher were provided throughout the protocol to ensure maximal effort.

Dynamometer data were analyzed using a custom-written MATLAB program (Mathworks, Natick, Massachusetts). For MVICs, a trained researcher manually selected the end of the contraction to identify the point with the greatest torque production. For each MVDC at 180 deg·s^{-1}, the same researcher manually selected multiple time points to ensure that peak torque was selected during the isovelocity phase of contraction. These analyses provided: peak isometric torque (Nm), peak isokinetic torque (Nm), and peak unloaded velocity (deg·s^{-1}) for each participant. Peak isometric and isokinetic torque were defined as the greatest torque value acquired from the three contractions. These steps are illustrated in Figure 5.3.

Statistical Analyses

All data were tested for normality using the Shapiro-Wilk test prior to further analysis. All data are reported as mean ± standard deviation (SD) with the significance level set to $\alpha \leq 0.05$. Independent t tests were used to detect potential differences between males and females for all primary outcome variables. Simple linear regressions were used to quantify the relationships between muscle size (mCSA, muscle volume) and muscle function (peak torque and peak velocity) in this study group. Simple linear regression models were also used to test the hypothesis that there would be no relationship between FF and muscle architecture (mean tract length, mean curvature, mean pennation angle, and variability in fascicle orientation) or diffusion (MD, FA) properties. Additionally, coefficients of variation were calculated for these variables with the equation:

$$CoV = (SD/mean) * 100 \quad \textit{Equation 9}$$

where CoV is the coefficient of variation, SD is the standard deviation of all values.

To test the hypothesis that there was no relationship between fat content and muscle function, simple linear regression models were used for all variables acquired via isokinetic dynamometer (peak isometric and isokinetic torque, peak contraction velocity). To test the hypothesis that there was no relationship between architecture or diffusion and muscle function, a simple linear regression model was used for all variables acquired via isokinetic dynamometer. To test the combined effect of fat content and architecture on muscle function, all variables with a significant F value in simple linear regression analyses were used in a multiple linear regression model, with muscle volume as the base model (Table 5.3).

RESULTS

Descriptive and performance data for the 39 participants (21 female) are displayed in Table 5.1. Muscle composition, architecture and diffusion variables are shown in Table 5.2. Group differences between males and females are also noted. Figure 5.4 depicts sex differences in muscle function.

Pooled Regression Analyses

Figure 5.5 depicts the pooled relationships between muscle size and muscle strength. There was relationship between FF and tract length ($r^2 = 0.11$; $p = 0.05$). There were no relationships between FF and curvature ($r^2 = 0.00$; $p = 0.96$), pennation angle ($r^2 = 0.03$; $p = 0.34$), or variability in fascicle orientation ($r^2 = 0.02$;

p = 0.37). When normalizing to muscle height (r^2 = 0.00; p = 0.97), and femur length (r^2 = 0.00; p = 0.90), differences in the relationship between fat fraction and tract length were eliminated.

There were no relationships between fat and isometric torque (r^2 = 0.01; p = 0.50), isokinetic torque (r^2 = 0.03; p = 0.32), or peak contraction velocity (r^2 = 0.06; p = 0.13).

There were relationships between isometric torque and two measures of muscle architecture: curvature (r^2=0.17, p=0.01), and pennation angle (r^2=0.16, p=0.02). There were no relationships between isometric torque and tract length (r^2=0.01, p=0.64) or variability in fascicle orientation (r^2=0.10, p=0.07). For isokinetic torque, there was a relationship only with curvature (r^2=0.21, p=0.01). There were no relationships between tract length (r^2=0.01, p=0.61), pennation angle (r^2=0.08, p=0.10) or variability in fascicle orientation (r^2=0.05, p=0.18). There were no relationships between peak contraction velocity and tract length (r^2=0.03, p=0.33), curvature (r^2=0.01 p=0.53), pennation angle (r^2=0.02, p=0.39) or variability in fascicle orientation (r^2=0.00, p=0.92).

Sex differences between regressions for some measures of fat, architecture, and function can be found in Figures 5.6-5.9.

There were relationships between markers of diffusion and some of our study variables. The MD was related to isometric torque (r^2=0.13, p=0.03). However, MD was not related to isokinetic torque (r^2=0.05, p=0.18), peak contraction velocity (r^2=0.00, p=0.71), or FF (r^2=0.02, p=0.40). The FA was related to both isometric and

isokinetic torque (Figure 5.10). However, FA was not related to peak contraction velocity (r^2=0.04, p=0.25), or FF (r^2=0.06, p=0.14).

Multiple Regression Models

Table 3 shows the results of a series of multiple linear regression models using mCSA and muscle volume as a base model due to their strong relationships with isometric strength (r^2 = 0.86 and 0.85, respectively; Figure 5.5). Curvature and pennation angle were added to the model independently to estimate the effects of each of these variables on the relationship with muscle function.

DISCUSSION

This study evaluated the relationships between fat content and muscle architecture as well as muscle function of muscle via Dixon, DTI, and isokinetic dynamometry in adults 21-45 years old. The effect of biological sex was also explored. This study also evaluated the relationship between these variables and measures of diffusion. A main finding of this study was the negative association between FF and tract length, in partial support of our first hypothesis. In agreement with our second hypothesis, fat content was not associated with muscle function *in vivo*. Additionally, there was a positive relationship between muscle curvature and both measures of muscle strength. Pennation angle was positively associated with isometric, but not isokinetic strength. These results suggest that fat content may interrupt muscle fascicle lengths, but does not disrupt muscle structure enough to impair maximal muscle function. Other notable results included no relationship between fat content and measures of diffusion, in one of the only concurrent investigations of these variables in healthy adults.

Relationships Between Muscle Size & Architecture with Muscle Performance

Measures of muscle size were strongly associated with maximal muscle torque, as expected. Fat-free muscle CSA and muscle volume explained 86% and 85% of the variation in isometric torque in our sample (Figure 5.5). Our values are greater than those previously reported in various ambulatory muscles, which has ranged from 48-79% (9, 30, 121). Compared to isometric torque, mCSA and volume explained a lower percentage of the difference in isokinetic strength with values of 76% and 72%, respectively (Figure 5.5). Regarding muscle architecture and muscle function, both muscle curvature and pennation angle showed significant relationships in our sample. The association between pennation angle and maximal torque is reasonable, because greater angles likely reflect greater contractile area in adults. However, the use of pennation angle in characterization of function performance has been questioned in recent studies (146), as increased pennation angles will only relate to muscle strength to the extent that the increase is due to increases in lean tissue, rather than edema or fibrosis. Muscle curvature is a relatively new variable investigated by DTI, with limited data available in the literature. Curvature is a variable of interest in future studies that wish to investigate changes in intramuscular pressure or joint angle from contraction. Increased intramuscular pressure has been shown to affect strain development and perfusion patterns (53, 173, 213); curvature may prove to be an understudied variable in this area. It may also be worthwhile to clarify the functional role of muscle curvature in skeletal muscle mechanics by explaining the changes in muscle curvature and strength at different joint angles. Variability in fascicle orientation did not have a relationship with any measure of fat content or function in

our cohort. However, it may still be a variable of interest in study groups with high levels of fat infiltration (>20%) or functional deficits as a descriptor of muscle disorganization that offers different information than tract length.

Relationships Between Fat Content with Architecture & Diffusion

Our data showed that greater levels of FF were associated with shorter tract lengths in healthy adults (Figure 5.6). This result provides preliminary evidence of a potential mechanism for fat-induced muscle dysfunction in groups with high FF. Good reliability for tract lengths has been demonstrated in muscle (3, 20), and our results suggest that accumulation may interrupt fascicles along the muscle length. This may partially explain why muscle size is not always the best predictor of functional capacity, such as in the case of obese individuals (95, 154). Longer muscle fascicles can produce force at greater speeds and over greater lengths compared with shorter fibers (17). Therefore, fat-induced muscle impairment may be most evident with high levels of fat accumulation at faster dynamic movements. Notably, FF did not have a relationship with either MD or FA, in contrast to a previous finding in boys with Duchenne's muscular dystrophy (143). In their study, fat content had associations of 62-75% with both MD and FA in various thigh muscles, though the measures of fat infiltration were qualitatively evaluated on an ordinal scale. This lack of sensitivity in fat measurement limits application to functional tasks as the full range of variation between values is not captured. Measures of FF are often not reported in DTI studies, and tractography (which is required for architectural data), is only performed in a portion of investigations. Because effective acquisition of DTI data requires fat suppression, drawing

conclusions about the effect of fat content on muscle architecture requires a dedicated MR technique for fat quantification in addition to DTI acquisition. A study by Williams et al. concluded that diffusion properties of muscle can be effectively estimated when the water represents > 55% of the MR signal, or the upwards of 45% infiltration of fat (248). This supports the conclusion that these DTI measures can be practically applied to a wide range of muscle types. Qualitative and quantitative disorganization of muscle structure with a concurrent increase in FF has been investigated previously (193). However, measurements of both fat content and architecture have been almost exclusively in populations with advanced neuromuscular disease (59, 193). Therefore, it is not clear whether pathology, decreased physical activity, or other factors may be the primary drivers for the disruption of structure or functional impairment in these populations. Muscle architecture measurement by DTI is also commonly reported in the calf muscles, making it difficult to compare our values to those found in the literature (20, 21, 187, 216).

Relationships Between Fat Content and Muscle Function in vivo

Fat content was not associated with muscle performance in our study group (Figure 5.7). This supports the conclusion that modest levels of fat infiltration in the absence of aging, injury, or disease do not have a direct effect on mechanical muscle function. The FF values for our study were slightly higher, but still similar those reported in the literature for the quadriceps of healthy young adults, which are generally ≤ 10% (13, 49, 87). Because many investigations of older adults have found associations between fat content in the thigh and some measure of physical

function (25, 28, 50, 61, 68), it may be that changes that occur due to aging (e.g., diet, exercise, sarcopenia, protein turnover rate) are at least partially responsible for the variations in size and strength in this population. These findings are commonly reported in measures by MRI or computed tomography, which have been validated previously (172). Mobility impairment is known to take place concurrently with decreases in thigh attenuation by computed tomography and increases in FF by MRI, which have both been shown to represent intermuscular fat content (62, 74, 157). This, taken with our findings, would suggest fat accumulation in ambulatory muscles is a result of aging or inactivity, rather than a direct cause of decreased muscle functioning. This agrees with our findings in Study 1, which showed that despite a wide range of BMIs in moderately active younger adults (18.9-39.9 $kg \cdot m^{-2}$), there was not a large variation in measures of FF by MRI (7.8 ± 1.1%).

Sex-Based Comparisons

As expected, males had greater values for indices of body and muscle size, such as height, body mass, mCSA, and muscle volume. There was no difference in fat content between groups. Sex-based comparisons of intramuscular fat content are scarce, with most comparisons being made between appendicular and whole-body measurements. Tract length was the only architectural variable that was different between the groups, with males having 13% longer fiber tracts. However, this is likely due to the greater height and femur lengths of the males, as this difference was eliminated when normalizing to either variable ($p > 0.15$, both). Still, this demonstrates an association between fascicle lengths and fat deposition that can be explored in study designs investigating resistance exercise in training study designs.

Relationships between curvature and pennation with muscle strength appeared to be driven by males, but failed to reach statistical significance.

Fractional anisotropy was also greater in females. This result may be attributed to their smaller muscle size, leading to more anisotropic diffusion in their muscle. However, there were no sex-related differences in MD. Our findings related to the sex-based differences in measures of diffusion fully agreed with some studies (251), partially agreed with some studies (124, 209), and fully contrasted with others (71). For instance, there was no consistent trend in diffusion between muscle groups in these studies, as similar MD values were found when compared to other investigations of the thigh (124), and dorsiflexors (251), but were also in stark contrast to other values in the dorsiflexors (71). Measures of diffusion seem to be sensitive to differences in gender, age, and muscle group (32, 71, 188, 216). The relationship between fraction anisotropy and muscle strength (Figure 5.10) indicates that more anisotropic properties of diffusion in muscle are related to greater levels of muscle strength. Fractional anisotropy is reduced in instances of muscle injury (252), and larger muscle fiber size (14). This supports the idea that greater organization in muscle structure (i.e., architecture with tightly packed and unobstructed fascicles) is an independent predictor of muscle strength in healthy muscle. Higher FA values have also been reported at the ends of muscle. Our sample also has shown some variability in FA, rather than MD along the length of the thigh (Figure 5.11). This may be a consideration when evaluating different muscle lengths in future studies.

Combined Effects of Fat & Architecture on Muscle Function Are Not Known

It is worth bringing attention to a review by Jiang et al., which summarized the impact of fat infiltration on muscle architecture and capacity (114). This review noted the dearth of studies that concurrently evaluated fat infiltration, architecture, and capacity in muscle, pointing out that only three of the studies reviewed included all components in the same sample. Additionally, most of the measures of fat infiltration and all the measures of architecture that were included in this review were obtained using ultrasound, which has many clear limitations. First, the authors mention that muscle thickness was the only measure of muscle architecture which was assessed jointly with fat content. Our study has delineated the clear differences between muscle size and architecture, and muscle thickness would be more accurately defined as a measure of muscle size, analogous with mCSA. Second, ultrasound is not a reliable method of fat quantification. Echo intensity is the primary variable in ultrasound analyses, and is meant to represent fat content. However, it has been postulated that echo intensity more consistently represents fibrous tissue rather than fat in ultrasound (192). Therefore, it is misleading to say that there have been many studies which have compared fat content, architecture, and muscle function in the same cohort prior to our study. Still, this review highlights some clear gaps in the field which our study has addressed, namely: *1)* a sample of young, moderately active adults to control for the effects of aging and disease, *2)* the use of sensitive and robust methods for fat and architecture quantification of the entire thigh *3)* inclusion of multiple variables to quantify architecture (e.g., curvature, pennation angle, variability in fascicle orientation) and

4) standardized measures of muscle function under isometric and isokinetic conditions. Muscle volume and mCSA were used in multiple regression with significant measures of muscle architecture, however muscle curvature nor pennation angle added any additional explanation for the variance in muscle strength. Muscle size and curvature may be so closely related in healthy muscle, that these variables do not predict muscle function independently. More investigation is still needed to clarify the role of curvature in muscle function.

Limitations

There were limitations to this study. One limitation was that we drew our conclusions from the use of a fat content measure that represents the entire quadriceps muscle group, whereas the muscle architecture measures represent only the vastus lateralis muscle. The DTI analyses were limited to the vastus lateralis for several reasons, primarily because of the restrictions of surface coil acquisition areas. Additionally, DTI analyses are time-consuming and labor-intensive, so evaluating the primary knee extensor in the quadriceps was deemed suitable for our study question. Still, the strength of our sample size and analysis of the entire thigh allowed us to draw confident conclusions about the effect of fat content on muscle structure and mechanical function. Another potential limitation was our method for calculating measures of muscle diffusion and FF. By averaging the values of each axial slice into a single value for FF, MD, and FA, we may be "washing out" potential variability in muscle composition or diffusion within our study group. This may be a consideration in future research that evaluates separate study groups with more pronounced differences in composition, diffusion, or architecture.

Conclusions

Our results show that fat content is related to shorter fascicle length, but does not have any relationship with maximal muscle strength or contraction velocity in adults aged 21 to 45 years of age. Modest fat content values or moderate levels of activity may explain the lack of association between fat content and muscle performance. Based on our findings, mCSA, fascicle length, muscle curvature, and pennation angle, but not fat content, are key determinants of force production. Tract length was the only measure of muscle architecture that differed between sexes, a difference that was eliminated when adjusting for height and femur length. The cause for our findings related to muscle diffusion between males and females is unclear, however fractional anisotropy was shown to be an indepdnet predictor of muscle strength, likely due to its characterization of a more organized muscle structure. Future research should compare the relationships between fat content, architecture, and functional capacity between groups with known differences in muscle structure and function (e.g., younger vs. older; neuromuscular disorders vs. controls), also combining DTI and reliable fat quantification techniques. Studies should also investigate the relationship between FF and performance in submaximal or fatiguing tasks. These study designs will allow researchers to determine the role of fat content and the usefulness of the additional measures of muscle architecture beyond fascicle length and pennation angle.

Acknowledgements

The authors thank Nicholas Remillard, M.S., Luke Arieta, M.A., Elena Bliss, MRT, and Carol Bigelow, PhD, for their help on various parts of this study. We also thank all of the individuals who volunteered to participate in this research.

Funding

This work was funded by NIH R21 AR073511 and NIH/NIAMS R01 AR073831

Table 5.1. Group characteristics

Variable	All Participants (n=39)	Males (n=18)	Females (n=21)	p-value, sex
Age (years)	30 ± 7 (21- 45)	30 ± 7 (22 - 44)	30 ± 7 (21 - 45)	0.99
Height (cm)	171 ± 9 (158 -191)	178 ± 8 (168 - 191)	166 ± 6 (158 -180)	< 0.001
Body Mass (kg)	82 ± 19 (50 - 124)	89.3 ±19.2 (64 - 96)	76.0 ± 16.9 (50 - 116)	0.03
Body Mass Index ($kg \cdot m^{-2}$)	28.0 ± 5.9 (18.7 - 39.9)	28.2 ± 5.7 (22.6 - 26.2)	27.8 ± 6.1 (18.7 - 39.9)	0.84
Physical Activity ($counts \cdot day^{-1}/1000$)	251 ± 103 (42 - 549)	237 ± 100 (42 - 522)	263 ± 106 (154 - 549)	0.46
Moderate-Vigorous Physical Activity ($min \cdot day^{-1}$)	36 ± 18 (4 - 96)	33 ± 18 (4 - 70)	39 ± 19 (13 - 96)	0.38
Isometric Torque (Nm)	211 ± 7 (100 - 470)	275 ± 66 (164 - 470)	157 ± 32 (100 - 218)	< 0.001
Isokinetic Torque (Nm)	126 ± 45 (50 - 246)	163 ± 36 (96 - 246)	94 ± 21 (50 - 135)	< 0.001
Peak Velocity ($deg \cdot s^{-1}$)	442 ± 28 (346 - 490)	451 ± 21 (409 - 490)	433 ± 31 (346 - 488)	0.02

Data are mean ± SD. Range noted in parentheses. Bold line separates data from all participants and data for sex comparisons. p values are given for comparisons between males and females.

Table 5.2. Muscle composition, architecture, and diffusion characteristics

Variable	All Participants (n=39)	Coefficient of Variation (%)	Males (n=18)	Females (n=21)	p-value, sex
Composition					
mCSA (cm^2)	66.8 ± 18.6 (35.5 – 115.3)	27.9	82.8 ± 12.7 (63.3 – 115.3)	53.1 ± 9.6 (35.5 – 73.9)	< 0.001
Muscle Volume (cm^3)	1071 ± 394 (422 - 2190)	36.7	1393 ± 336 (785 - 2190)	795 ± 158 (422 - 1078)	< 0.001
FF (%)	7.6 ± 1.4 (4.8 – 12.1)	19.0	7.2 ± 1.5 (4.8 – 10.1)	7.9 ± 1.3 (5.8 – 12.1)	0.12
Architecture					
Tract Length (mm)	69.2 ± 13.1 (35.5 – 94.4)	18.9	74.2 ± 11.9 (58.7 – 94.4)	65.1 ± 12.8 (35.5 – 90.5)	0.04
Curvature (m^{-1})	11.6 ± 2.8 (7.5 – 18.8)	23.9	12.7 ± 2.7 (8.5 – 18.8)	10.8 ± 2.6 (7.5 – 17.6)	0.04
Pennation Angle (°)	15.8 ± 3.7 (10.1 – 25.0)	23.5	16.5 ± 3.0 (12.9 – 22.8)	15.2 ± 4.2 (10.1 – 25.0)	0.31
Variability in fascicle orientation (SD ε1)	29.4 ± 7.8 (20.4 – 52.3)	26.5	30. ± 6.0 (20.4 – 44.0)	28.5 ± 9.0 (14.6 – 52.3)	0.45
Diffusion					
MD ($mm \cdot s^{-1}$)	1.62 ± 0.06 (1.48 – 1.76)	3.8	1.64 ± 0.06 (1.53 – 1.76)	1.59 ± 0.06 (1.48 – 1.76)	0.02
FA (dimensionless)	0.20 ± 0.02 (0.17 – 0.26)	9.8	0.18 ± 0.01 (0.17 – 0.20)	0.21 ± 0.02 (0.18 – 0.26)	< 0.001

Data are mean ± SD. Range noted in parentheses. Bold line separates data from all participants and data for sex comparisons. p values are given for comparisons between males and females. mCSA = Fat-free muscle cross-sectional area; FF = Fat Fraction; MD = Mean Diffusivity; FA = Fractional Anisotropy

Table 5.3. Multiple regression analyses for muscle isometric torque

Variable	Model 1	Model 2	Model 3
mCSA (cm^2)	-	β = 0.91 (3.3,4.6); p<0.001	β= 0.96 (3.5,4.8); p<0.001
Curvature (m^{-1})	-	β = 0.04 (-2.8,5.2); p=0.54	-
Pennation Angle (°)	-	β = 0.07 (-4.6,1.6); p=0.34	-

Variable	Model 1	Model 2	Model 3
Muscle volume (cm^3)	-	β = 0.91 (0.16,0.21); p<0.001	β= 0.96 (0.17,0.22); p<0.001
Curvature (m^{-1})	-	β = 0.09 (-0.90,6.0); p=0.14	-
Pennation Angle (°)	-	β = 0.00 (-2.7,2.8); p=0.99	-

Relationships between mCSA and muscle volume as base predictors for isometric strength. The standardized β coefficient and 95% confidence interval noted in parentheses. Significance level are provided for each model. Model 1: Base model; Model 2: Base model + curvature; Model 3: Base model + pennation angle

Figure 5.1. Timeline of Study events. Chronological timeline of events between study days and data collection order.

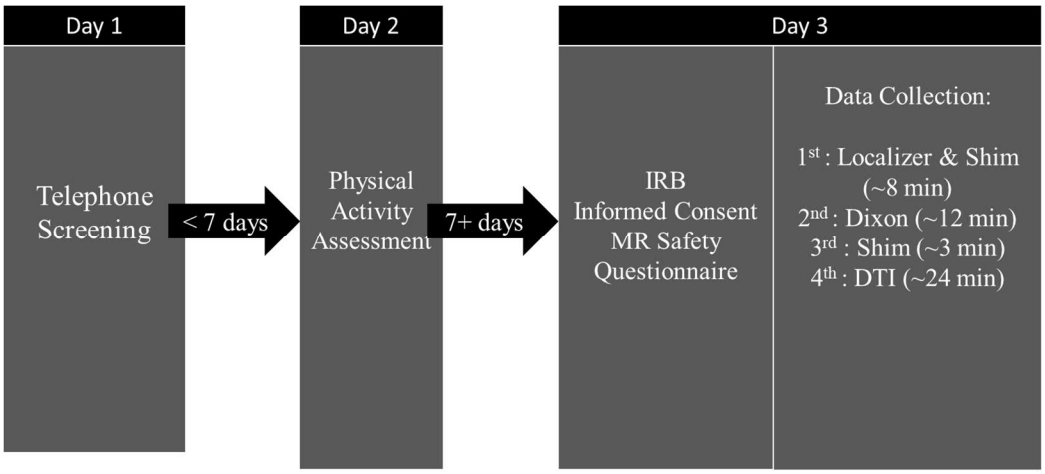

Figure 5.2. Diffusion tensor imaging tractography of vastus lateralis muscle. *A)* Creation of imaging mask *B)* Selection of seed points for tract propagation *C)* Representative image of fiber tracts for the vastus lateralis muscle. Axial slices from the Dixon MRI are shown at top, middle and bottom.

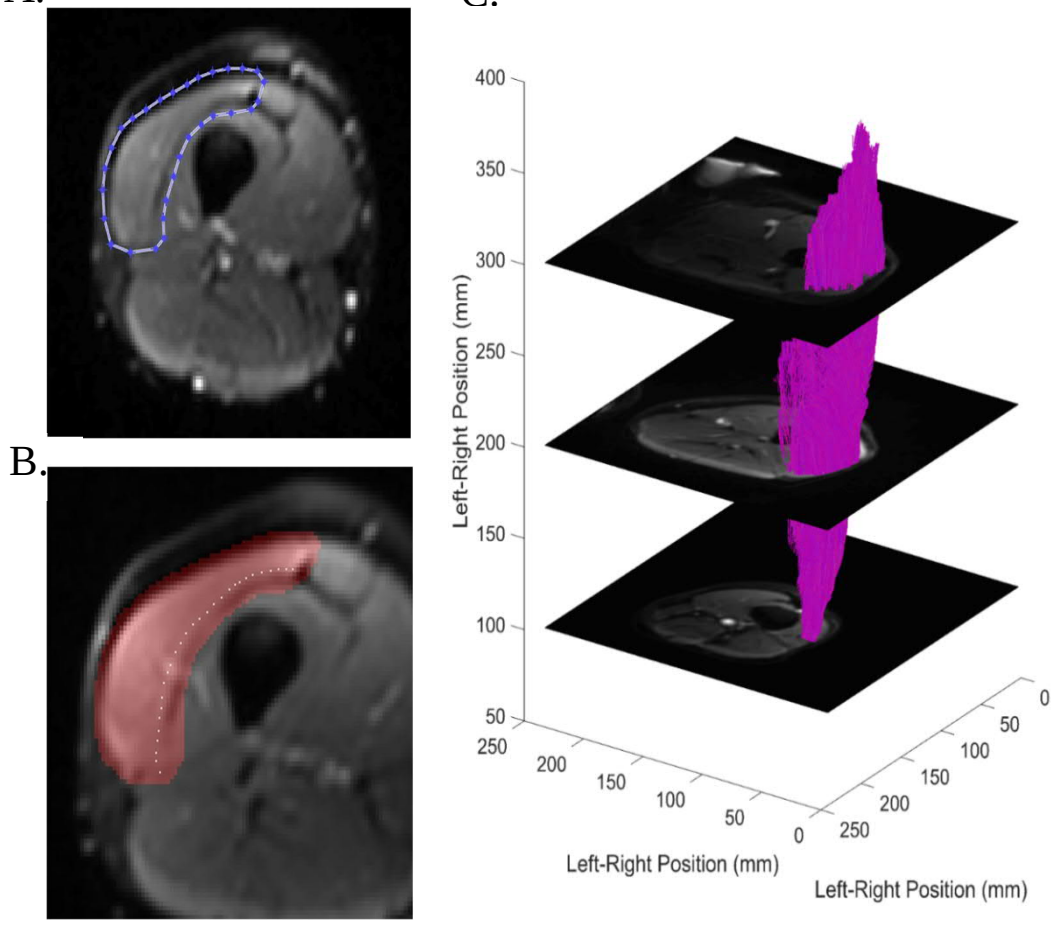

Figure 5.3. Analysis of maximal torque in knee extensors. *A)* Torque trace for maximal voluntary isometric contraction. The red star is manually selected by a trained researcher and represents the end of contraction. *B)* Torque trace for a single maximal voluntary dynamic contraction. Start of contraction is depicted by red star, start of isovelocity phase by green star, end of velocity overshoot artifact by blue star, end of isovelocity phase by purple star, and end of contraction by black star. Peak torque value is identified between start and end of contraction within in the isovelocity phase. The red line with arrow indicates direction of cursor movement in processing.

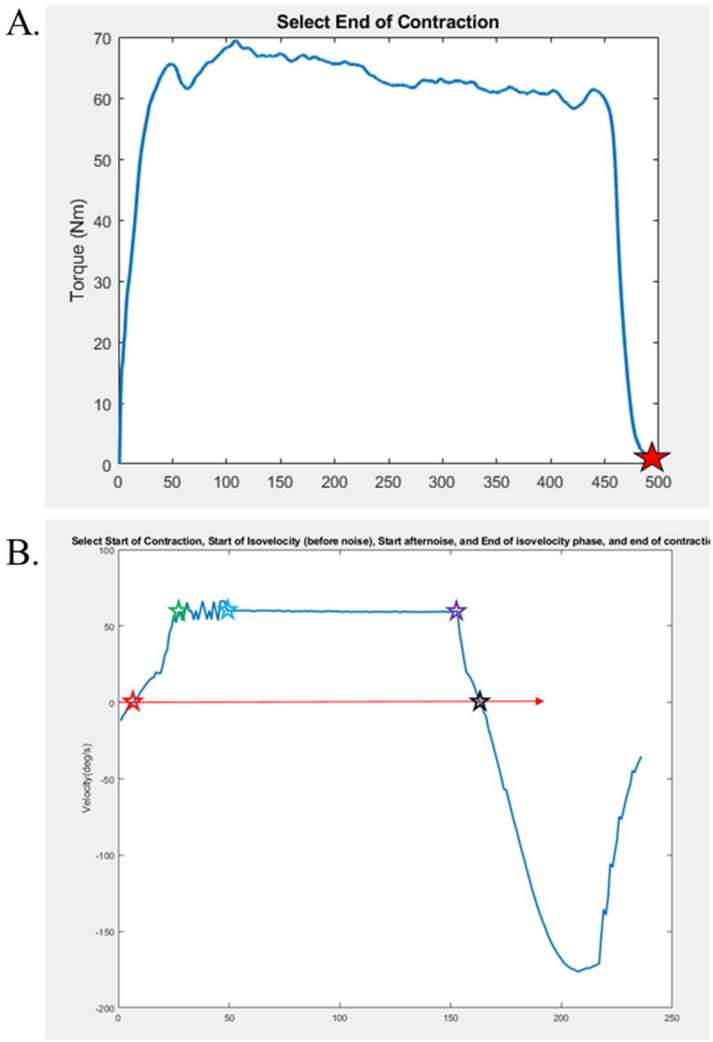

Figure 5.4. Sex differences in muscle function. Box plots for peak isometric (0 deg·s^{-2}) and isokinetic (180 deg·s^{-2}) torque, and peak contraction velocity. Asterisks indicate p<0.001 for differences between males (n=18) and females (n=21). The difference in peak velocity between males and females did not attain statistical significance (p=0.07). Outliers (outside 1st or 3rd quartile + 1.5*Interquartile range) are depicted with filled blue (females) and red (males) circles.

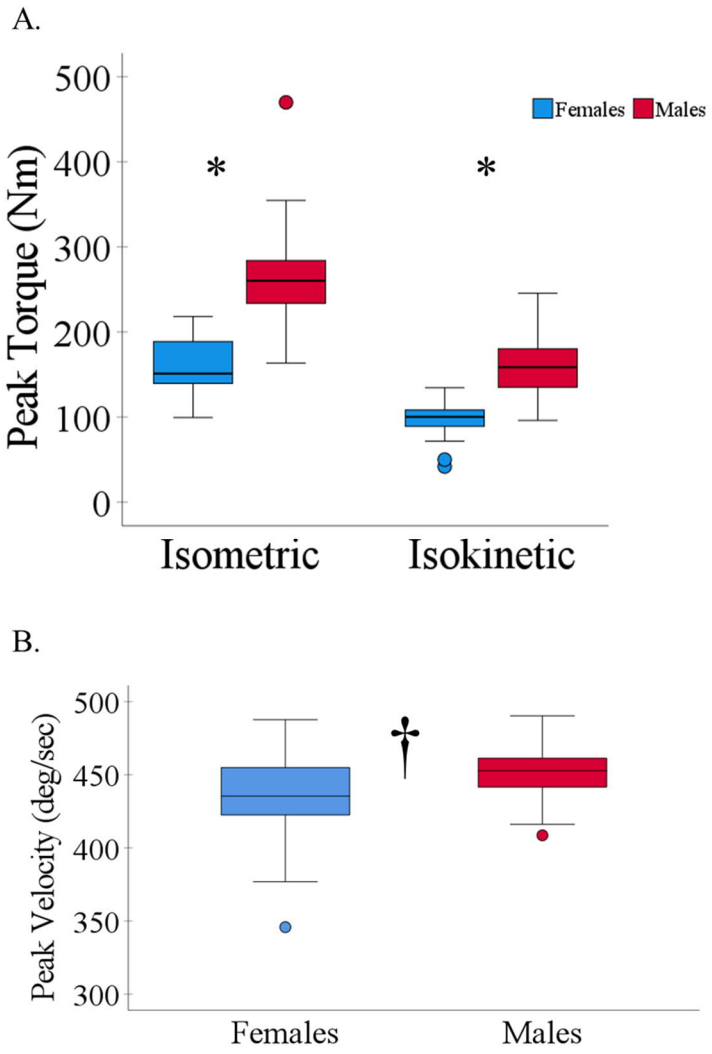

Figure 5.5. Relationships between muscle size and strength. *A)* Relationship between muscle cross-sectional area (mCSA) and maximal isometric torque *B)* Relationship between muscle volume and maximal isometric torque *C)* Relationship between muscle cross-sectional area (mCSA) and maximal isokinetic torque *D)* Relationship muscle volume and maximal isokinetic torque.

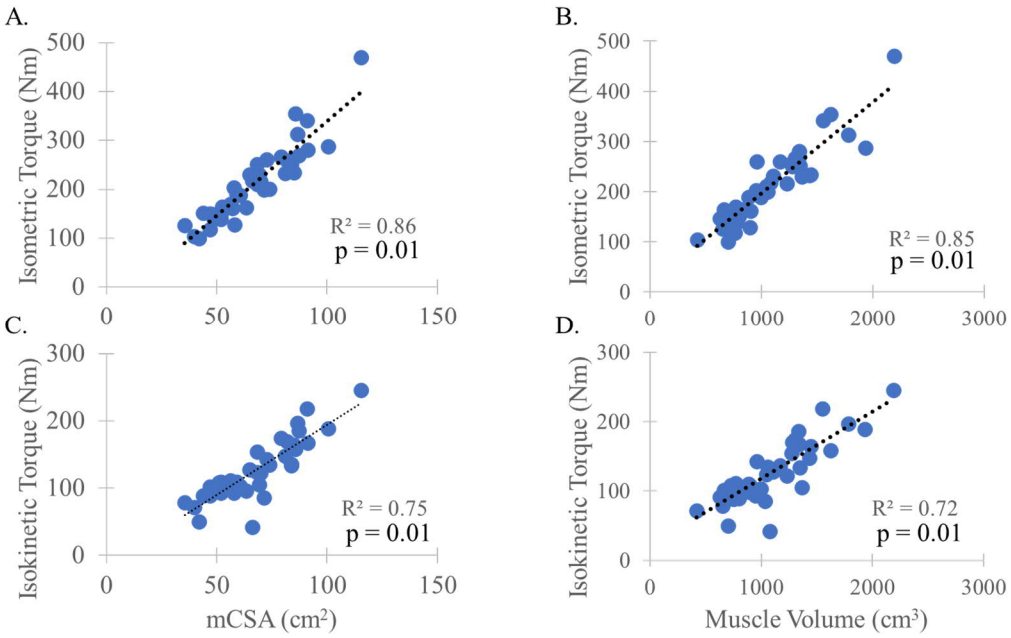

Figure 5.6. Relationships between fat content and muscle architecture. *A)* Relationship between fat fraction and tract length *B)* Relationship between fat fraction and pennation angle *C)* Relationship between fat fraction and muscle curvature. Blue dots represent females and orange dots represent males. The r^2 and p value on the left represents women (blue) and right represents men (orange).

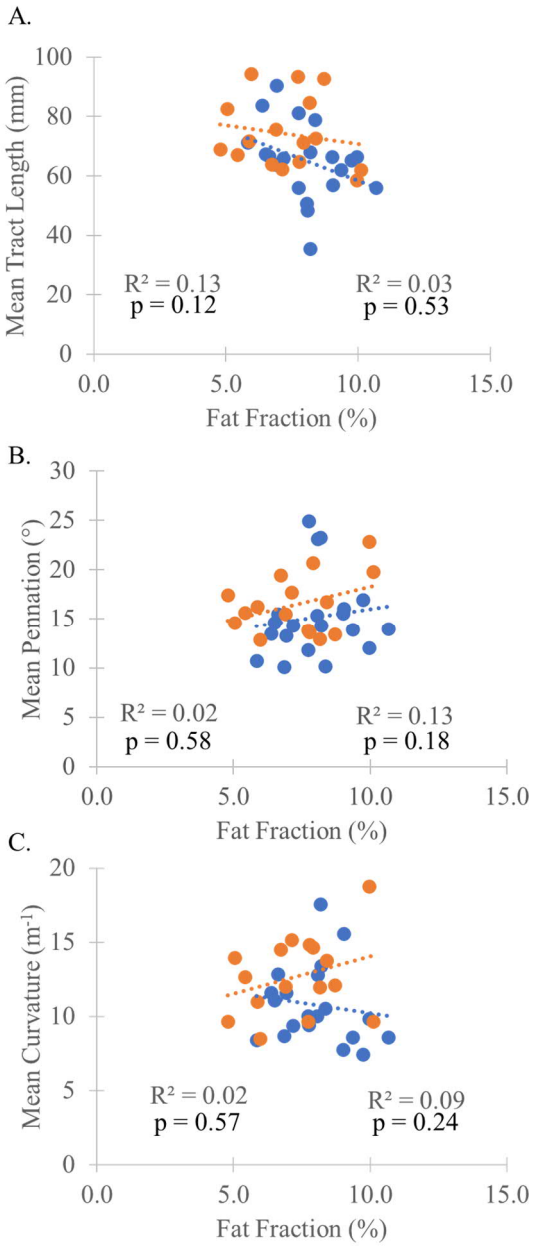

Figure 5.7. Relationships between fat content and muscle function. *A)* Relationship between fat fraction and isometric torque *B)* Relationship between fat fraction and isokinetic torque *C)* Relationship between fat fraction and peak contraction velocity. Blue dots represent females and orange dots represent males. The r^2 and p value on the left represent women (blue) and right represent men (orange).

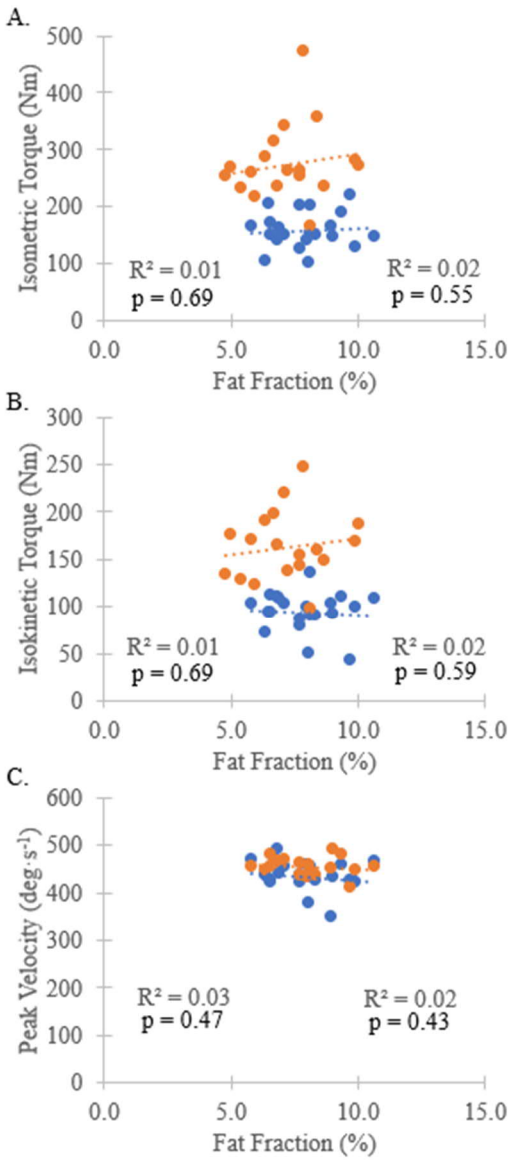

Figure 5.8. Relationships between muscle curvature and muscle function. Panels *A)* Relationship between muscle curvature and maximal isometric torque *B)* Relationship between muscle curvature and maximal isokinetic torque *C)* Relationship between muscle curvature and peak contraction velocity. Blue dots represent females and orange dots represent males. The r^2 and p value on the left represent women (blue) and right represent men (orange).

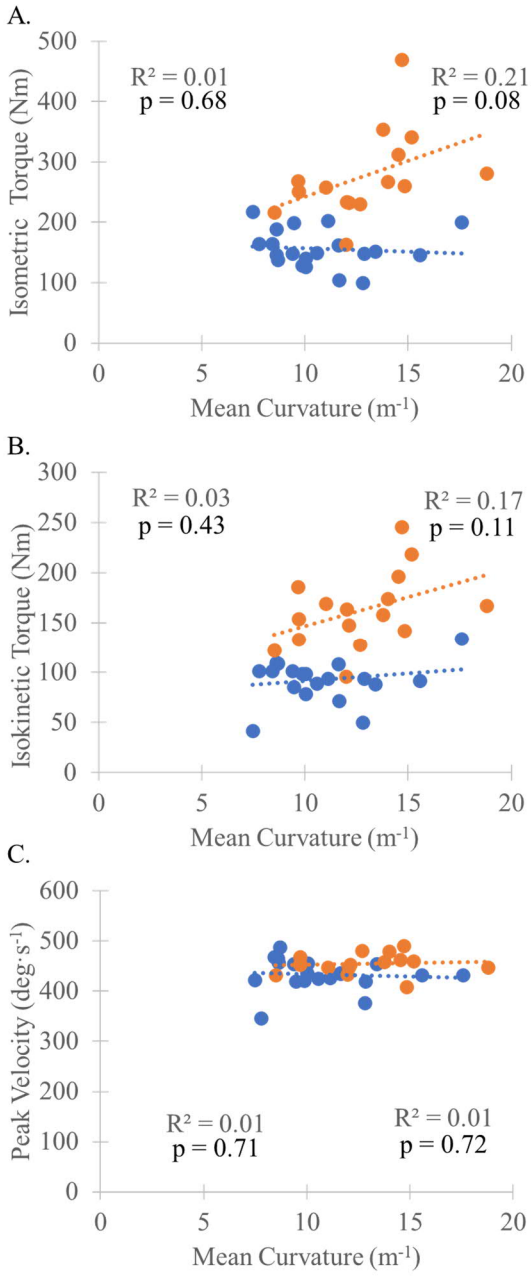

Figure 5.9. Relationships between pennation angle and muscle function. Panels *A)* Relationship between pennation angle and maximal isometric torque *B)* Relationship between pennation angle and maximal isokinetic torque *C)* Relationship between pennation angle and peak contraction velocity. Blue dots represent females and orange dots represent males. The r^2 and p value on the left represent women (blue) and right represent men (orange).

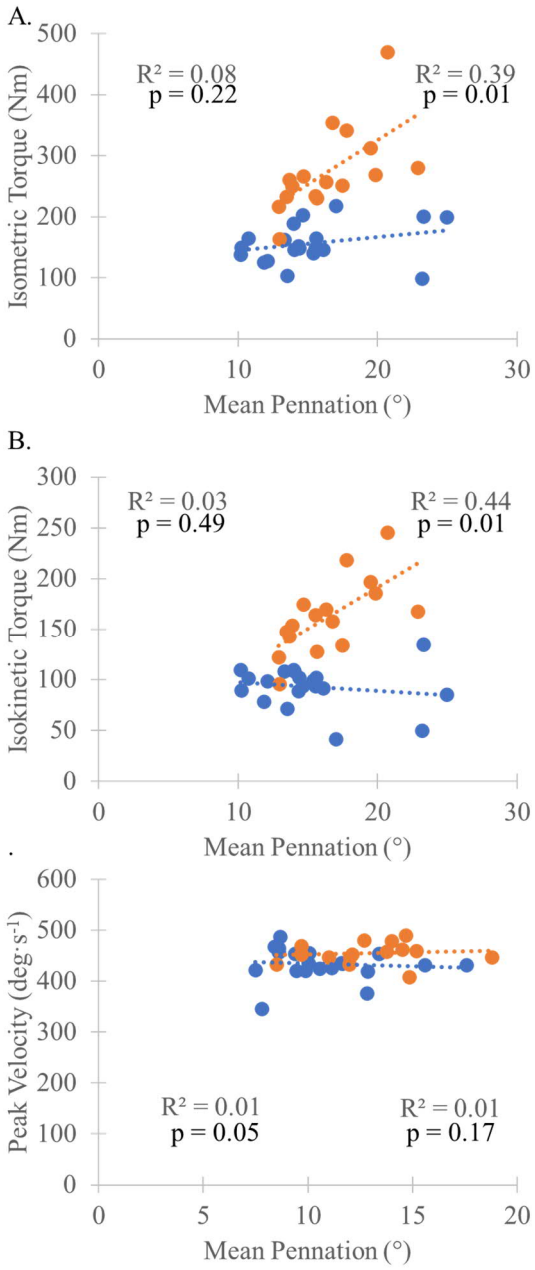

Figure 5.10. Relationships between fractional anisotropy and maximal strength. *A)* Relationship between fractional anisotropy and maximal isometric torque *B)* Relationship between fractional anisotropy and maximal isokinetic torque.

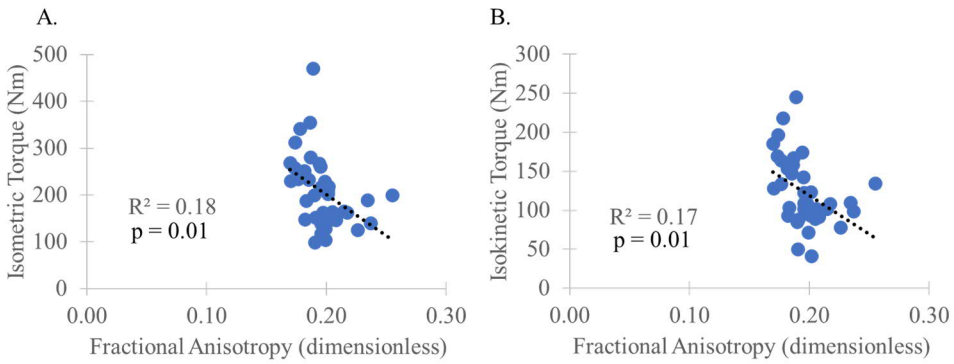

Figure 5.11. Mean diffusivity and fractional anisotropy of the vastus lateralis for a single male participant. Values for mean diffusivity (blue) and fractional anisotropy (orange) along the length of the femur (knee=0%; hip=100%).

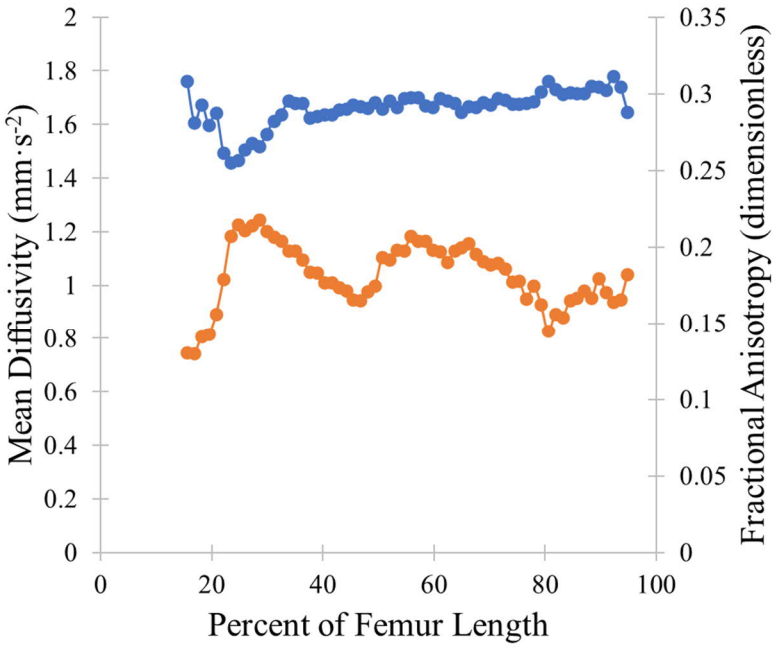

CHAPTER 6

STUDY 3: INTRAMYOCELLULAR LIPID CONTENT DOES NOT EXPLAIN VARIATIONS IN FAT FRACTION AND IS NOT RELATED TO SINGLE FIBER FUNCTION

ABSTRACT

Size, function, and fat accumulation in skeletal muscle can be quantified at multiple scales. However, we do not know whether measures of fat and function at the organ or organism level are indicative of fat or function at the level of single fiber. Understanding the patterns of fat accumulation in healthy, young adults can clarify the role of fat content in muscle impairment. The purpose of this study was to quantify the agreement between fat content and function at the cellular and organ levels in healthy young adults. We also quantified the relationship between intramyocellular lipid (IMCL) content and single fiber function. Twenty healthy young adults (31 ± 8 years; 11 female) were evaluated by magnetic resonance imaging, isokinetic dynamometry, oil red o, and sinusoidal analysis. Muscle torque (Nm) across multiple contraction velocities (0-240 $deg \cdot s^{-1}$), specific tension ($mN \cdot mm^{-2}$), and cross-bridge kinetics (myosin attachment rate (s^{-1}), myosin attachment time (ms), myofilament stiffness ($kN \cdot m^{-2}$) for myosin heavy chain (MHC) I and IIA fibers. Fat fraction (FF) was not related to IMCL ($r^2 = 0.05$; $p=0.34$) and muscle torque was not related to specific tension in MHC I ($r^2<0.13$; $p>0.07$) or MHC IIA ($r^2<0.04$; $p>0.42$). Muscle torque was also not related to cross-bridge kinetics in MHC I ($r^2<0.05$; $p>0.18$) or MHC IIA fibers ($r^2<0.06$; $p>0.18$). Finally, IMCL was not related to any measures of cross-bridge kinetics in MHC I ($r^2<0.12$; $p>0.13$) or MHC IIA ($r^2<0.03$; $p>0.46$) fibers. Our results show that measures of muscle fat at the organ level do not reflect IMCL content in young adults. Additionally, single fiber kinetics did not explain *in vivo* muscle function in healthy young adults, contrary to previous studies. We conclude that IMCL content

does not impair single fiber function in our sample of young adults. Greater accumulation of IMCL or significant changes in fiber structure may be necessary to induce functional impairment.

INTRODUCTION

The size, function, and composition (i.e., proportion of contractile to non-contractile tissue) of human skeletal muscle can be quantified at multiple levels, such as cellular, organ, or organism. Despite a noted relationship between fat and muscle function (48, 153, 155, 207, 240), studies comparing fat content at the cellular and organ level in humans is scarcely available in the literature (Figure 6.1). This makes it difficult to determine whether measures of fat at the organ or organism level, which are easier to acquire, are indicative of fat content within the cell. Patterns of fat deposition can also change due to aging and disease (99, 211). Therefore, measures of fat at the single fiber level (i.e., cellular) could potentially provide different information than those at the whole muscle level (i.e., organ). Regarding muscle function, several factors (e.g., cross-bridge kinetics, shortening velocity) dictate force in single fibers, and subsequently whole muscle (45, 166, 167). Interestingly, fiber area or function is preserved in some clinical populations when compared to controls, despite differences in whole muscle function (100, 201). Evaluating measures of fat deposition or function from the cellular or organ level alone may cause researchers to draw erroneous conclusions about how to characterize the health or functioning of an individual (i.e., organism). Further, the role of fat in the potential disruption of the mechanical processes of force production has not been clarified, particularly at the cellular level.

Muscle strength is a crucial factor in mobility and physical function (92), underscoring the importance of elucidating the factors that contribute to muscle force. The size of a muscle, specifically its cross-sectional area (mCSA), is the best

predictor of its maximal strength at the organ level (161, 207). While maximal isometric (i.e., static) strength is a useful marker in the characterization of adults in various cohorts, assessment of muscle strength under dynamic conditions is more practical in the evaluation of functional tasks (52). There are differences in strength between many groups (e.g., older vs. younger, clinical vs. controls), even when adjusting for muscle size (91, 149, 222). This indicates that there are other factors that contribute to variations in muscle strength. There is general agreement that peripheral, rather than central mechanisms are primarily responsible for muscle weakness in healthy adults (120, 138, 227). Therefore, a focus on the peripheral factors that may cause muscle impairment is a logical research area. Measurements performed *in vitro* have the advantage of eliminating the effects of neurological function or force transmission via intermuscular tissues, thus allowing the focus to be on muscle cells and their sub-structures. At the cellular level, factors other than fiber CSA have been shown to better predict fiber tension, such as myofilament stiffness (166). Additionally, with an increase in organizational scale there are more structural components that contribute to the transmission of force. Therefore, fat and function may have different relationships within the cellular and organ levels.

Both composition and function can be measured in various ways in skeletal muscle, which can pose challenges in the interpretation of their relationship. Intracellular fat content is commonly measured using *in vitro* techniques such as electron microscopy and oil red o (ORO) staining, due to their high accuracy and direct measurement of fat (210). However, like any invasive technique, sampling location, area, and tissue processing are considerations for accurate interpretation

and analysis. At the organ level, intermuscular fat refers to tissue located between muscle groups, while intramuscular fat content refers to fat within a muscle (85). Different imaging techniques such as ultrasound, computed tomography, and magnetic resonance imaging (MRI) can be employed to assess both areas, which is generally more feasible than the use of *in vitro* analyses. However, these *in vivo* methods represent primarily extracellular, rather than intracellular fat deposits (2), and may lead to different conclusions, based upon our Study 1 (Chapter 4). Compared with ultrasound and computed tomography, MRI offers greater versatility in application by easily combining multiple acquisition techniques (e.g., spectroscopy, T1 weighted imaging). Magnetic resonance imaging also has the added benefit of not exposing participants to ionizing radiation (57, 243). Considering mCSA explains 35-79% of the variation in maximal strength for the ambulatory muscles of healthy adults (30, 121, 161), fat content at the single fiber or whole muscle levels may explain part of this relationship between size and strength.

To this end, the first aim of this study was to compare fat content at the cellular and organ levels in healthy young adults. We compared lipid area fraction (%) and fat fraction (%) to determine the relationship between cellular and organ level fat content. Our first hypothesis was that there would be no relationship between cellular and whole muscle fat content (%), due to our in Study 1, which found no relationship between histochemical staining, MRI, and magnetic resonance spectroscopy. Our second aim was to compare single fiber characteristics (specific fiber tension ($mN \cdot mm^{-2}$), myosin attachment rate (s^{-1}), and myosin attachment time (ms), myofilament stiffness ($kN \cdot m^{-2}$)) in MHC I and IIA fibers to specific torque at

multiple contraction velocities (0-240 $Nm \cdot s^{-2}$) to determine the relationship between cellular and organ level function. Our second hypothesis was that there would be a relationship between MHC IIA but not MHC I fibers for all single fiber characteristics at all contraction velocities. This was due to previous findings that have demonstrated a relationship between single fiber kinetics and whole muscle function in older adults (166–168). Our third aim was to evaluate the relationship between fat content and muscle function in fibers. We compared *in vitro* lipid area fraction (%) to all single fiber characteristics in MHC I and IIA fibers to determine the relationship between cellular fat content and muscle function. Our hypothesis was that *in vitro* lipid area fraction (%) would have a relationship with MHC IIA, but not MHC I fibers for all single fiber characteristics. We believed that greater levels of lipid content would not impair function in MHC I fibers when compared to MHC IIA fibers due to their physiological predisposition for oxidative energy production in the body. These findings will contribute to the literature by demonstrating whether whole muscle characteristics are also observed at the single fiber level in the absence of age-related changes or chronic disease. This study will also be the first to compare single fiber fat content with function in healthy young adults.

METHODS

Participants

Participants between 21-45 years of age were recruited to be relatively sedentary and free of cardiovascular, musculoskeletal, neurological, or metabolic disease. All participants had a body mass index (BMI) between 18.5-39.9 $kg \cdot m^{-2}$ and were not

taking any medications known to affect physical or muscular function. Study procedures were approved by the Institutional Review Board at the University of Massachusetts Amherst (Appendices A-C). After determining eligibility and MR safety via telephone screening (Appendix D), all participants were scheduled for a visit to the Life Science Laboratories at the University of Massachusetts Amherst where they completed an informed consent, medical history (Appendix E), and MR safety questionnaire (Appendix F). Descriptive characteristics were recorded for all participants. Height and body mass were collected with a scale (SECA Model 769, Hamburg, Germany).

Physical Activity Assessment

To account for potential influences of habitual physical activity (PA) on our outcomes, PA was measured for each participant using uniaxial GT1M accelerometers (ActiGraph, Pensacola, FL). Participants wore accelerometers on their right hip for at least 7 days prior to study selection, and maintained an activity diary during that period. Data were collected at 80 Hz and averaged over 60-s epochs. Daily activity counts (arb. units), MVPA (min) and wear time (hours) were determined using ActiLife software (ActiGraph, Pensacola, FL). The first 7 valid (>10 hr wear time) days were analyzed for each participant. Standard cutpoints (232) were used to determine minutes of moderate-to-vigorous physical activity (MVPA), and wear time was calculated as described by Choi et al. (35). Physical activity logs were used to validate wear time, and exclude atypical days due to travel illness, etc. (Appendix H).

Muscle Biopsy Acquisition and Storage

Percutaneous needle biopsies of the vastus lateralis muscle were performed in a under local lidocaine anesthesia and in the fasted state, as previously described (170). Muscle tissue was partitioned into samples for oil red o (ORO) staining on intact fibers. For ORO analyses, muscle bundles were frozen in embedding medium (OCT; Sakura, Torrance, CA) in isopentane cooled with liquid N_2 and stored at -80°C until analyzed.

Myosin Heavy Chain Determination

Muscle fiber bundles were examined for determination of MHC composition, as previously described (177) with slight modifications. Briefly, 6 μm thick cross-sections were incubated with primary and secondary antibodies, which fluoresced at different wavelengths for MHC I, IIA and IIX isoforms. These antibodies were then measured using a Keyence BZ-X800 microscope (Osaka, Japan) to produce blue, red, and green images which corresponded to the various MHC isoforms. The composite image was analyzed for each MHC isoform (I, I/IIA, IIA, IIAX and IIX) and fiber size using Image J software (NIH, Bethesda, MD, USA).

Fiber Lipid Content Determination

Muscle fiber bundles were examined for intramyocellular lipid (IMCL) content using ORO staining, as previously described (128). After staining, 6 μm thick cross-sections were imaged using a Keyence BZ-X800 microscope and images for each fiber were analyzed for lipid droplet size (mm), area fraction occupied by lipid droplets (%), and number of droplets per area (#) using Fiji/ImageJ software (NIH,

Bethesda, MD, USA). All collection and analyses of single muscle fiber compositional assessments were conducted by trained individuals in the Muscle Biology Laboratory at the University of Massachusetts Amherst.

Fiber Tension Measurement

Fibers were prepared for mechanical measurements and mounted on the experimental apparatus as previous described (170), except that bromophenol blue was used as an indicator dye instead of toluidine blue during the fixing of the ends of the fiber. Briefly, fibers were placed in relaxing solution (15°C), and manually stretched to a sarcomere length of 2.65 μm, as this resembles *in vivo* sarcomere length in human skeletal muscle (33). Sarcomere length was determined with a camera (Point Grey, FLIR Integrated Imaging Solutions, Inc., Richmond, BC, Canada) which was integrated with ImageJ software (NIH, Bethesda, MD, USA). Fibers were placed in pre-activating solution, moved to activating solution with force measured at its plateau, and placed back into relaxing solution. Initial activation was performed at 15°C, which improves fiber stability versus initial activation at 25°C. Temperature was then increased to 25°C, sarcomere length reset to 2.65 μm and cross-sectional area (CSA) determined by measuring fiber width on the apparatus' compound microscope. The height of fibers was estimated based upon the height-to-width ratio measured via microscope prior to mounting and presuming fiber CSA is elliptical. Fibers were placed in pre-activating solution, moved to activating solution with specific tension ($mN \cdot mm^{-2}$) measured at its plateau, sinusoidal analysis performed, and moved back into relaxing solution.

In vitro Estimation of Molecular Kinetics

Myosin-actin cross-bridge kinetics and myofilament properties were derived using sinusoidal analysis, as previously described (170). Briefly, sinusoidal analysis was performed in activation solution at 25°C at the specific tension plateau by applying small-amplitude, sinusoidal strain (normalized length, or length per change in length) to one end of the fiber at 48 frequencies from 0.125 to 200 Hz, while sinusoidal stress output (normalized force, or force per cross-sectional area) were measured at the other end of the fiber. The stress output was divided into its elastic and viscous components, then fit with a six-parameter equation to estimate specific steps in the cross-bridge cycle, including myosin attachment time (t_{on}), myosin attachment rate (s^{-1}), and myofilament stiffness ($kN \cdot m^2$). For myofilament stiffness, k represents the degree to which the cross-bridge is purely elastic or purely viscous.

In vivo Intramuscular Fat Content Determination

Scans for all participants were performed on a Siemens Skyra 3T scanner, 70-cm bore MR system (Siemens Healthcare, Erlangen, Germany) running on VE11C platform. Participants were positioned supine on the exam table with feet oriented toward the scanner. Gradient-echo scout images were used to confirm optimal leg positioning in the isocenter and correct coil positioning over the muscle. Serial images of the dominant thigh were acquired in all participants from the lateral epicondyle of the femur to the greater trochanter of the hip. Images were acquired using an 18-channel phased array coil combined with a spine coil built into the exam table. To limit movement, the coil was secured to the thigh using inelastic straps. A six-point Dixon technique was applied to generate water- (W) and fat- (F) only

images using a 2D gradient echo sequence (73). Parameters were as follows: image resolution (1.25 x 1.25 x 5 mm^3), TR = 35ms; slice thickness = 5 mm; 24 slices, FOV = 240 x 240 mm^2; TE =2.46, 6.15; 3.69, 7.38; 4.92, 8.61 ms; matrix = 192×192 mm^2; GRAPPA factor = 2; flip angle = 15°, bandwidth = 1090 Hz/pixel, 1 average, and acquisition time = 12 min.

Water and fat images were reconstructed offline using the MATLAB Fatty Riot algorithm (219). Methods for calculation of fat-free muscle cross-sectional area (mCSA), muscle volume, and fat signal fraction (FF, %) began with identifying and recording the anatomical landmarks for the femur (lateral epicondyle and greater trochanter). Then, all slices in which all four quadriceps muscles are visible were identified, and a single region of interest (ROI) was drawn around the entire quadriceps muscle group in each slice. Subcutaneous fat, bone, and regions of intermuscular fat or connective tissue were excluded as much as possible when drawing each ROI. Mean FF was calculated on a pixel-by-pixel basis as:

$$FF = 100\% * F/(W + F) \qquad \textit{Equation 10}$$

Where W is the water signal intensity and F is the fat signal intensity. Fat signal fraction, referred to as fat fraction was calculated as an average of the values for each ROI. The mCSA for each ROI was calculated as total area of the ROI minus the fat area.

In Vivo Muscle Strength Measurements

Measures of maximal knee extensor muscle torque (Nm) and peak velocity ($deg \cdot s^{-1}$) were collected as indices of muscle performance *in vivo* using a Biodex System 4

dynamometer (Biodex Medical Systems, Inc., Shirley, NY, USA). Prior to muscle performance testing, participants performed a 5-minute, unloaded warm up on a stationary bicycle. Next, they were seated on the dynamometer in an upright position with a 110° hip angle. Chair and dynamometer settings were adjusted for each participant to correctly align the axis of rotation with the femoral condyle to ensure participant safety and accurate torque measurements. The experimental protocol consisted of 2 maximal voluntary isometric contractions (MVICs) followed by 6 randomized sets of 3 repetitions of isokinetic maximal voluntary dynamic contractions (MVDCs). Participants were instructed to "kick as hard and fast as possible" for each concentric contraction, and then "relax". After the MVDCs, participants performed a third MVIC to evaluate potential fatigue that may have occurred during the MVDC protocol. The MVICs were performed at 100° of knee flexion (180° being a straight leg) and lasted 3-4 s. The MVDCs were performed over an 80° range of motion, from a starting point at 90° of knee flexion to 10° of knee flexion (almost fully extended). Peak contraction velocity was estimated using isokinetic contraction speeds of 500 $deg \cdot s^{-1}$, which were essentially unloaded contractions (torque was not recorded for these contractions). Visual feedback and verbal encouragement from the researcher were provided throughout the protocol to ensure maximal effort.

Dynamometer data were analyzed using a custom-written MATLAB program (Mathworks, Natick, Massachusetts). For MVICs, a trained researcher manually selected the end of the contraction. For each MVDC, the same trained researcher manually selected multiple time points on a plot of velocity over time: the start of

contraction, the start of the isovelocity phase, the end of the dynamometer artifact, the end of the isovelocity phase, and the end of contraction. These analyses provided: peak isometric torque (Nm), peak isokinetic torque (Nm), and peak unloaded velocity ($deg \cdot s^{-1}$) for each participant. Peak isometric and isokinetic torque were defined as the greatest torque value acquired from one of the three total contractions via post-processing. These steps are illustrated in Study 2.

Statistical Analyses

All data are reported as mean ± standard deviation (SD) with the significance level set to $\alpha \leq 0.05$. All hypotheses were tested using linear regression analyses. Cellular and whole muscle area were calculated in the quantification of fat content; therefore, these variables were also tested with linear regression. Specific torque ($Nm \cdot cm^{-2}$) and specific tension ($mN \cdot mm^{-2}$) were selected to compare measures of muscle function that were normalized to CSA at the fiber and whole muscle levels.

RESULTS

Descriptive data for all participants, including muscle composition, are shown in Table 1. Our sample of young adults were moderately active and had a range of BMIs from normal body weight (18.5 – 24.9 $kg \cdot m^{-2}$) to obese class 2 (30.0 – 34.9 $kg \cdot m^{-2}$). There was a greater rage for all single fiber measurements in MHC IIA fibers when compared to MHC I. Values for fiber and whole muscle function are given in Table 2.

In contrast to our first hypothesis, lipid area fraction (%) and FF (%), had no relationship ($r^2 = 0.05$; $p = 0.34$) (Figure 6.2). Lipid droplet size ($r^2 = 0.05$; $p = 0.69$)

nor the number of droplets per area ($r^2 = 0.02$; $p = 0.46$) were related to FF. In an exploratory analysis, there were significant correlations between mCSA *in vivo* and fiber CSA *in vitro* for both MHC I ($r^2 = 0.53$; $p=0.02$) and MHC IIA ($r^2 = 0.50$; $p<0.001$) fibers (Figure 6.2). Notably, lipid area fraction ($r^2= 0.02$; $p = 0.45$), nor FF ($r^2 = 0.00$; $p=0.76$) had a relationship with BMI.

In contrast to our second hypothesis, isometric torque (Nm) did not have a relationship with MHC I ($r^2 = 0.02$; $p = 0.611$), or MHC IIA ($r^2 = 0.01$; $p = 0.65$) fiber specific tension ($mN \cdot mm^{-2}$). Similarly, isometric torque (Nm) did not have a relationship with MHC I ($r^2 = 0.02$; $p=0.60$) or MHC IIA ($r^2 = 0.05$; $p = 0.35$) myosin attachment rate (s^{-1}). Isometric torque ($Nm \cdot cm^{-2}$) had no relationship with MHC I ($r^2 = 0.00$; $p = 0.83$) or MHC IIA ($r^2 = 0.00$; $p = 0.38$) myosin attachment time (ms). Isometric torque ($Nm \cdot cm^{-2}$) also had no relationship with MHC I ($r^2 = 0.04$; $p = 0.57$) or MHC IIA ($r^2 = 0.02$; $p = 0.24$) myofilament stiffness ($kN \cdot m^{-2}$). These results are displayed in Figures 6.3 and 6.4. Table 6.3 shows the linear regression analyses for cellular and organ level muscle function across all *in vivo* contraction velocities. There were no significant relationships between cellular measures of fiber function and any marker of *in vivo* muscle performance. Additionally, there were no correlations between absolute measures of muscle torque (Nm) and any cellular measures of muscle function in MHC I or IIA fibers.

In contrast to our third set of hypotheses evaluating the relationship between fat content and muscle function in fibers, fiber specific tension ($mN \cdot mm^{-2}$) did not have a relationship with MHC I ($r^2 = 0.13$ $p = 0.13$), or MHC IIA ($r^2 = 0.02$; $p = 0.54$) lipid area fraction (%). Similarly, lipid area fraction (%) did not have a relationship

with MHC I (r^2 = 0.01; p = 0.65) nor MHC IIA (r^2 = 0.00; p = 0.74) myosin attachment rate (s^{-1}) or MHC I (r^2 = 0.00; p = 0.94) nor MHC IIA (r^2 = 0.02; p = 0.60) myosin attachment time (ms). Myofilament stiffness ($kN \cdot m^{-2}$) did not have a relationship with MHC I (r^2 = 0.01 p = 0.38), or MHC IIA (r^2 = 0.02; p = 0.46) lipid area fraction (%). These results are displayed in Figures 6.5 and 6.6.

DISCUSSION

This study evaluated muscle with *in vitro* and *in vivo* techniques to compare the compositional and functional characteristics of whole muscle to those of single fibers in adults 21-45 years old. This study also investigated the relationship between cellular measures of fat content and muscle function. Our results showed no relationship for measures of fat (i.e., IMCL and FF) or function (i.e., myosin attachment rate, myosin attachment time, specific tension, myofilament stiffness, specific torque) between the cellular and organ levels. We also did not find a relationship between IMCL content and any measures of cellular function in MHC I or MHC IIA fibers. There was a relationship between the CSA of single fibers and mCSA of whole muscle, with a stronger relationship for MHC IIA fibers compared to MHC I. These results suggest that fat content at the whole muscle level does not reflect fat within the cells of the vastus lateralis. This finding, combined with the lack of agreement between IMCL, FF, and BMI provides insight into the patterns of fat distribution in young adults. Body fat percentage is strongly associated with BMI across age and sex (72), however this accumulation of fat does not seem to be located within intramuscular or intracellular compartments in young adults. The findings related to muscle function show that single fiber kinetics do not explain variations in whole muscle performance in static or dynamic conditions in young adults. Lastly, our results indicate that the limited IMCL accumulation is a reason for the lack of relationship with any measures of single fiber function. This is notable, because a report has previously shown a relationship between cellular fat content and function in older adults (36).

Relationships between cellular and organ level fat content

Measures of whole muscle FF by MRI did not reflect cellular IMCL content in our sample of healthy young adults. Cellular lipid content represented a nominal percentage of fiber CSA in our sample, despite a wide range of BMIs. There have been lipid area fraction values of up to 9% in older adults (36), and previous work in obese adults and those with type 2 diabetes mellitus have shown greater lipid area fractions (80). This indicates that IMCL deposition is possible at significantly greater levels, though lipid accumulation at intracellular locations may not be a typical storage depot for fat in the absence of aging or pathological conditions. There have been many comparisons of intramuscular fat deposits between modalities (55, 57, 86, 172, 249), but few studies which have compared fat content between intracellular and intramuscular locations. In these investigations, the study group is most commonly older adults (36, 224). These findings cannot be extrapolated to a younger cohort, because fat is redistributed from subcutaneous to visceral and ectopic depots with age; this redistribution occurs despite a maintenance or decrease in total body fat (48, 211). Nonetheless, equipment which measures global and regional body fat is commonly utilized due to its availability and ease of use. Therefore, individuals should be aware that high levels of global or regional body fat levels may not represent IMCL within the muscle fibers of young, healthy adults. This is likely because the accumulation of lipids is occurring outside of the cell in this group. This finding contrasts with a study by Goodpaster and colleagues, which reported associations of 43-77% in various muscles of the trunk and lower body when comparing fat measurement by ORO to computed tomography

(77). This is noteworthy because quantification of IMCL in healthy adults is useful in determining the oxidative potential of muscle or estimation of insulin resistance for type 2 diabetes risk. Their sample included 10 obese subjects with type 2 diabetes mellitus, compared to 11 total obese subjects free of other conditions in this study. Activity levels, BMI status, and presence of type 2 diabetes are all factors that could individually contribute to varied fat content and distribution patterns. Additionally, computed tomography is less accurate than Dixon imaging for IMCL quantification, due to lower resolution and no true separation of IMCL and EMCL (210); all could explain the differences in the findings.

Relationships between cellular and organ level muscle function

Like our findings regarding fat content, function in whole muscle did not reflect function in single fibers in our sample of young adults. Studies of single fiber force production generally seek to understand the impact of aging (66, 107, 142) or clinical pathology on fiber function (100, 131, 132). Additionally, preservation of fiber CSA or force in older adults and clinical populations has been reported in some studies (65, 100, 131), with the opposite result in others (66, 163). Despite the importance of this work, researchers must also examine the relationships between single fiber and whole muscle function in healthy, younger adults to determine the extent to which cellular function can be expected to dictate whole muscle performance. Our findings did show a strong relationship between MHC IIA fiber CSA and whole muscle mCSA in younger adults. It may be that MHC IIA fiber CSA is a better predictor for whole muscle performance in active young adults, with increases in CSA still leading to relatively greater proportions of strongly bound

cross-bridges when compared to findings in older adults (166). Aging, inactivity, or disease may cause decreases in the relative concentrations of contractile proteins or the effectiveness of the cross-bridge cycle, which may be a larger factor in whole muscle performance. Even then, previous findings have suggested single fiber mechanics, specifically contractile velocity may have a greater relationship with dynamic, rather than isometric function (167, 169).Nonetheless, our results can be evaluated jointly with an investigation by Reid and colleagues, which reported no differences in fiber CSA or specific tension between healthy middle-aged (~47 years) and mobility impaired (~77 years) older adults (199). This was despite differences in whole muscle CSA, fat content, specific power, and neuromuscular activation (199). Their study also noted a similar degree of fat accumulation and neuromuscular function (e.g., specific torque, tension) between healthy middle aged and older adults (~74 years). Miller et al. reported a relationship between MHC IIA fiber tensions and isokinetic power in healthy younger and older adults with similar materials, acquisition, and processing, but different statistical methods (167). Intracellular lipids were not measured in these studies, so we cannot determine whether IMCL content was a modulating factor in single fiber performance.

Relationships between IMCL and measures of fiber function

Our data suggest that IMCL does not impair fiber function, contrary to previous findings in older adults (36, 224), and animal models (7, 16, 56). Relationships between measures of fat content and fiber kinetics were virtually nonexistent in our sample of young adults, suggesting that the effects of aging or disease are a significant contributor to impairment of fiber function. Both human studies reported

greater lipid area fractions (2.4-9.4%), though the study by Choi et al. evaluated lipid content by fiber type (36, 224), which likely contributed to the differences in our findings as well. A study of boys with Duchenne's muscular dystrophy found that a FF of 20% was associated with a high risk of functional reduction, and FF values ≥ 75% were unable to perform a standardized test of muscle strength (69). Though there are numerous factors that can contribute to muscle dysfunction in musculoskeletal disorders, this indicates that there may also be a threshold where muscle function is impaired in healthy adults. There has been evidence of a paradox in fat accumulation, whereby the IMCL concentrations of endurance athletes are like those observed in obese or diabetic populations (76). However, the superior oxidative capacity and insulin sensitivity of endurance trained athletes (despite comparable lipid content) is likely due to the increases in mitochondria size, number, mitochondrial contact with lipid droplets, and clearance rate of lipid byproducts (228). Similarly, the maintenance of structural integrity in the fiber may be sufficient to counteract any potential deficits caused by increased IMCL content in active, young adults. We are only aware of two studies which compared measures of fat and function at the cellular and organ levels, both in older adults (36, 224). Our study is the first to demonstrate a lack of relationship between IMCL content and fiber function in younger, healthy adults. This finding can be taken together with our results from Study 2, which showed no relationship between FF and knee extensor torque in a younger sample. The lack of agreement between fat and function at the cellular and organ levels in our findings is notable, because the relationship between fat and function appears to vary between model type, age, and

disease status. Therefore, researchers that wish to elucidate the mechanisms of fat-induced muscle dysfunction must evaluate these variables within the same population, muscle group, and organizational level to draw sound conclusions about their relationship.

Limitations

Our study has several limitations. Measures of whole muscle function represent the performance of all knee extensors, and measures of fat content represent only the quadriceps muscle group. Alternatively, data that represent cellular composition and function were acquired from a snapshot of fibers in the vastus lateralis, which themselves only represent ~one third of quadriceps muscle volume (unpublished observations). Another limitation was that the IMCL content analyzed via ORO was averaged across the entire CSA in this study. Muscles with greater oxidative properties (e.g., soleus) have greater lipid content when compared to muscles with more glycolytic properties (e.g., gastrocnemius) (108). The vastus lateralis is a mixed muscle type, so averaging the lipid content from this muscle group may have washed out potential differences in the relationship between IMCL and fiber function. Future studies may want to quantify lipid content in each fiber type, and use other modalities that can investigate the relationship between fat content and single fiber function exclusively in the vastus lateralis.

Conclusion

Our results show that fat content nor muscle function are related between the cellular and organ levels. Investigators who are interested in elucidating the effects

of fat on muscle function (e.g., metabolic, mechanical) should be aware that measures of fat content at the organ level may not accurately estimate intracellular lipid content. Similarly, muscle function at the organ level does not necessarily reflect fiber tension or molecular kinetic in young adults. Our results also suggest that fat content does not directly impair muscle force production. The negative effects of fat infiltration may be more evident in submaximal and dynamic contractions. Additionally, greater accumulation of IMCL (>3%) or degradation of fiber integrity may be necessary to cause significant functional impairment.

Acknowledgements

The authors thank Nicholas Remillard, M.S., Luke Arieta, M.A., Christopher Hayden, M.S., Phillip Woods, M.S., Brent Momb, M.S., Shayelia Stanley B.S., Aurora Foster, M.S., Elena Bliss, MRT, Stuart Chipkin, M.D., and Carol Bigelow, PhD for their help on various parts of this study. We also thank all of the individuals who volunteered to participate in this research.

Funding

This work was funded by NIH R21 AR073511 and NIH R01 AG047245

Table 6.1. Participant characteristics

Variable	Mean ± SD	Range
Whole Body		
Age (years)	31 ± 8	21 - 45
Height (cm)	173 ± 10	158 - 191
Weight (kg)	89 ± 19	50 - 123
Body Mass Index ($kg \cdot m^{-2}$)	29.6 ± 5.5	18.9 - 39.9
Physical Activity ($counts \cdot day^{-1}/1000$)	285 ± 119	42 - 549
Moderate-Vigorous Physical Activity ($min \cdot day^{-1}$)	42 ± 21	4 - 96
Whole Muscle		
mCSA (cm^2)	69.9 ± 20.5	42 -115
FF (%)	7.7 ± 1.1	6.4 -10.0
Single Fiber		
MHC I Fiber CSA (μm^2)	5415 ± 1350	3704 - 9657
MHC IIA Fiber CSA (μm^2)	5826 ± 2114	3078 - 12016
ORO Lipid Area Fraction (%)	2.2 ± 0.74	0.92 - 3.63
ORO Lipid Droplets/CSA (#)	0.036 ± 0.014	0.018 - 0.063
ORO Average Lipid Droplet Area (mm^2)	0.50 ± 0.08	0.38 - 0.65

N = 20 (11 female). mCSA = muscle Cross-Sectional Area, FF= Fat fraction, MHC= Myosin Heavy Chain, ORO = Oil Red O.

Table 6.2. Muscle function *in vitro* and *in vivo*

Variable	Mean ± SD	Range
Whole Muscle		
Peak Torque (Nm)	225 ± 85	100 - 470
Specific Torque ($Nm \cdot cm^{-2}$)	3.2 ± 0.4	2.4 – 4.1
MHC I Fibers		
Fibers Analyzed Per Person (#)	8 ± 4	1 - 17
Specific Tension ($mN \cdot mm^{-2}$)	141 ± 22	96 - 146
Myosin Attachment Rate (s^{-1})	15 ± 2	11 - 19
Myosin Attachment Time (ms)	46 ± 9	34 - 67
Myofilament Stiffness ($kN \cdot m^{-2}$)	2688 ± 512	1642 - 3744
MHC IIA Fibers		
Fibers Analyzed Per Person (#)	5 ± 2	1- 8
Specific Tension ($mN \cdot mm^{-2}$)	189 ± 41	96 - 271
Myosin Attachment Rate (s^{-1})	48 ± 5	37 - 61
Myosin Attachment Time (ms)	16 ± 2	14 - 22
Myofilament Stiffness ($kN \cdot m^{-2}$)	5826 ± 2113	2571 - 8164

N = 20 (11 female). MHC= Myosin Heavy Chain.

Table 6.3. Relationships between single fiber kinetics and *in vivo* muscle performance

	MHC I Fibers			MHC IIA Fibers		
Contraction Velocity ($deg \cdot s^{-2}$)	Specific Tension ($mN \cdot mm^{-2}$)	Myosin Attachment Rate (ms)	Myosin Attachment Time (ms)	Specific Tension ($mN \cdot mm^{-2}$)	Myosin Attachment Rate (ms)	Myosin Attachment Time (ms)
0	r^2=0.04, p=0.61	r^2=0.04, p=0.60	r^2=0.05, p=0.83	r^2=0.04, p=0.65	r^2=0.01, p=0.35	r^2=0.01, p=0.38
60	r^2=0.13, p=0.07	r^2=0.05, p=0.18	r^2=0.04, p=0.19	r^2=0.04, p=0.59	r^2=0.05, p=0.18	r^2=0.00, p=0.31
120	r^2=0.02, p=0.43	r^2=0.03, p=0.54	r^2=0.04, p=0.57	r^2=0.03, p=0.52	r^2=0.05, p=0.71	r^2=0.04, p=0.57
180	r^2=0.02, p=0.41	r^2=0.04, p=0.58	r^2=0.00, p=0.33	r^2=0.02, p=0.42	r^2=0.05, p=0.82	r^2=0.05, p=0.74
240	r^2=0.00, p=0.33	r^2=0.06, p=0.30	r^2=0.03, p=0.24	r^2=0.02, p=0.45	r^2=0.05, p=0.76	r^2=0.05, p=0.73
500*	r^2=0.05, p=0.74	r^2=0.06, p=0.95	r^2=0.06, p=0.93	r^2=0.04, p=0.56	r^2=0.01, p=0.40	r^2=0.01, p=0.39

Relationships between single fiber kinetics as an independent variable and all contraction velocities as dependent variables. *Regressions for 500 $deg \cdot s^{-2}$ represent relationship between fiber kinetics maximal contraction velocity, rather than maximal torque.

Figure 6.1. Overview of selected studies of muscle composition and function

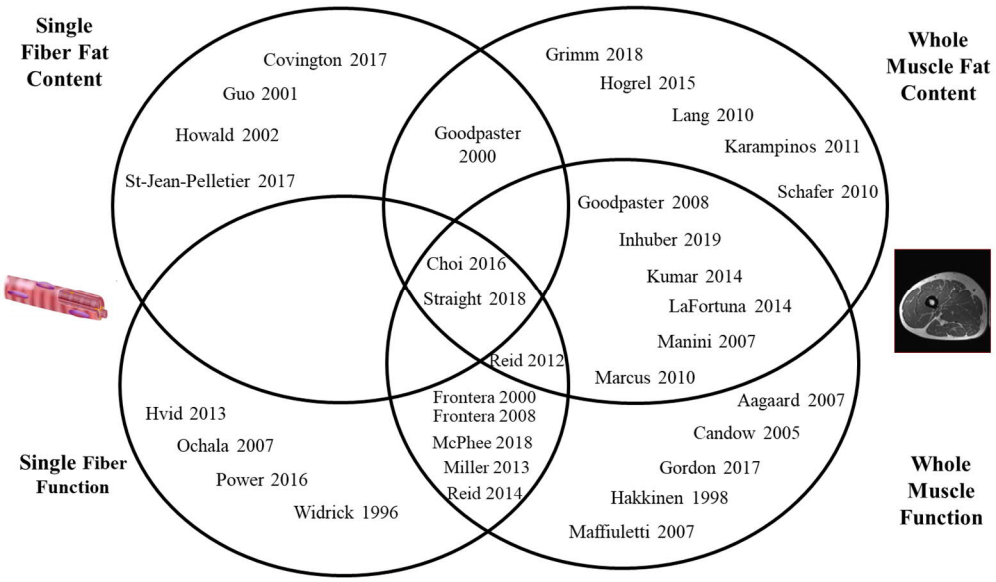

Figure 6.2. Relationships between whole muscle and single fiber composition. Panels *A and B)* Relationship between muscle cross-sectional area of quadriceps and cross-sectional areas of myosin heavy chain I and IIA fibers, respectively *C)* Relationship between fat fraction of quadriceps and lipid area fraction of single fibers.

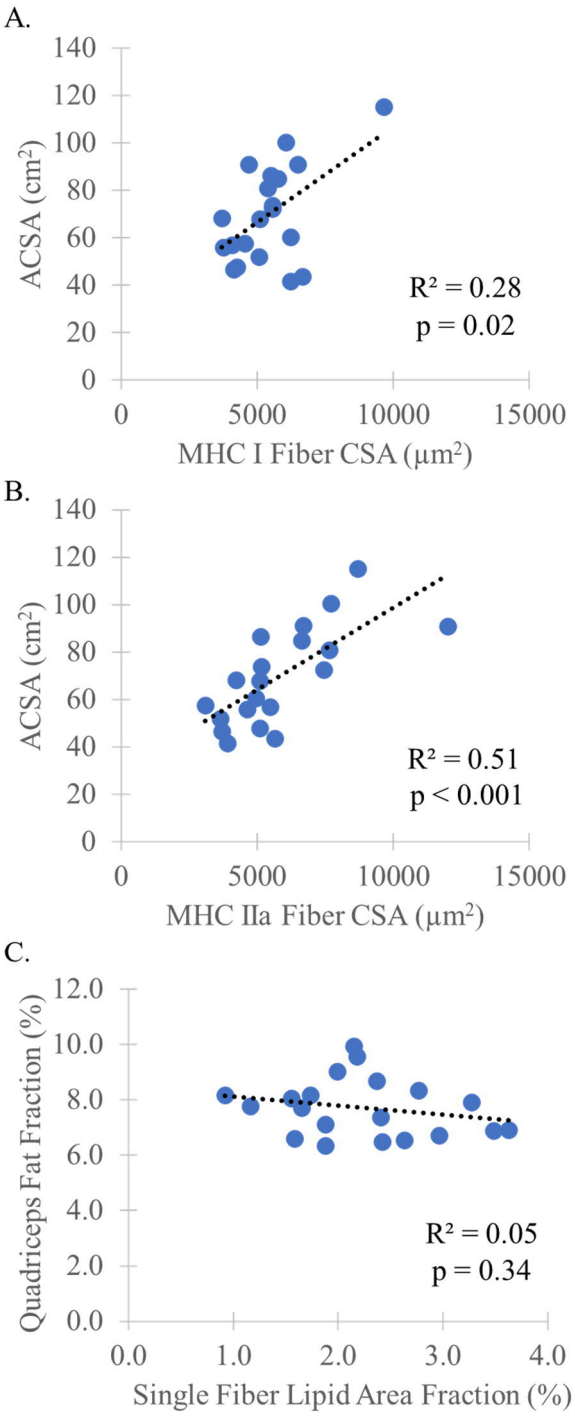

Figure 6.3. Relationships between MHC I fiber function and isometric torque. *A)* Relationship between absolute isometric torque and single fiber specific tension *B)* Relationship between absolute isometric torque and myofilament stiffness *C)* Relationship between absolute isometric torque and myosin attachment rate *D)* Relationship between absolute isometric torque and myosin attachment time. All data for single fibers represent myosin heavy chain I isoforms.

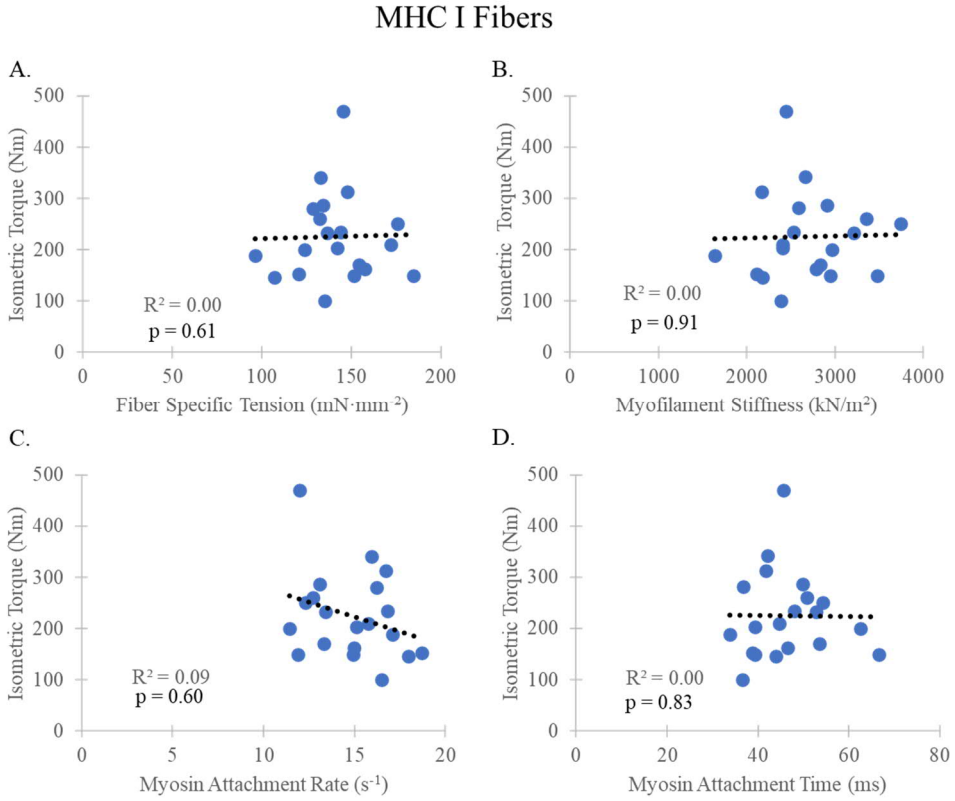

Figure 6.4. Relationships between MHC IIa fiber function and isometric torque. *A)* Relationship between absolute isometric torque and single fiber specific tension *B)* Relationship between absolute isometric torque and myofilament stiffness *C)* Relationship between absolute isometric torque and myosin attachment rate *D)* Relationship between absolute isometric torque and myosin attachment time. All data for single fibers represent myosin heavy chain IIa isoforms.

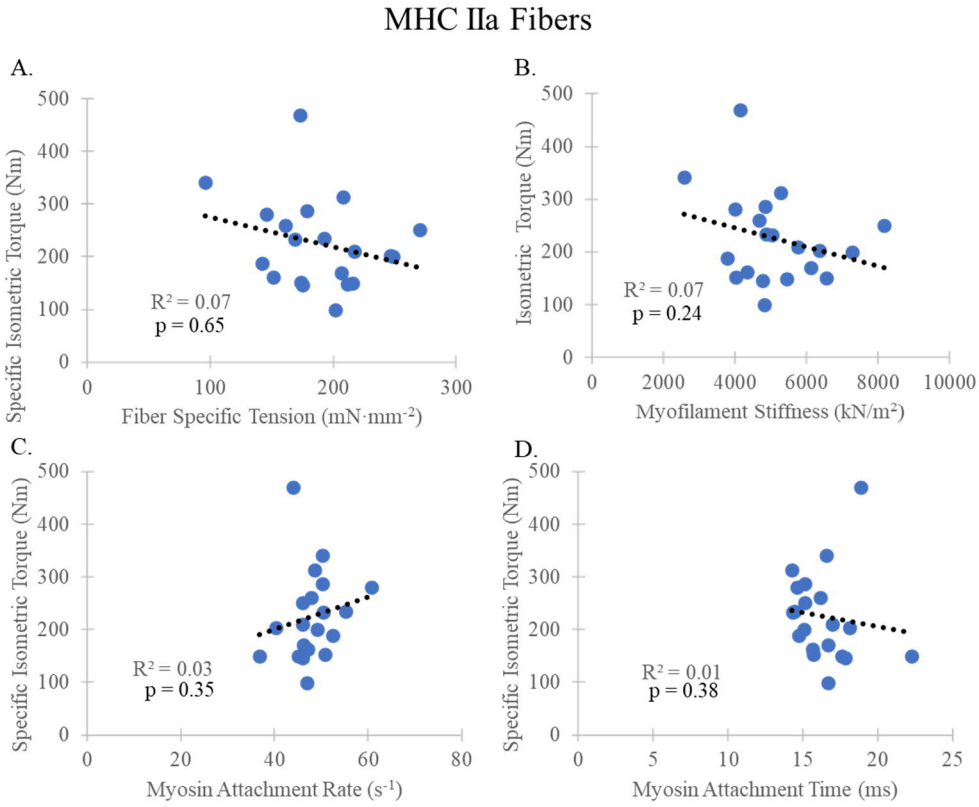

Figure 6.5. Relationships between lipid content and MHC I fiber function. *A)* Relationship between lipid area fraction and single fiber specific tension *B)* Relationship between lipid area fraction and myofilament stiffness *C)* Relationship between lipid area fraction and myosin attachment rate *D* Relationship between lipid area fraction and myosin attachment time. All data for single fibers represent myosin heavy chain I isoforms.

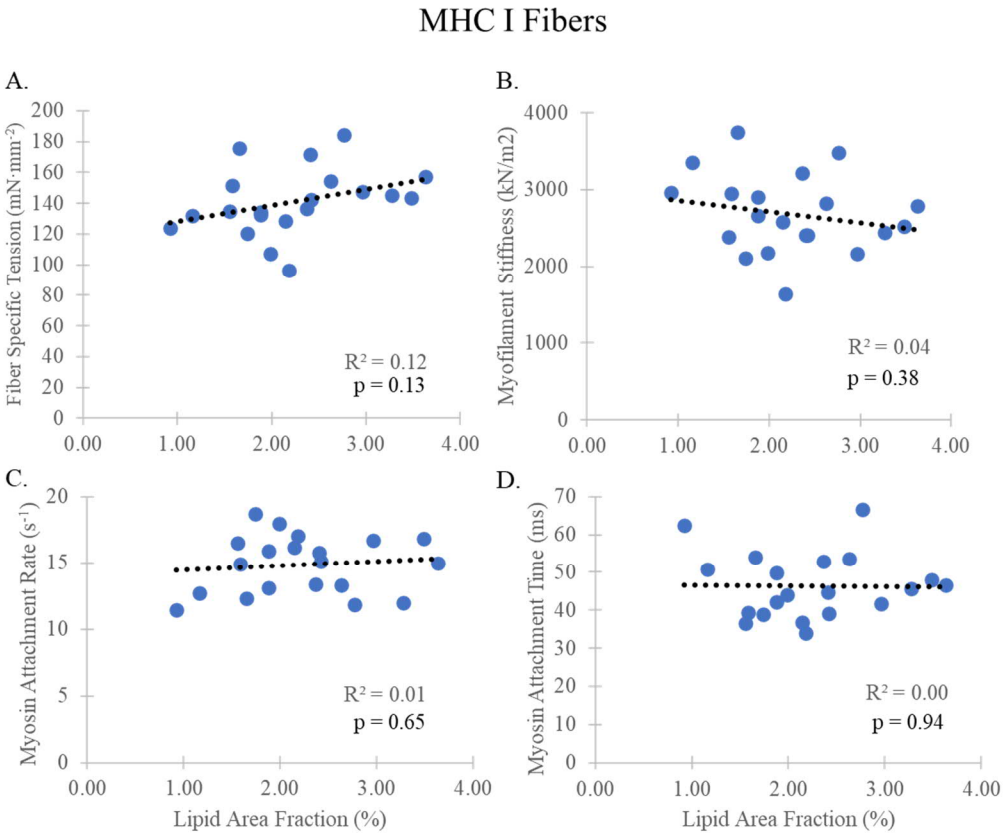

Figure 6.6. Relationships between lipid content and MHC IIa fiber function. *A)* Relationship between lipid area fraction and single fiber specific tension *B)* Relationship between lipid area fraction and myofilament stiffness *C)* Relationship between lipid area fraction and myosin attachment rate *D* Relationship between lipid area fraction and myosin attachment time. All data for single fibers represent myosin heavy chain IIa isoforms.

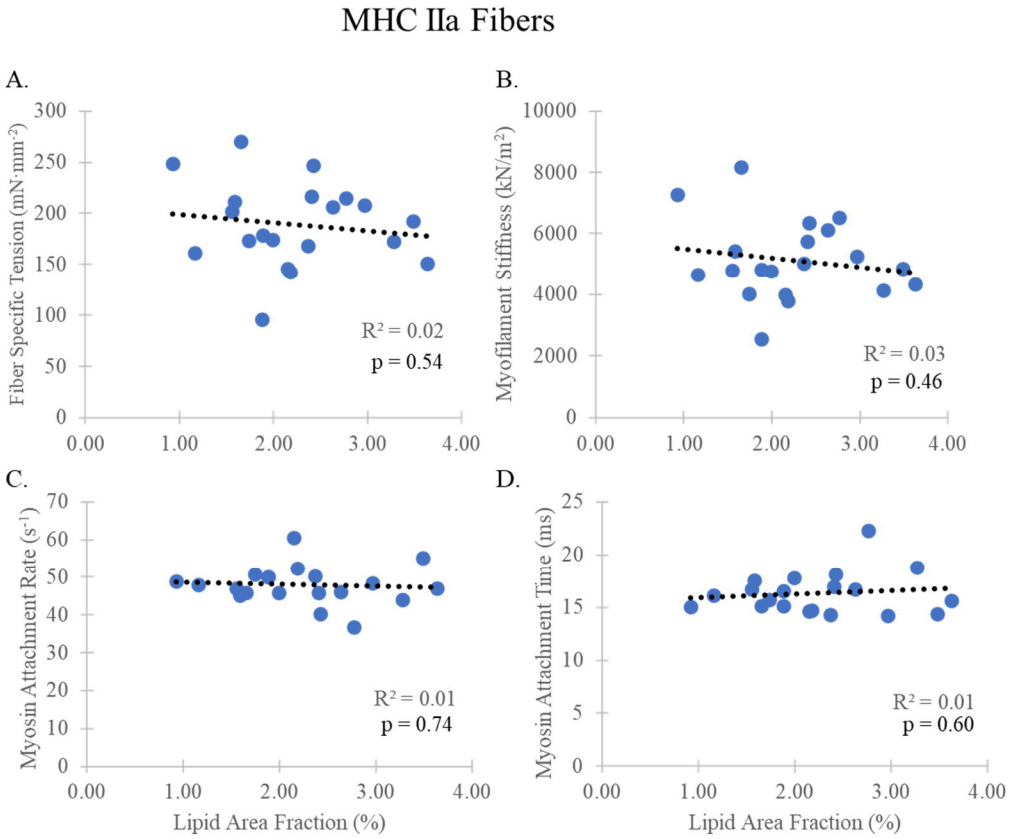

CHAPTER 7

DISSERTATION SUMMARY

The goal of this dissertation work was to clarify the role of fat content in the structure and mechanical function of human skeletal muscle. This goal was evaluated at multiple scales to identify the variables that may contribute to impairments in muscle strength. Size does not fully explain variations in muscle strength, therefore there are other factors that contribute to the observed differences in muscle function between many populations. Muscle size, fat content, architecture, and function are intricately linked, however many of the relationships between these components have not been evaluated in young adults. This dissertation is composed of three studies that utilized *in vitro* and *in vivo* techniques across multiple scales to identify other factors that may contribute to variations in mechanical muscle function, with a focus on the role of fat content. There have been many studies that have reported relationships between fat content and various measures of muscle performance (153, 178, 207, 229, 240). However, a clear limitation of these investigations is that most of these findings cannot be interpreted without consideration for the confounding effects of inactivity, aging, or disease on their outcomes. Unlike the mechanisms for fat-induced muscle impairment, the relationship between muscle architecture and mechanical function is well established (147). However, very few investigations have evaluated each of these components of muscle structure and their relationship with muscle function in the same study cohort. Another clear gap in this area is the lack of research that has evaluated muscle size, composition, and function (Figure 6.1) across multiples anatomical levels (e.g., molecular, cellular, organ, organism,

Figure 1.2). It was for these reasons that we sought to elucidate the potential effects of fat on the structure and function of skeletal muscle.

Fat is a tissue with clinical and functional relevance, and is stored in many depots throughout the body. Intramuscular fat has been increasingly used as a variable of interest for research in aging (48, 157) and clinical research (99, 202). Study 1 (Chapter 4) compared the fat content between three commonly used methods: Histochemical staining (HCS), magnetic resonance spectroscopy (MRS), and magnetic resonance imaging (MRI). Previous studies have shown agreement between *in vivo* methods of fat quantification (55, 57, 172), but few have compared *in vitro* and *in vivo* measures of IMCL. Further, this study provided details on the agreement between fat content at the cellular and organ levels. We expected *in vitro* and *in vivo* measurements of IMCL to agree with one another, since they are meant to measure lipids at the same location (H 1.1). We also hypothesized that IMCL would have a relationship with FF (%), due to the modest levels of fat content in our sample of young adults (H 1.2a, H 1.2b). A key finding was that quantification of IMCL content by ORO (%) and MRS (IMCL/TCr) do not agree with one another in this cohort. We also concluded that IMCL normalized to both TCr and water via MRS agreed with one another, but showed the most variation when compared to ORO and Dixon analyses (Figure 4.6). Our data should be used in combination with reviews comparing the strengths and limitations of different quantification methods (210) to ensure the appropriate method for their sample, and accurate interpretation of data between modality or muscle group.

In study 2 (Chapter 5), we quantified the relationships between quadriceps FF (%) and measures of muscle architecture (H 2.1a-c), and function (H 2.2). Muscle diffusion

characteristics and the effect of biological sex on study variables was also explored. Previous studies have estimated the effects of fat content and architecture on muscle function, but very few have evaluated both components in the same study cohort (114). Based on previous research (13, 39, 147, 155), we hypothesized that FF (%) would have relationship with pennation angle (°), tract length (mm), and curvature (m^{-1}) but not measures of muscle function (i.e., isometric, or isokinetic torque (Nm), peak contraction velocity ($deg \cdot s^{-2}$)). We expected fat content to derange the orderly structure of skeletal muscle, but we did not expect the levels of fat to be great enough to impair maximal muscle strength in moderately active young adults. We discovered a relationship between FF and tract length, suggesting that fat content interrupts muscle fascicles at the organ level of the quadriceps (Figure 1.1). However, FF was not related to any measures of muscle performance. This is contrary to consistent findings of a relationship between fat content and functional performance in older adults (36, 224), animal models (7, 16), and those with musculoskeletal disease (178, 250). This suggests that *1)* the effects of aging or disease have a greater effect on muscle strength than fat content or *2)* there is a threshold of fat accumulation that is necessary for fat to directly interfere with the process of force production. Muscle curvature was related to isometric and isometric torque, while pennation angle had a relationship only with isometric torque. Curvature has been highlighted as a potential variable of interest for research aimed at strain development and perfusion patterns, particularly in repeated or submaximal contractions. These results support inclusion of muscle curvature in future study design. Our findings provide novel data on architecture and diffusion by DTI, and their relationships with fat content and function along the length of the entire thigh.

Study 3 (Chapter 6) compared the fat content and function of whole muscle with single fibers *in vitro* and *in vivo.* This study also quantified the relationships between lipid content and cross-bridge kinetics in single fibers. Previous work has demonstrated a relationship between single fiber function and whole muscle performance (45, 168, 169). However, fiber area and function are preserved in some populations compared to controls, despite differences in whole muscle function (100, 201). There has also been limited research that has addressed the potential effects of IMCL on single fiber function (Figure 6.1). Based upon the results of study 1, we hypothesized that there would not be a relationship between measures of fat content at the whole muscle and single fiber levels (H 3.1). We expected single fiber and whole muscle strength to be related in MHC IIA fibers since these isoforms produce larger forces than MHC I fibers (144, 166) (H 3.2 a-c). Finally, we wanted to quantify the relationship between IMCL and single fiber kinetics (H 3.3 a-c). We expected MHC IIA fibers to have a stronger relationship with IMCL because MHC I fibers have an oxidative phenotype; therefore, they are designed to function with higher lipid content when compared to MHC IIa fibers. Like Study 1, there was no relationship between FF (%) and IMCL (%). Our sample had a wide range of BMIs, so this result provides insight into the patterns of fat infiltration in younger adults. Similarly, cross-bridge kinetics were not related to whole muscle function across a range of contraction velocities. This is a consequential finding, as it suggests cross-bridge kinetics play a minimal role in whole muscle performance in the absence of aging or musculoskeletal disease. Our final set of hypotheses were also not supported, as measures of IMCL were not related to cross-bridge kinetics. We are unaware of any other studies which have reported the relationship between IMCL and cross-bridge kinetics in young

adults. The implications of these findings are relevant to work on IMCL and function in other populations, because these results indicate that increased IMCL accumulation is an indicator of fiber dysfunction, rather than a direct cause.

Significance

This work proposed several questions that were addressed by our findings (page 37). In short, comparisons of fat content between some of the commonly used methods of fat quantification (e.g., ORO, MRS, and MRI) are not in agreement. Fat content at the organ level does not reflect IMCL content in moderately active young adults, regardless of BMI status. This provides insight on the patterns of fat accumulation in younger adults, which should be compared to data in older adults and those with musculoskeletal disease (99, 211). Intramyocellular lipid content *in vitro* does not have a relationship with single fiber function, suggesting that greater levels of lipid or a decline in structural integrity of myofibers may be necessary to impair function at this level. Fat content *in vivo* may potentially disrupt the length of muscle fascicles, but does not impair maximal muscle performance in the quadriceps, like our findings related to fat and function at the single fiber level. We also provided novel diffusion data in whole muscle, and information regarding the sex-based differences in diffusion and architecture by DTI. Our use of highly sensitive modalities at multiple organizational levels allowed us to provide a complete appraisal of the role of fat content in the disorganization of muscle structure and impairment of mechanical muscle function. Our findings, taken with the literature, suggest that greater fat fractions may disrupt muscle fascicle length, but not enough to impair maximal strength in this group. Our research also demonstrated that levels of fat accumulation in the body or quadriceps are not necessarily representative of cellular lipid

content. These data indicate that there may be a threshold of fat accumulation that is necessary to induce mechanical muscle dysfunction, even in healthy adults. Fat and mechanical function must be evaluated at the same anatomical scale for clear interpretations of their relationship in muscle. These conclusions have implications in the clarification of fat's contribution in muscle structure and function. In cohorts of young, moderately active adults that are free of musculoskeletal disease, it appears that fat content is not a major factor mechanical muscle function. The proposed mechanisms for fat-induced muscle impairment in our conceptual framework (Figure 1.1) have been updated with our findings in Figure 7.1.

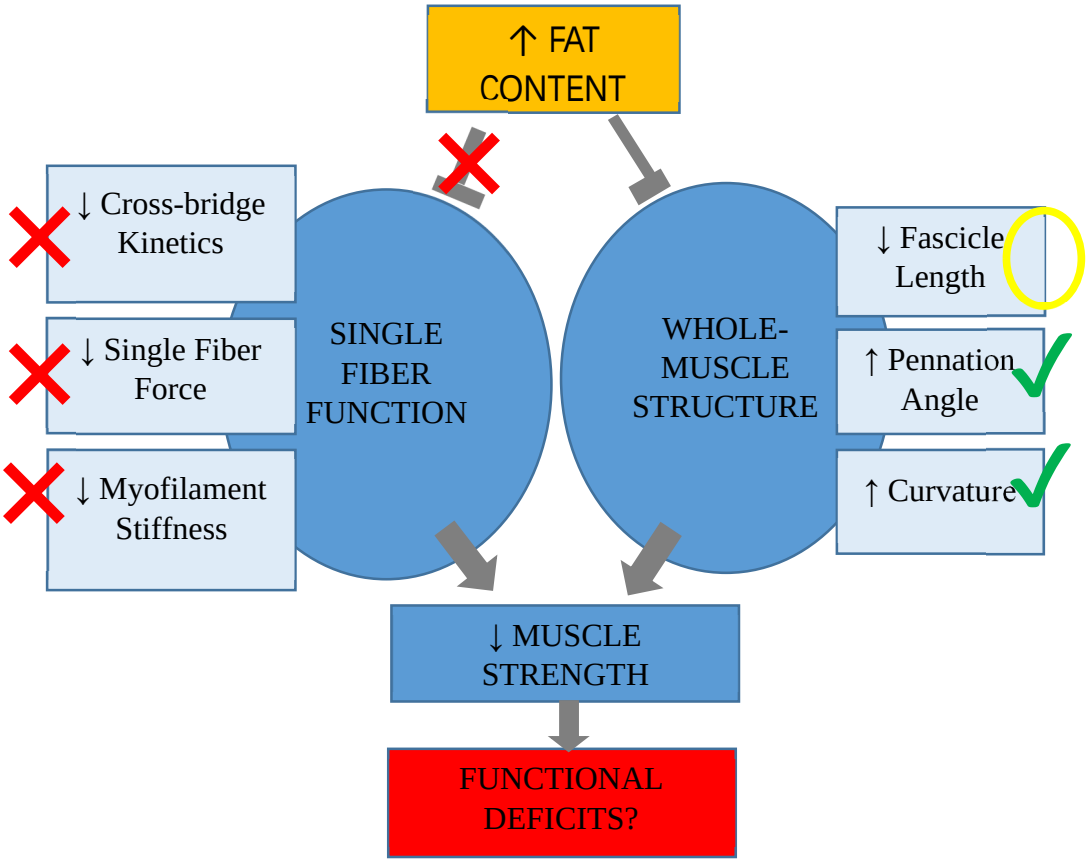

Figure 7.1. **Effects of fat content in limiting functional capacity.** Fat content was not related to any measures of single fiber function (red X). While fat content did have a modest relationship with fascicle length in whole muscle (yellow circle), this was not enough to impair muscle strength. Pennation angle and curvature were the only structural variables related to muscle strength in young adults (green check).

Future Directions

This dissertation provides a wealth of information about the role of fat content in the structure and function of skeletal muscle. While more research needs to be undertaken to clarify the exact mechanisms by which force may impair contractile function, our research has provided strong support for the view that fat content does not disrupt single fiber or whole muscle mechanical function in younger adults. These results are in direct conflict with conclusions drawn from work in older adults, those with pathological conditions, and animal models (7, 16, 36, 56, 178, 224). This dissertation used various sophisticated, sensitive, and reliable methods to pinpoint the specific variables worthy of

further investigation to explain the additional factors which contribute to variations in muscle function. The literature has compared the agreement between methods of *in vivo* fat quantification (54, 55, 86, 110, 172, 243), however our research has provided much needed data comparing IMCL measurement between *in vivo* and *in vitro* methods. Magnetic resonance imaging, ^{1}H-MRS, and ORO are all commonly used in the literature, and our findings can be referenced by clinicians, researchers, and practitioners to identify the modality that would be most suitable for their subject population or research question. Additionally, future work should take note of the modest IMCL and FF values in this sample, despite a wide range of BMIs. We propose that future studies continue to control for physical activity in the assessment of fat content whenever possible, so that researchers may quantify the contribution of physical activity on study outcomes. Dixon and DTI were used for quantification of fat and architecture, respectively. Currently, these MRI techniques are among the most comprehensive modalities, and can provide data across the length of a muscle. The use of Dixon imaging has been acknowledged as the gold standard for quantification (55, 152), however the utilization of DTI in the assessment of skeletal muscle is < 30 years old (11, 234). The additional data that was provided by DTI, such as muscle curvature and variability in fascicle orientation, are a starting point for an entire area of research on muscle structure. Specifically, alterations in joint position, and changes in intramuscular pressure. Some of this work has already been published (43, 53, 173). Researchers should also use DTI in populations with catalogued differences in fat content (e.g., younger vs. older, sedentary vs. highly active, clinical vs. controls) to determine if fat content is consistently associated with tract length. Future work is also needed to explain the sex-based differences in diffusion and

architecture to improve our understanding of how these variables may be interpreted in studies. Finally, future studies should both use static and dynamic measures of muscle performance to get a better understanding of the relationship between fat and function. Dynamic movements are more functionally relevant across populations, so study designs that incorporate submaximal bouts of exercise or fatigue protocols may be more effective at highlighting potential mechanisms for fat-induced muscle impairment.

APPENDIX A

INFORMED CONSENT DOCUMENT (PILOT GRANT PROJECT)

INFORMED CONSENT DOCUMENT
University of Massachusetts
Amherst, MA 01002

Project Title: Mechanical Disruption of Force Transmission by Adipose Tissue in Human Skeletal Muscle

Principal Investigator: Jane Kent, Ph.D
Co-Investigators: Joseph Gordon, M.S.; Miles Bartlett, M.A; Liam Fitzgerald, M.S.; Julia Miehm, B.S.; Mark Miller, Ph.D.; Chad Straight, Ph.D.; John Chase, M.S; Rajakumar Nagarajan, Ph.D.

Your written informed consent is required before you can participate in this project. Please read this document carefully and then sign your name on the last page if you agree to participate. This document is in accordance with regulations for the Protection of Human Research Subjects (45 CFR 46). You are encouraged to ask questions at any time before, during or after participating.

Purpose: Overweight and obesity are significant public health problems and, at this time, we do not know how fat tissue that is deposited inside muscle may affect the muscle's ability to produce force. Thus, the purpose of this study is to understand how fat tissue may interfere with muscle function, which may help us identify ways in which we might reverse obesity-related muscle weakness.

Eligibility: To participate in this study you must be healthy and between 24-45 years of age. You may not have any: neurological or neuromuscular disease; a history of stroke, peripheral vascular disease, cardiac or pulmonary disease; be a smoker; or have a history of any metabolic diseases/disorders. You may not be pregnant. You may not have any metal implants or anything that would prevent you from undergoing a magnetic resonance imaging (MRI) study.

Procedures: Prior to your visit, you were screened by telephone interview for general health, medical history, current medications, usual physical activity habits, and eligibility for the study. Because you are qualified for this study, you were invited to the Life Sciences Laboratories building at the University of Massachusetts Amherst for today's visit. Your next steps are as follows:

Step 1: Paperwork and Magnetic Resonance Scanning (~90 minutes)

Upon arriving at the Life Sciences Laboratories, you will be asked to read this Informed Consent document. We encourage you to ask any questions you may have about the study procedures. Following completion of this consenting procedure, you will be asked to complete a Medical History Form, Physical Activity

Readiness Questionnaire, and Magnetic Resonance Safety Questionnaire. We will then measure your blood pressure while you are seated, and obtain your height and weight.

Next, we will review your Magnetic Resonance Safety Questionnaire, have you remove all jewelry, and change into paper scrub pants. We will scan you for metal using a hand-held metal detector. You will also walk through a metal detector similar to those used at airports, and then we will escort you to the Magnet Room, where you will be positioned on your back on the exam bed, with your arms resting comfortably at your side. We will lay a flexible mat on the thigh of your dominant leg, and move you into the magnet. We will use the flexible mat to obtain images of your thigh muscles. This will take about 15 minutes. We will then remove you from the magnet and replace the mat with a small curved piece of plastic that contains a pair of copper coils. This set of coils is similar to the mat, but provides information about the chemical composition of your muscle using a technique called magnetic resonance spectroscopy (MRS). Together, the MRI and MRS techniques will allow us to measure the amount and location of fat deposited within your thigh muscles. These measures will be obtained while you are lying quietly on the exam bed. Altogether, we expect these procedures to take about 1 hour.

Step 2: Muscle Strength (~30 minutes)

After we have completed the MRI and MRS procedures, we will escort you upstairs to the Human Testing Center to perform a muscle contraction protocol. To begin, you will perform 5 minutes of light cycling exercise on a stationary bike, and then 2-3 sets of knee-extension contractions, which will allow you to warm up and become familiarized with our testing equipment. Then, you will perform 2-3 maximal isometric (i.e., 'static') contractions, each lasting 3-4 seconds, with at least one minute of rest between contractions. You will then perform multiple sets (approximately 5-8) of 3 maximal-effort dynamic (i.e., with movement) contractions at speeds ranging from very slow to very fast. Again, at least one minute of rest will be given between each set of 3 contractions. We expect these procedures to take about 30 minutes.

Lastly, before leaving, we will give you a small device to wear at your waist, which will measure the amount and intensity of your physical activity over the next 7 days. We will instruct you on how and when to wear this device, and how to keep a simple physical activity log book. At the end of this 7-day period, a member of the Muscle Physiology Laboratory will pick up the device and your log book at a time and location that is most convenient for you.

Subject Enrollment/Length of Study: We expect to enroll 20 participants in this study. Your participation will include one visit lasting approximately 2 hours.

Possible Risks and Discomforts: There are minimal risks associated with the procedures used in this research study. During any type of exercise, there are slight health risks, such as cardiovascular events, muscle soreness, and fatigue, but these risks are minimal during the type of testing used here. Any muscle soreness that you might develop would be expected to go away in 2-3 days.

Magnetic Resonance Spectroscopy (MRS) and Imaging (MRI) – The United States Food and Drug Administration (FDA) has established guidelines for magnet strength and exposure to radio waves, and we carefully observe those guidelines. No ill effects have been reported for the radio wave exposure associated with this protocol. Please note that no ionizing radiation, such as used in x-rays, is involved with this technique. Some people may feel uncomfortable or anxious while in the MR scanner, which is a large magnet. If this happens to you, you may ask to stop the study at any time and we will take you out of the scanner. On rare occasions, some people might feel dizzy, get an upset stomach, have a metallic taste, feel tingling sensations, or experience muscle twitches. These sensations usually go away quickly but please tell the research staff if you experience them.

MRI and MRS pose some risks for certain people. If you have a pacemaker or certain types of metal objects inside your body, you may not be in this study because the strong magnet used for these MR studies might harm you. Another risk is a metallic object flying through the air toward the magnet and hitting you. To reduce this risk, we require that all people involved with the study remove all metal from their person and all metal objects from their pockets. Nothing metal can be brought into the magnet room at any time. Also, once you are in the magnet, the door to the room will be closed so that no one accidentally brings a metal object near the magnet while you are in it.

Please read the Magnetic Resonance Safety Questionnaire and complete it very carefully. Those questions are for your safety. Take a moment now to be sure that you have read this and be sure to ask any questions and tell us any information you think might be important. **Even if you think that it is probably okay, we would rather have you ask us to make sure.**

If you experience significant claustrophobia during the MR testing, you will be removed immediately. You will be positioned feet-first in the magnet and your head will remain near the opening, which will minimize the chances of claustrophobia.

What if there is an unexpected finding on my MRI scan? The investigators for this research project are not licensed or trained diagnosticians or clinicians. The testing performed in this project is not intended to find abnormalities, and the images or data collected do not comprise a diagnostic or clinical study. However, on occasion the investigators may perceive an abnormality. When this occurs, UMass Amherst researchers will consult with a specialist. If the specialist determines that additional inquiry is warranted, the researcher will contact you. In such a case, you are advised to consult with a licensed physician to determine whether further examination or treatment would be prudent. Although the images collected for this research project do not comprise a diagnostic or clinical study, the images can be made available to you for clinical follow-up.

Confidentiality: Steps are taken to protect the identities of participants and the data collected in this study. The Informed Consent, Physical Activity Readiness Questionnaire, and MR Safety Questionnaire (all of which will have your name on them) will be stored and locked in a filing cabinet within a locked office. All other data collection sheets will be coded with your participant number and the study title instead of your name, so that no potential identifiers can be linked back to you. Data collection sheets and lists of participant codes and names are kept separate from all other study materials. All electronic data will be kept on a password-protected computer in a locked office. Any data that are published or used in a presentation will not include any names or identifiers that could link back to you.

In Case of Injury: In the unlikely event of an injury resulting directly from participation in this study, we will do everything we can to assist you in seeking medical treatment. The University of Massachusetts does not have a program for compensating participants for injury or complications related to human subject research.

Benefits: You will receive no direct benefit from participating in this study.

Costs and Reimbursement: There is no cost to participate in this study. You will be given a $20 gift card if you complete all of the procedures planned for this visit.

Withdrawal from Participation: Participation in this research is voluntary. You have the right to withdraw or refuse to continue from the study at any point, without prejudice.

Alternative Procedures: The procedures described above are non-invasive techniques that are commonly used in muscle research. There are no other non-invasive techniques that can be used to obtain the information necessary with the high-quality resolution required for this study.

Request for Additional Information: You are encouraged to ask questions about the study. The investigators will attempt to answer all of your questions to the best of their knowledge. The investigators fully intend to conduct the study with your best interest, safety, and comfort in mind. Please address any questions regarding the study to the Muscle Physiology Laboratory. Our phone number is (413) 545-5305. We can also be reached by email at umassmplab@umass.edu. You may also address questions to Dr. Kent by calling her at (413) 545-9477 or by emailing her at jkent@kin.umass.edu. If you would like to speak with someone not directly involved in the research study, you may contact the Human Research Protection Office at the University of Massachusetts via email at humansubjects@ora.umass.edu; telephone (413) 545-3428; or mail at the Human Research Protection Office (HRPO), Mass Venture Center, 100 Venture Way, Suite 116, Hadley, MA, 01035.

Subject Statement of Voluntary Consent: By signing this form, I am agreeing to voluntarily enter this study. I understand that, by signing this document, I do not waive any of my legal rights. I have had a chance to read this consent form, and it was explained to me in a language that I use and understand. I have had the opportunity to ask questions and have received satisfactory answers. A copy of this signed Informed Consent Form will be given to me.

Participant's name (please print) Address

Signature Phone Number Date

STUDY REPRESENTATIVE STATEMENT:
The investigator has read and understands the federal regulations for the Protection of Human Research Subjects (45 CFR 46) and agrees to comply with all of its clauses to the best of their ability. The investigator also pledges to consider the best interests of the subject beyond the explicit statement contained in the aforementioned federal regulations and to exercise professional expertise to protect the rights and welfare of the subject.

Signature of Person Obtaining Consent Name (please print) Date

APPENDIX B

INFORMED CONSENT DOCUMENT (NIH R21)

INFORMED CONSENT DOCUMENT
University of Massachusetts
Amherst, MA 01002

Project Title: *Mechanical Disruption of Force Transmission by Adipose Tissue in Skeletal Muscle*

Principal Investigator: Jane Kent, Ph.D
Co-Investigators: Joseph Gordon III, M.S.; Miles Bartlett, M.A; Liam Fitzgerald, M.S.; Julia Miehm, B.S.; Mark Miller, Ph.D.; Chad Straight, Ph.D.; Rajakumar Nagarajan, Ph.D.

Your written informed consent is required before you can participate in this project. Please read this document carefully and then sign your name on the last page if you agree to participate. This document is in accordance with regulations for the Protection of Human Research Subjects (45 CFR 46). You are encouraged to ask questions at any time before, during or after participating.

Purpose: Overweight and obesity are significant public health problems and, at this time, we do not know how fat tissue that is deposited inside muscle may affect the muscle's ability to produce force. If fat located in muscle reduces its strength, then overweight and obese people may have a decreased ability to engage in physical activities that promote health. Thus, the purpose of this study is to understand how fat tissue may interfere with muscle function, which may help us identify ways in which we might reverse obesity-related muscle weakness. We will use several innovative techniques to measure the strength, anatomy and pattern of fat in your thigh muscles. In some people, we will also take a small amount of muscle tissue from your thigh, in order to study how well muscle cells contract at a very basic level.

Eligibility: To participate in this study you must be healthy and between 24-45 years of age. You must have a Body Mass Index (BMI) of 18.5-24.9 ("normal" BMI) or 30-40 Kg/m^2 ("high" BMI), and may not have any: neurological or neuromuscular disease; a history of stroke, peripheral vascular disease, cardiac or pulmonary disease; be a smoker; or have a history of any metabolic diseases/disorders. You may not be pregnant. You may not have any metal implants or anything that would prevent you from undergoing a magnetic resonance imaging (MRI) study.

Procedures: Before your visit, you were screened by telephone interview for general health, medical history, current medications, usual physical activity habits, and overall eligibility for the study. Because you are qualified for this study, you

were invited to the Life Sciences Laboratories building at the University of Massachusetts Amherst for today's visit. Your next steps are as follows:

Visit 1: Paperwork, Familiarization and Physical Activity Monitor (~60 minutes)

Upon arriving at the Life Sciences Laboratories, you will be asked to read this Informed Consent document. We encourage you to ask any questions you may have about the study procedures. Following completion of this consenting procedure, you will be asked to complete a Medical History Form, Physical Activity Readiness Questionnaire, and Magnetic Resonance Safety Questionnaire. We will then measure your blood pressure and heart rate, and obtain your height and weight.

Next, you will be familiarized with the muscle strength testing procedures on our dynamometer, which is a leg exercise machine similar to one you may have seen at a gym. You will practice 2-3 sets of knee-extension contractions, until you are comfortable with this procedure. Then, we will give you a physical activity monitor, which is a small device worn around your waist. This will measure the amount and intensity of your daily physical activity for 7 days. We will also give you information on how and when to wear this device, and how to record your physical activity in a log book. At the end of this 7-day period, the monitor will be returned at visit 2, or a member of the Muscle Physiology Laboratory will pick up the device and physical activity log book at a time and location that is most convenient for the participant. At the end of this first visit, we will walk downstairs to the Human Magnetic Resonance Center, and show you where the MRI studies will take place during your second visit.

Visit 2: Magnetic Resonance and Muscle Strength Measures (~90 minutes)

Upon arrival at the Human Magnetic Resonance Center, we will review your Magnetic Resonance Safety Questionnaire, and have you remove all jewelry and change into paper scrub pants. We will scan you for metal using a hand-held metal detector. You will also walk through a metal detector similar to those used at airports. We will then escort you into the Magnet Room, where you will be positioned on your back on the exam bed, with your arms resting comfortably at your side. We will lay a flexible mat on the thigh of your dominant leg, and move you into the magnet. We will use the flexible mat to obtain images of your thigh muscles. This will take about 30 minutes. We will then remove you from the magnet and replace the mat with a small curved piece of plastic that contains a pair of copper coils. This set of coils is similar to the mat, but provides information about the biochemistry of your muscle using a technique called magnetic resonance spectroscopy (MRS). Together, the MRI and MRS techniques will allow us to measure the amount and location of fat deposited within your thigh muscles. These measures will be obtained while you are lying quietly on the exam bed. Altogether, we expect these procedures to take about 1 hour.

After we have completed the MRI and MRS procedures, we will walk you upstairs to the Human Testing Center to perform the muscle strength protocol. To begin, you will perform 5 minutes of light cycling exercise on a stationary bike. Next, we will position you on the dynamometer (as at Visit 1) and have you perform 2-3 maximal-effort static contractions, each lasting 3-4 seconds, with at least one minute of rest between contractions. Then, you will perform 7-8 sets of 3 maximal-effort dynamic (i.e., with movement) contractions at speeds ranging from very slow to very fast. Again, at least one minute of rest will be given between each set of 3 contractions. We expect these procedures to take about 30 minutes.

Visit 3: ***Skeletal Muscle Biopsy (~90-120 minutes)***

Upon arriving at the Life Sciences Laboratories for your biopsy, a small amount of blood (20 mL or ~2 tablespoons) will be taken from your forearm. After this, you will undergo a biopsy of one thigh muscle (vastus lateralis) that underwent the study procedures from day 2 under localized lidocaine anesthesia. The biopsy procedure allows us to obtain muscle tissue to test the function of the individual fibers or cells that make up your muscles.

You will be instructed not to consume any anti-inflammatory drugs (i.e., Ibuprofen or aspirin) or any aspirin-containing drugs such as Alka-Seltzer, Pepto-Bismol, or certain decongestants that contain anti-inflammatory drugs (i.e. Dristan) for 24 hours before and 4 days after your muscle biopsy, to reduce your risk of bleeding. You will be given a telephone number that may be used to reach the Muscle Biology Laboratory. If you are unsure as to whether a medication you intend to take contains aspirin, it is strongly advised that you call one of the study investigators before taking the medication. A trained physician will perform the needle biopsy procedure, which involves the removal and examination of a small piece of muscle tissue. You will first be given a local anesthetic. Then, a small incision (about ½ inch) will be made in your skin and fascia. A needle will then be inserted into your muscle, and a small "plug" of tissue will be removed from the muscle. This “plug” is about the size of 2-3 grains of rice. More than one needle insertion may be needed to obtain a large enough specimen for testing and examination.

The muscle that we will biopsy is located at the outer thigh, about mid-way between your knee and hip. You will feel some pressure or "tugging" sensations. Many people experience mild discomfort, but some volunteers find the biopsy procedure to be painful. If there is pain, the physician will provide more anesthetic to the area to reduce the pain. The anesthetic is called Lidocaine (like Novocaine) and may burn or sting when injected (before the area becomes numb). After the anesthetic wears off, the area may be sore for about a week, and this soreness may limit your activity. You will be contacted by a member of the Muscle Physiology Laboratory for a biopsy wound check 2-3 days following this procedure, and muscle tissue collected may be used for future unspecified research.

Subject Enrollment/Length of Study: We expect to enroll 48 participants in this study. Your participation will include 2-3 visits lasting a total of 3-5 hours. Approximately 18 of the 48 participants will complete only visits 1 and 2, and approximately 30 participants will complete all 3 visits.

Possible Risks and Discomforts: During any type of exercise, there are slight health risks, such as cardiovascular events, muscle soreness, and fatigue, but these risks are minimal during the type of testing used here. Any muscle soreness that you might develop would be expected to go away in 2-3 days. Potential risks and discomforts associated with the MR and biopsy procedures are described next. There is also a slight risk of a breach of confidentiality with documents that indicate your identity, but this risk is minimized by taking the steps presented in the confidentiality section.

Magnetic Resonance Spectroscopy (MRS) and Imaging (MRI): The United States Food and Drug Administration (FDA) has established guidelines for magnet strength and exposure to radio waves, and we carefully observe those guidelines. No ill effects have been reported for the radio wave exposure associated with the planned measures. Please note that no ionizing radiation, such as used in x-rays, is involved with this technique. Some people may feel uncomfortable or anxious while in the MR scanner, which is a large magnet. If this happens to you, you may ask to stop the study at any time and we will take you out of the scanner. On rare occasions, some people might feel dizzy, get an upset stomach, have a metallic taste, feel tingling sensations, or experience muscle twitches. These sensations usually go away quickly but please tell the research staff if you experience them.

MRI and MRS pose some risks for certain people. If you have a pacemaker or certain types of metal objects inside your body, you cannot be in this study because the strong magnet used for these MR studies might harm you. Another risk to participants is a metallic object flying through the air toward the magnet and hitting you. To reduce this risk, we require that all people involved with the study remove all metal from their person and all metal objects from their pockets. Nothing metal can be brought into the magnet room at any time. Also, once you are in the magnet, the door to the room will be closed so that no one accidentally brings a metal object near the magnet while you are in it.

Please read the Magnetic Resonance Safety Questionnaire and complete it very carefully. These questions are for your safety. Take a moment now to be sure that you have read this and be sure to ask any questions and tell us any information you think might be important. **Even if you think that it is probably okay, we would rather have you ask us to make sure.**

If you experience significant claustrophobia during the MR testing, you will be removed immediately. You will be positioned feet-first in the magnet and your head will remain near the opening, which will minimize the chances of claustrophobia.

Skeletal Muscle Biopsy: The risks are small and may include the following: infection (a slight risk any time the skin is broken), bleeding of the site, hematoma (blood collected beneath the skin that under very rare conditions could require surgery), bruising of the area, and damage to the muscle tissue or other tissues in the area (very rare). These risks are very low because there are no big blood vessels near the biopsy site and because the muscle tissue usually stops any bleeding by pressing against itself. Also, studies have shown that the muscle rapidly repairs itself after the biopsy. It is possible that you may have temporary numbness around the biopsy site for several days to weeks. At the biopsy site, a small scar about 1 cm long or less could result, but usually this will fade in time. Risks are minimized by having a trained and qualified medical physician perform the biopsy.

What if there is an unexpected finding on my MRI scan? The investigators for this research project are not licensed or trained diagnosticians or clinicians. The testing performed in this project is not intended to find abnormalities, and the images or data collected do not comprise a diagnostic or clinical study. However, occasionally in the process of research, investigators may perceive an abnormality, the health implications of which may not be clear. When this occurs, UMASS Amherst researchers will consult with a radiologist. If the radiologist determines that an additional inquiry is warranted, the researcher will then contact you regarding the radiologist's opinion of the unexpected finding(s).

In such a case, you are advised to consult with a licensed physician to determine whether further examination or treatment would be prudent. Although the images collected for this research project do not comprise a diagnostic or clinical study, the images can be made available to you for clinical follow-up. The costs for any care that will be needed to diagnose or treat an unexpected finding(s) would not be paid for by University of Massachusetts, Amherst. These costs would be your responsibility. If you have further tests done by your licensed physician, those results will then become part of your medical record, which may affect your current and future health or life insurance. Regardless of the health implications, the discovery of an unexpected finding(s) may cause you to feel anxious or worried. You may wish to talk to your physician or a qualified mental health clinician. You can contact the Center for Counseling and Psychological Health (CCPH) at (413) 545-2337 (Mon-Fri from 8-5pm) - on weekends or after 5pm, call (413) 577-5000 and ask for the CCPH clinician on call. You can also contact the Psychological Services Center at 413-545-0041 (Monday-Friday 8am-5pm) or psc@psych.umass.edu. In a serious emergency, remember that you can also call 911 for immediate assistance."

Confidentiality: Steps are taken to protect the identities of all participants and the data collected in this study. The Informed Consent, Physical Activity Readiness Questionnaire, MR Safety Questionnaire, and Telephone Screening Form (all of which will have your name on them) will be stored and locked in a filing cabinet within a locked office. All other data collection sheets will be coded with your participant number and the study title instead of your name, so that no potential

identifiers can be linked back to you. Data collection sheets and lists of participant codes and names are kept separate from all other study materials. All electronic data will be kept on a password-protected computer in a locked office. Any data that are published or used in a presentation will not include any names or identifiers that could link back to you.

In Case of Injury: In the unlikely event of an injury resulting directly from participation in this study, we will do everything we can to assist you in seeking medical treatment. The University of Massachusetts does not have a program for compensating participants for injury or complications related to human subject research.

Benefits: You will receive no direct benefit from participating in this study, although you will be provided with personalized information about your health that you may find interesting and/or useful.

Certificate of Confidentiality: The following procedures will be used to protect the confidentiality of your study records. The records and measurements obtained from this study are for research purposes only and will not be included in your medical records. Confidentiality will be maintained throughout the studies. All study data will carry an identifying code, not the actual participant's name to ensure confidentiality. A master key that links names and codes and any identifiable health information will be maintained in a separate and secure location. Identifiable data, including signed consent documents, and the master key will be kept separately from the study data, in a locked cabinet that can only be accessed by the investigators. All electronic data will be stored on a secure server and password-protected computers. The master key will be destroyed 6 years after the close of the study. Only Dr. Kent will have access to this data. At the conclusion of this study, the researchers will publish their findings. Information will be presented in summary format and you will not be identified in any publications or presentations. Research resources generated with funds from this grant will be freely distributed, as available, to qualified academic investigators for non-commercial research. Final data will be shared primarily through peer-reviewed publication. Raw data will be considered for sharing under the rules indicated below. Raw datasets to be released for sharing will not contain identifiers. Data and associated documentation will be made available to users only under a signed and properly executed data-sharing agreement that provides for specific criteria under which the data will be used, including but not limited to a commitment to: 1) using the data only for research purposes; 2) securing the data using appropriate computer technology; and 3) destroying or returning the data after analyses are completed. This research is covered by a Certificate of Confidentiality from the National Institutes of Health (NIH). The researchers with this Certificate may not disclose or use information, documents, or biospecimens that may identify you in any federal, state, or local civil, criminal, administrative, legislative, or other action, suit, or proceeding, or be used as evidence, for example, if there is a court subpoena, unless you have

consented for this use. Information, documents, or biospecimens protected by this Certificate
cannot be disclosed to anyone else who is not connected with the research except, if there is a federal, state, or local law that requires disclosure (such as to report child abuse or communicable diseases but not for federal, state, or local civil, criminal, administrative, legislative, or other proceedings); if you have consented to the disclosure, including for your medical treatment; or if it is used for other scientific research, as allowed by federal regulations protecting research subjects. The Certificate cannot be used to refuse a request for information from personnel of the United States federal or state government agency sponsoring the project that is needed for auditing or program evaluation by the NIH which is funding this project. You should understand that a Certificate of Confidentiality does not prevent you from voluntarily releasing information about yourself or your involvement in this research. If you want your research information released to an insurer, medical care provider, or any other person not connected with the research, you must provide consent to allow the researchers to release it.

Costs and Reimbursement: There is no cost to participate in this study. If you take part in just Visits 1 and 2 (no muscle biopsy), you will be given $40 cash for completing these procedures. If you complete all three visits (including the muscle biopsy), you will be given an additional $150 cash, for a total of $190.

Withdrawal from Participation: Participation in this research is voluntary. You have the right to withdraw or refuse to continue from the study at any point, without prejudice.

Alternative Procedures: The planned procedures include techniques that are commonly used in muscle research. There are no other techniques that can be used to gather the information needed for this project with the kind of high-quality of resolution that is needed in order to answer our research questions.

Request for Additional Information: You are encouraged to ask questions about the study. The investigators will attempt to answer all of your questions to the best of their knowledge. The investigators fully intend to conduct the study with your best interest, safety, and comfort in mind. Please address any questions regarding the study to the Muscle Physiology Laboratory. Our phone number is (413) 545-5305. We can also be reached by email at umassmplab@umass.edu. You may also address questions to Dr. Kent by calling her at (413) 545-9477 or by emailing her at jkent@kin.umass.edu. If you would like to speak with someone not directly involved in the research study, you may contact the Human Research Protection Office at the University of Massachusetts via email at humansubjects@ora.umass.edu; telephone (413) 545-3428; or mail at the Human Research Protection Office (HRPO), Mass Venture Center, 100 Venture Way, Suite 116, Hadley, MA, 01035.

Subject Statement of Voluntary Consent: By signing this form, I am agreeing to voluntarily enter this study. I understand that, by signing this document, I do not waive any of my legal rights. I have had a chance to read this consent form, and it was explained to me in a language that I use and understand. I have had the opportunity to ask questions and have received satisfactory answers. A copy of this signed Informed Consent Form will be given to me.

_____

Participant's name (please print) Address

_____

Signature Phone Number Date

STUDY REPRESENTATIVE STATEMENT:
The investigator has read and understands the federal regulations for the Protection of Human Research Subjects (45 CFR 46) and agrees to comply with all of its clauses to the best of their ability. The investigator also pledges to consider the best interests of the subject beyond the explicit statement contained in the aforementioned federal regulations and to exercise professional expertise to protect the rights and welfare of the subject.

_____

Signature of Person Obtaining Consent Name (please print) Date

APPENDIX C

INFORMED CONSENT (SUB 21; BIOPSIES FOR YOUNG ADULTS)

INFORMED CONSENT DOCUMENT
University of Massachusetts
Amherst, MA 01003

Project Title: *Sub21: Mechanical Disruption of Force Transmission by Adipose Tissue in Skeletal Muscle*

Principal Investigator: Jane Kent, Ph.D.
Co-Investigators: Joseph Gordon III, M.S.; Luke Arieta, B.S.; Miles Bartlett, M.A.; Stuart Chipkin, MD.; Liam Fitzgerald, M.S.; Christopher Hayden, B.S.; Julia Miehm, M.S.; Mark Miller, Ph.D.; Rajakumar Nagarajan, Ph.D.; Chad Straight, Ph.D.

Your written informed consent is required before you can participate in this project. Please read this document carefully, initial each page and sign your name on the last page if you agree to participate. This document is in accordance with regulations for the Protection of Human Research Subjects (45 CFR 46). You are encouraged to ask questions at any time before, during or after participating.

Purpose: Overweight and obesity are significant public health problems and, at this time, we do not know how fat tissue that is deposited inside muscle may affect its ability to produce force. If fat located in muscle reduces its strength, then overweight and obese people may have a decreased ability to engage in physical activities that promote health. The purpose of this study is to understand how fat tissue may interfere with muscle function, which may help us identify ways to reverse obesity-related muscle weakness. We will use several innovative techniques to measure the anatomy and pattern of fat in your thigh muscles.

Eligibility: You may be eligible for this study based upon your being eligible for the "Sex-specific adaptation to different resistance exercise programs in older adults" study (Protocol #2017-4206). To participate in this study you must be healthy and between 65-75 years old. You may not have: neurological or neuro-muscular disease; a history of stroke, peripheral vascular disease, cardiac or pulmonary disease; be a smoker; or have a history of any metabolic diseases/disorders. You may not have any metal implants or anything that would prevent you undergoing a magnetic resonance imaging (MRI) study.

Procedures:

Visit 1: Paperwork and Anthropometrics (~30 minutes)

At Visit 1, you will be asked to read this Informed Consent document. We encourage you to ask any questions you may have about the study procedures. Once consenting is complete, we will review your Health History Questionnaire and MR Safety Screening Questionnaire that was completed previously for the "Sex-specific

adaptation to different resistance exercise programs in older adults" study to determine if any information has changed. We will measure your height, body mass, blood pressure, and heart rate.

Visit 2: Magnetic Resonance Imaging (~90 minutes)

At Visit 2 in the Human Magnetic Resonance Center, we will review your MR Safety Screening Questionnaire, have you remove all jewelry and change into paper scrub pants if needed. We will scan you for metal using a hand-held metal detector, and you will walk through a metal detector similar to those at airports. We will escort you into the Magnet Room, where you will be positioned on your back on the exam bed, with your arms resting comfortably at your sides. We will lay a flexible mat on the thigh of your dominant leg to obtain images of your thigh muscles, and move you into the magnet. This measurement will take about 50 minutes. We will remove you from the magnet and replace the mat with a small curved piece of plastic that contains a pair of copper coils. Before the next scan, you may use the restroom or stretch at this time if needed. This set of coils is similar to the mat, but provides information about the biochemistry of your muscle using magnetic resonance spectroscopy (MRS). This measurement will take about 20 minutes. Together, the MRI and MRS techniques will allow us to measure the amount and location of fat deposited within your thigh muscles.

Subject Enrollment/Length of Study: We expect to enroll 16 participants in this study. Your participation will include 2 visits lasting a total of approximately 2 hours.

Possible Risks and Discomforts: Potential risks and discomforts associated with the MR procedure are described next. There is also a slight risk of a breach of confidentiality with documents that indicate your identity, but this risk is minimized by taking the steps presented in the confidentiality section.

Magnetic Resonance Spectroscopy (MRS) and Imaging (MRI): The United States Food and Drug Administration (FDA) has established guidelines for magnet strength and exposure to radio waves, and we carefully observe those guidelines. No ill effects have been reported for the radio wave exposure associated with the planned measures. Please note that no ionizing radiation, such as used in x-rays, is involved with this technique. Some people may feel uncomfortable or anxious while in the MR scanner, which is a large magnet. If this happens to you, you may ask to stop the study at any time and we will take you out of the scanner. On rare occasions, some people might feel dizzy, get an upset stomach, have a metallic taste, feel tingling sensations, or experience muscle twitches. These sensations usually go away quickly but please tell the research staff if you experience them.

MRI and MRS pose some risks for certain people. If you have a pacemaker or certain types of metal objects inside your body, you cannot be in this study because the strong magnet used for these MR studies might harm you. Another risk to participants is a metallic object flying through the air toward the magnet and hitting you. To reduce this risk, we require that all people involved with the study remove

all metal from their person and all metal objects from their pockets. Nothing metal can be brought into the magnet room at any time. Also, once you are in the magnet, the door to the room will be closed so that no one accidentally brings a metal object near the magnet while you are in it.

Please read the MR Safety Screening Questionnaire and complete it very carefully. These questions are for your safety. Take a moment now to be sure that you have read this and be sure to ask any questions and tell us any information you think might be important. **Even if you think that it is probably okay, we would rather have you ask us to make sure.**

If you experience significant claustrophobia during the MR testing, you will be removed immediately. You will be positioned feet-first in the magnet and your head will remain near the opening, which will minimize the chances of claustrophobia.

What if there is an unexpected finding on my MRI scan? The investigators for this research project are not licensed or trained diagnosticians or clinicians. The testing performed in this project is not intended to find abnormalities, and the images or data collected do not comprise a diagnostic or clinical study. However, occasionally in the process of research, investigators may perceive an abnormality, the health implications of which may not be clear. When this occurs, UMASS Amherst researchers will consult with a radiologist. If the radiologist determines that an additional inquiry is warranted, the researcher will then contact you regarding the radiologist's opinion of the unexpected finding(s). In such a case, you are advised to consult with a licensed physician to determine whether further examination or treatment would be prudent. Although the images collected for this research project do not comprise a diagnostic or clinical study, the images can be made available to you for clinical follow-up. The costs for any care that will be needed to diagnose or treat an unexpected finding(s) would not be paid for by University of Massachusetts, Amherst. These costs would be your responsibility. If you have further tests done by your licensed physician, those results will then become part of your medical record, which may affect your current and future health or life insurance. Regardless of the health implications, the discovery of an unexpected finding(s) may cause you to feel anxious or worried. You may wish to talk to your physician or a qualified mental health clinician. You can contact the Center for Counseling and Psychological Health (CCPH) at (413) 545-2337 (Mon-Fri from 8-5pm) - on weekends or after 5pm, call (413) 577-5000 and ask for the CCPH clinician on call. You can also contact the Psychological Services Center at 413-545-0041 (Monday-Friday 8am-5pm) or psc@psych.umass.edu. In a serious emergency, remember that you can also call 911 for immediate assistance.

In Case of Injury: In the unlikely event of an injury resulting directly from participation in this study, we will do everything we can to assist you in seeking medical treatment. The University of Massachusetts does not have a program for compensating participants for injury or complications related to human research.

Benefits: You will receive no direct benefit from participating in this study, although you will be provided with personalized information about your health that you may find interesting and/or useful.

Confidentiality: Steps are taken to protect the identities of all participants and the data collected in this study. Your Informed Consent and any other forms with your name on them will be stored and locked in a filing cabinet within a locked room. All other data collection sheets will be coded with your participant number and study title instead of your name, so that no potential identifiers can be linked back to you. Data collection sheets and lists of participant codes and names are kept separate from all other study materials. All electronic data will be kept on a password-protected computer in a locked room. Any data that are published or used in a presentation will not include any names or identifiers that could link back to you.

The following procedures will be used to protect the confidentiality of your study records. The records and measurements obtained from this study are for research purposes only and will not be included in your medical records. Confidentiality will be maintained throughout the studies. All study data will carry an identifying code, not the actual participant's name to ensure confidentiality. A master key that links names and codes and any identifiable health information will be maintained in a separate and secure location. Identifiable data, including signed consent documents, and the master key will be kept separately from the study data, in a locked cabinet that can only be accessed by the investigators. All electronic data will be stored on a secure server and password-protected computers. The master key will be destroyed 6 years after the close of the study. At the conclusion of this study, the researchers will publish their findings. Information will be presented in summary format and you will not be identified in any publications or presentations. Research resources generated with funds from this grant will be freely distributed, as available, to qualified academic investigators for non-commercial research. Final data will be shared primarily through peer-reviewed publication. Raw data will be considered for sharing under the rules indicated below. Raw datasets to be released for sharing will not contain identifiers. Data and associated documentation will be made available to users only under a signed and properly executed data-sharing agreement that provides for specific criteria under which the data will be used, including but not limited to a commitment to: 1) using the data only for research purposes; 2) securing the data using appropriate computer technology; and 3) destroying or returning the data after analyses are completed.

Certificate of Confidentiality: This research is covered by a Certificate of Confidentiality from the National Institutes of Health (NIH). The researchers with this Certificate may not disclose or use information, documents, or biospecimens that may identify you in any federal, state, or local civil, criminal, administrative, legislative, or other action, suit, or proceeding, or be used as evidence, for example, if there is a court subpoena, unless you have consented for this use. Information, documents, or biospecimens protected by this Certificate cannot be disclosed to

anyone else who is not connected with the research except, if there is a federal, state, or local law that requires disclosure (such as to report child abuse or communicable diseases but not for federal, state, or local civil, criminal, administrative, legislative, or other proceedings); if you have consented to the disclosure, including for your medical treatment; or if it is used for other scientific research, as allowed by federal regulations protecting research subjects. The Certificate cannot be used to refuse a request for information from personnel of the United States federal or state government agency sponsoring the project that is needed for auditing or program evaluation by the NIH which is funding this project. You should understand that a Certificate of Confidentiality does not prevent you from voluntarily releasing information about yourself or your involvement in this research. If you want your research information released to an insurer, medical care provider, or any other person not connected with the research, you must provide consent to allow the researchers to release it.

Costs and Reimbursement: There is no cost to participate in this study. If you take part in this study you will be given $30 cash for completing these procedures.

Withdrawal from Participation: Participation in this research is voluntary. You have the right to withdraw or refuse to continue the study at any point, without prejudice.

Alternative Procedures: The planned procedures include techniques that are commonly used in muscle research. There are no other techniques that can be used to gather the information needed for this project with the high-quality of resolution that is needed in order to answer our research questions.

Request for Additional Information: You are encouraged to ask questions about the study. The investigators will attempt to answer all of your questions to the best of their knowledge. The investigators fully intend to conduct the study with your best interest, safety, and comfort in mind. Please address any questions regarding the study to the Muscle Physiology Laboratory. Our phone number is (413) 545-5305. We can also be reached by email at umassmplab@umass.edu. You may also address questions to Dr. Kent by calling her at (413) 545-9477 or by emailing her at jkent@kin.umass.edu. If you would like to speak with someone not directly involved in the research study, you may contact the Human Research Protection Office at the University of Massachusetts via email at humansubjects@ora.umass.edu; telephone (413) 545-3428; or mail at the Human Research Protection Office (HRPO), Mass Venture Center, 100 Venture Way, Suite 116, Hadley, MA, 01035.

Subject Statement of Voluntary Consent: By signing this form, I am agreeing to voluntarily enter this study. I understand that, by signing this document, I do not waive any of my legal rights. I have had a chance to read this consent form, and it was explained to me in a language that I use and understand. I have had the

opportunity to ask questions and have received satisfactory answers. A copy of this signed Informed Consent Form will be given to me.

_____

Participant's name (please print) Address

_____

Signature Phone Number Date

STUDY REPRESENTATIVE STATEMENT: The investigator has read and understands the federal regulations for the Protection of Human Research Subjects (45 CFR 46) and agrees to comply with all of its clauses to the best of their ability. The investigator also pledges to consider the best interests of the subject beyond the explicit statement contained in the aforementioned federal regulations and to exercise professional expertise to protect the rights and welfare of the subject.

_____

Signature of Person Obtaining Consent Name (please print) Date

APPENDIX D

TELEPHONE SCREENING FORM

Screened by:_____ Date:_____ Status:_____

TELEPHONE SCREENING FORM: MR STUDIES

1) Name_____

2) Phone # (Circle preferred contact): Best time/day to contact: _____

   a. Home _____ Message? Yes No

   b. Work _____ Message? Yes No _____

   c. Cell _____ Message? Yes No _____

3) Email: _____

4) Age_____ Sex_____ Height _____ Weight _____ BMI _____

(calculate)

5) How did you find out about this study?_____

6) Have you ever participated in a research study before? _____

   a. Are you currently participating in any other research studies right now?_____

      i. If yes, describe:_____

      _____

      ii. End date: _____

7) Current health status (general)_____

8) Do you have any physical limitations? _____

9) Are you pregnant?_____

10) Do you, or have you ever had, any of the following:

   a. Stroke?_____

   b. Peripheral vascular disease?_____

c. Cardiac disease?_____

d. Pulmonary disease?_____

e. Neurological disease?_____

f. Arthritis in the lower leg?_____

Have you used ambulatory devices during the last month (i.e., ankle-foot orthotic, cane, wheelchair, etc.)?

_____

11) Do you smoke or have you ever smoked before? _____ For how long? _____ Quit? _____

12) Do you have any allergic reactions? _____

13) Do you have any significant past medical history? (e.g., hypertension, CAD, etc.)

_____

14) Current medications:

Drug Name	Classification	Dosage	Frequency	Duration	Prescribed for?

a. Do you take any Statins?_____ If yes, please describe:

_____

b. Do you take any beta-blockers, sedatives, tranquilizers, or other medication that may impair physical function?_____

If yes, please describe:_____

_____

15) Current physical activity level (regular exercise, none, athlete, etc.) _____

16) Has your Doctor ever told you not to exercise? _____ If yes, please describe:_____

17) What was the date of your last doctor's visit?

_____

18) Is fatigue a problem for you? _____ Leg fatigue? _____

19) What type of transportation will you be using? _____ Will you need a parking pass? _____

20) Would you like to be contacted again for future studies? Yes No

*Inform participant that eligibility will be confirmed during first visit, and they may be deemed ineligible at that time.

21) Comments:_____

_____

22) Go through Magnetic Resonance Safety Questionnaire:

APPENDIX E

MEDICAL HISTORY FORM

Please fill out and sign below in ink. This record is confidential.

Medical History

Do you take any prescribed or over-the-counter medications? Please include vitamins, herbs, or other dietary supplements. If yes please list the dose, frequency and duration of use.

Do you take any statins? If yes, please indicate name and dose:_____

Have you ever been told by a physician that you should not exercise?

Yes ____ No ____ If yes, please explain:

Do you have or have you EVER had any of the following problems? Check if YES and provide details below.

____ Heart disease/rheumatic fever ____ Thyroid disorder ____Asthma
____ High blood pressure ____ Claustrophobia ____ Allergies

____ Elevated Cholesterol ____ Anemia ____Stroke

____ Epilepsy or seizure disorder ____Diabetes _Dizziness

____ Blurred or double vision ____ Orthopedic or joint problems (e.g., arthritis)

____ Shortness of breath or difficulty in breathing

____Phlebitis, blood-clots, varicose veins, peripheral vascular disease

Details, if relevant:

Lifestyle

Do you smoke cigarettes? Yes ____ No ____

Do you drink alcohol? Yes ____ No ____

Do you get regular exercise? Yes ____ No ____

If yes, number of times per week _____

Have you had surgery? Yes ____ No ____

If yes, when was this? _____

Is there any other information that you feel we should know about before you participate in the study? If yes please explain in the space below.

Signature: _____ Date: _____

APPENDIX F

MR SAFETY SCREENING QUESTIONNAIRE

MR Safety Screening Questionnaire

Participant's Name (print): _____Today's date: _____

Study Name: _____ Investigator: _____

Year of birth: _____ Gender: _____ Height: _____ Weight: _____

Please read the following questions carefully. It is very important for us to know if you have any **metal devices** or **metal parts** anywhere in your body. If you do not understand a question, please ask us to explain!

1. Yes ☐ No☐ Do you get upset or anxious in small spaces (claustrophobia)?
2. Yes ☐ No☐ Did you ever have an aneurysm clip implanted during brain surgery?
3. Yes ☐ No☐ Do you have embolization coils (Gianturco) in your brain?
4. Yes ☐ No☐ Do you have a Carotid Artery Vascular clamp?
5. Yes ☐ No☐ Do you have a "shunt" (a tube to drain fluid) in your brain, spine or heart?
6. Yes ☐ No☐ Do you have a Vagus nerve stimulator to help you with convulsions or with epilepsy?
7. Yes ☐ No☐ Have you ever had metal removed from your eyes by a doctor?
8. Yes ☐ No☐ Have you ever worked with metal? (For example in a machine shop)?
9. Yes ☐ No☐ Do you have implants in your eyes? Have you ever had cataract surgery?
10. Yes ☐ No☐ Do you wear colored contact lenses or permanent eye liner?
11. Yes ☐ No☐ Do you have shrapnel or metal in your head, eyes or skin?
12. Yes ☐ No☐ Do you have implants in your ear (like cochlear implants) or a hearing aid?
13. Yes ☐ No☐ Do you wear braces on your teeth or have a permanent retainer?
14. Yes ☐ No☐ Do you have a heart pacemaker or a heart defibrillator?
15. Yes ☐ No☐ Do you have a filter for blood clots (Umbrella, Greenfield, bird's nest)?
16. Yes ☐ No☐ Do you have any stents (small metal tubes used to keep blood vessels open)?
17. Yes ☐ No☐ Did you ever have a device implanted in your body such as a nerve stimulators?
18. Yes ☐ No☐ Do you have an implanted pump to deliver medication?
19. Yes ☐ No☐ Do you have metal joints, rods, plates, pins, screws, nails, or clips in any part of your body?
20. Yes ☐ No☐ Have you ever had a gunshot wound? Or a B-B gun injury?
21. Yes ☐ No☐ Do you wear a patch to deliver medicines through the skin?
22. Yes ☐ No☐ Do you have any devices to make bones grow (like bone growth or bone fusion stimulators)?
23. Yes ☐ No☐ Do you have body-piercing or a tattoo?
24. Yes ☐ No☐ Have you ever had any surgery? Please list all:

FOR WOMEN

25. Yes ☐ No☐ Do you use a diaphragm, IUD, or cervical pessary?
26. Yes ☐ No☐ Do you think there is any possibility that you might be pregnant? Date of last menstrual period?

IMPORTANT INSTRUCTIONS: Before entering the Magnet Room, you must remove all metallic objects including hearing aids, dentures, partial plates, keys, beeper, cell phone, eyeglasses, hair pins, barrettes, jewelry including body piercing jewelry, watch, safety pins,

paperclips, money clip, credit cards, bank cards, magnetic strip cards, coins, pens, pocket knife,nail clipper, tools, clothing with metal fasteners, and clothing with metallic threads in material.

I attest that the above information is correct to the best of my knowledge. I have read and understand the entire contents of this form and have had the opportunity to ask questions regarding the information on this form and regarding the MR procedure that I am about to undergo.

Participant Signature: _____ Date**: _____**

MR Operator Signature: _____Date: _____

APPENDIX G

PHYSICAL ACTIVITY READINESS QUESTIONNAIRE

2016 PAR-Q+

The Physical Activity Readiness Questionnaire for Everyone

The health benefits of regular physical activity are clear; more people should engage in physical activity every day of the week. Participating in physical activity is very safe for MOST people. This questionnaire will tell you whether it is necessary for you to seek further advice from your doctor OR a qualified exercise professional before becoming more physically active.

GENERAL HEALTH QUESTIONS

Please read the 7 questions below carefully and answer each one honestly: check YES or NO.	YES	NO
1) Has your doctor ever said that you have a heart condition ☐ OR high blood pressure ☐?	☐	☐
2) Do you feel pain in your chest at rest, during your daily activities of living, **OR** when you do physical activity?	☐	☐
3) Do you lose balance because of dizziness **OR** have you lost consciousness in the last 12 months? Please answer **NO** if your dizziness was associated with over-breathing (including during vigorous exercise).	☐	☐
4) Have you ever been diagnosed with another chronic medical condition (other than heart disease or high blood pressure)? **PLEASE LIST CONDITION(S) HERE:** _____	☐	☐
5) Are you currently taking prescribed medications for a chronic medical condition? **PLEASE LIST CONDITION(S) AND MEDICATIONS HERE:** _____	☐	☐
6) Do you currently have (or have had within the past 12 months) a bone, joint, or soft tissue (muscle, ligament, or tendon) problem that could be made worse by becoming more physically active? Please answer **NO** if you had a problem in the past, but it *does not limit your current ability* to be physically active. **PLEASE LIST CONDITION(S) HERE:** _____	☐	☐
7) Has your doctor ever said that you should only do medically supervised physical activity?	☐	☐

If you answered NO to all of the questions above, you are cleared for physical activity.
Go to Page 4 to sign the PARTICIPANT DECLARATION. You do not need to complete Pages 2 and 3.

- Start becoming much more physically active – start slowly and build up gradually.
- Follow International Physical Activity Guidelines for your age (www.who.int/dietphysicalactivity/en/).
- You may take part in a health and fitness appraisal.
- If you are over the age of 45 yr and **NOT** accustomed to regular vigorous to maximal effort exercise, consult a qualified exercise professional before engaging in this intensity of exercise.
- If you have any further questions, contact a qualified exercise professional.

If you answered YES to one or more of the questions above, COMPLETE PAGES 2 AND 3.

Delay becoming more active if:

- You have a temporary illness such as a cold or fever; it is best to wait until you feel better.
- You are pregnant - talk to your health care practitioner, your physician, a qualified exercise professional, and/or complete the ePARmed-X+ at **www.eparmedx.com** before becoming more physically active.
- Your health changes - answer the questions on Pages 2 and 3 of this document and/or talk to your doctor or a qualified exercise professional before continuing with any physical activity program.

2016 PAR-Q+

FOLLOW-UP QUESTIONS ABOUT YOUR MEDICAL CONDITION(S)

1. Do you have Arthritis, Osteoporosis, or Back Problems?

If the above condition(s) is/are present, answer questions 1a-1c — If **NO** ☐ go to question 2

1a.	Do you have difficulty controlling your condition with medications or other physician-prescribed therapies? (Answer **NO** if you are not currently taking medications or other treatments)	YES ☐ NO ☐
1b.	Do you have joint problems causing pain, a recent fracture or fracture caused by osteoporosis or cancer, displaced vertebra (e.g., spondylolisthesis), and/or spondylolysis/pars defect (a crack in the bony ring on the back of the spinal column)?	YES ☐ NO ☐
1c.	Have you had steroid injections or taken steroid tablets regularly for more than 3 months?	YES ☐ NO ☐

2. Do you currently have Cancer of any kind?

If the above condition(s) is/are present, answer questions 2a-2b — If **NO** ☐ go to question 3

2a.	Does your cancer diagnosis include any of the following types: lung/bronchogenic, multiple myeloma (cancer of plasma cells), head, and/or neck?	YES ☐ NO ☐
2b.	Are you currently receiving cancer therapy (such as chemotheraphy or radiotherapy)?	YES ☐ NO ☐

3. Do you have a Heart or Cardiovascular Condition? *This includes Coronary Artery Disease, Heart Failure, Diagnosed Abnormality of Heart Rhythm*

If the above condition(s) is/are present, answer questions 3a-3d — If **NO** ☐ go to question 4

3a.	Do you have difficulty controlling your condition with medications or other physician-prescribed therapies? (Answer **NO** if you are not currently taking medications or other treatments)	YES ☐ NO ☐
3b.	Do you have an irregular heart beat that requires medical management? (e.g., atrial fibrillation, premature ventricular contraction)	YES ☐ NO ☐
3c.	Do you have chronic heart failure?	YES ☐ NO ☐
3d.	Do you have diagnosed coronary artery (cardiovascular) disease and have not participated in regular physical activity in the last 2 months?	YES ☐ NO ☐

4. Do you have High Blood Pressure?

If the above condition(s) is/are present, answer questions 4a-4b — If **NO** ☐ go to question 5

4a.	Do you have difficulty controlling your condition with medications or other physician-prescribed therapies? (Answer **NO** if you are not currently taking medications or other treatments)	YES ☐ NO ☐
4b.	Do you have a resting blood pressure equal to or greater than 160/90 mmHg with or without medication? (Answer **YES** if you do not know your resting blood pressure)	YES ☐ NO ☐

5. Do you have any Metabolic Conditions? *This includes Type 1 Diabetes, Type 2 Diabetes, Pre-Diabetes*

If the above condition(s) is/are present, answer questions 5a-5e — If **NO** ☐ go to question 6

5a.	Do you often have difficulty controlling your blood sugar levels with foods, medications, or other physician-prescribed therapies?	YES ☐ NO ☐
5b.	Do you often suffer from signs and symptoms of low blood sugar (hypoglycemia) following exercise and/or during activities of daily living? Signs of hypoglycemia may include shakiness, nervousness, unusual irritability, abnormal sweating, dizziness or light-headedness, mental confusion, difficulty speaking, weakness, or sleepiness.	YES ☐ NO ☐
5c.	Do you have any signs or symptoms of diabetes complications such as heart or vascular disease and/or complications affecting your eyes, kidneys, **OR** the sensation in your toes and feet?	YES ☐ NO ☐
5d.	Do you have other metabolic conditions (such as current pregnancy-related diabetes, chronic kidney disease, or liver problems)?	YES ☐ NO ☐
5e.	Are you planning to engage in what for you is unusually high (or vigorous) intensity exercise in the near future?	YES ☐ NO ☐

2016 PAR-Q+

6. Do you have any Mental Health Problems or Learning Difficulties? *This includes Alzheimer's, Dementia, Depression, Anxiety Disorder, Eating Disorder, Psychotic Disorder, Intellectual Disability, Down Syndrome*

If the above condition(s) is/are present, answer questions 6a-6b If **NO** ☐ go to question 7

6a.	Do you have difficulty controlling your condition with medications or other physician-prescribed therapies? (Answer **NO** if you are not currently taking medications or other treatments)	YES ☐ NO ☐
6b.	Do you have Down Syndrome **AND** back problems affecting nerves or muscles?	YES ☐ NO ☐

7. Do you have a Respiratory Disease? *This includes Chronic Obstructive Pulmonary Disease, Asthma, Pulmonary High Blood Pressure*

If the above condition(s) is/are present, answer questions 7a-7d If **NO** ☐ go to question 8

7a.	Do you have difficulty controlling your condition with medications or other physician-prescribed therapies? (Answer **NO** if you are not currently taking medications or other treatments)	YES ☐ NO ☐
7b.	Has your doctor ever said your blood oxygen level is low at rest or during exercise and/or that you require supplemental oxygen therapy?	YES ☐ NO ☐
7c.	If asthmatic, do you currently have symptoms of chest tightness, wheezing, laboured breathing, consistent cough (more than 2 days/week), or have you used your rescue medication more than twice in the last week?	YES ☐ NO ☐
7d.	Has your doctor ever said you have high blood pressure in the blood vessels of your lungs?	YES ☐ NO ☐

8. Do you have a Spinal Cord Injury? *This includes Tetraplegia and Paraplegia*

If the above condition(s) is/are present, answer questions 8a-8c If **NO** ☐ go to question 9

8a.	Do you have difficulty controlling your condition with medications or other physician-prescribed therapies? (Answer **NO** if you are not currently taking medications or other treatments)	YES ☐ NO ☐
8b.	Do you commonly exhibit low resting blood pressure significant enough to cause dizziness, light-headedness, and/or fainting?	YES ☐ NO ☐
8c.	Has your physician indicated that you exhibit sudden bouts of high blood pressure (known as Autonomic Dysreflexia)?	YES ☐ NO ☐

9. Have you had a Stroke? *This includes Transient Ischemic Attack (TIA) or Cerebrovascular Event*

If the above condition(s) is/are present, answer questions 9a-9c If **NO** ☐ go to question 10

9a.	Do you have difficulty controlling your condition with medications or other physician-prescribed therapies? (Answer **NO** if you are not currently taking medications or other treatments)	YES ☐ NO ☐
9b.	Do you have any impairment in walking or mobility?	YES ☐ NO ☐
9c.	Have you experienced a stroke or impairment in nerves or muscles in the past 6 months?	YES ☐ NO ☐

10. Do you have any other medical condition not listed above or do you have two or more medical conditions?

If you have other medical conditions, answer questions 10a-10c If **NO** ☐ read the Page 4 recommendations

10a.	Have you experienced a blackout, fainted, or lost consciousness as a result of a head injury within the last 12 months **OR** have you had a diagnosed concussion within the last 12 months?	YES ☐ NO ☐
10b.	Do you have a medical condition that is not listed (such as epilepsy, neurological conditions, kidney problems)?	YES ☐ NO ☐
10c.	Do you currently live with two or more medical conditions?	YES ☐ NO ☐

PLEASE LIST YOUR MEDICAL CONDITION(S) AND ANY RELATED MEDICATIONS HERE: _____

_____

GO to Page 4 for recommendations about your current medical condition(s) and sign the PARTICIPANT DECLARATION.

2016 PAR-Q+

If you answered NO to all of the follow-up questions about your medical condition, you are ready to become more physically active - sign the PARTICIPANT DECLARATION below:

- It is advised that you consult a qualified exercise professional to help you develop a safe and effective physical activity plan to meet your health needs.
- You are encouraged to start slowly and build up gradually - 20 to 60 minutes of low to moderate intensity exercise, 3-5 days per week including aerobic and muscle strengthening exercises.
- As you progress, you should aim to accumulate 150 minutes or more of moderate intensity physical activity per week.
- If you are over the age of 45 yr and **NOT** accustomed to regular vigorous to maximal effort exercise, consult a qualified exercise professional before engaging in this intensity of exercise.

If you answered **YES** to **one or more of the follow-up questions** about your medical condition:

You should seek further information before becoming more physically active or engaging in a fitness appraisal. You should complete the specially designed online screening and exercise recommendations program - the **ePARmed-X+ at www.eparmedx.com** and/or visit a qualified exercise professional to work through the ePARmed-X+ and for further information.

Delay becoming more active if:

- You have a temporary illness such as a cold or fever; it is best to wait until you feel better.
- You are pregnant - talk to your health care practitioner, your physician, a qualified exercise professional, and/or complete the ePARmed-X+ **at www.eparmedx.com** before becoming more physically active.
- Your health changes - talk to your doctor or qualified exercise professional before continuing with any physical activity program.

- You are encouraged to photocopy the PAR-Q+. You must use the entire questionnaire and NO changes are permitted.
- The authors, the PAR-Q+ Collaboration, partner organizations, and their agents assume no liability for persons who undertake physical activity and/or make use of the PAR-Q+ or ePARmed-X+. If in doubt after completing the questionnaire, consult your doctor prior to physical activity.

PARTICIPANT DECLARATION

- All persons who have completed the PAR-Q+ please read and sign the declaration below.
- If you are less than the legal age required for consent or require the assent of a care provider, your parent, guardian or care provider must also sign this form.

I, the undersigned, have read, understood to my full satisfaction and completed this questionnaire. I acknowledge that this physical activity clearance is valid for a maximum of 12 months from the date it is completed and becomes invalid if my condition changes. I also acknowledge that a Trustee (such as my employer, community/fitness centre, health care provider, or other designate) may retain a copy of this form for their records. In these instances, the Trustee will be required to adhere to local, national, and international guidelines regarding the storage of personal health information ensuring that the Trustee maintains the privacy of the information and does not misuse or wrongfully disclose such information.

NAME _____ DATE _____

SIGNATURE _____ WITNESS _____

SIGNATURE OF PARENT/GUARDIAN/CARE PROVIDER _____

For more information, please contact

www.eparmedx.com

Email: eparmedx@gmail.com

Citation for PAR-Q+

Warburton DER, Jamnik VK, Bredin SSD, and Gledhill N on behalf of the PAR-Q+ Collaboration. The Physical Activity Readiness Questionnaire for Everyone (PAR-Q+) and Electronic Physical Activity Readiness Medical Examination (ePARmed-X+). Health & Fitness Journal of Canada 4(2):3-23, 2011.

The PAR-Q+ was created using the evidence-based AGREE process (1) by the PAR-Q+ Collaboration chaired by Dr. Darren E. R. Warburton with Dr. Norman Gledhill, Dr. Veronica Jamnik, and Dr. Donald C. McKenzie (2). Production of this document has been made possible through financial contributions from the Public Health Agency of Canada and the BC Ministry of Health Services. The views expressed herein do not necessarily represent the views of the Public Health Agency of Canada or the BC Ministry of Health Services.

Key References

1. Jamnik VK, Warburton DER, Makarski J, McKenzie DC, Shephard RJ, Stone J, and Gledhill N. Enhancing the effectiveness of clearance for physical activity participation: background and overall process. APNM 36(S1):S3-S13, 2011.
2. Warburton DER, Gledhill N, Jamnik VK, Bredin SSD, McKenzie DC, Stone J, Charlesworth S, and Shephard RJ. Evidence-based risk assessment and recommendations for physical activity clearance: Consensus Document. APNM 36(S1):S266-s298, 2011.
3. Chisholm DM, Collis ML, Kulak LL, Davenport W, and Gruber N. Physical activity readiness. British Columbia Medical Journal. 1975;17:375-378.
4. Thomas S, Reading J, and Shephard RJ. Revision of the Physical Activity Readiness Questionnaire (PAR-Q). Canadian Journal of Sport Science 1992;17:4:338-345.

01-01-2016

APPENDIX H

PHYSICAL ACTIVITY LOG

INFORMATION ABOUT THE ACTIVITY MONITOR

The Activity Monitor is a small, plastic box containing electronic circuitry. When you wear the Activity Monitor, it measures how much you are moving.

Please remember a few important things about the monitor:

- Snap the belt around your waist.
- The monitor should be worn around your waist and positioned at the top of the right hipbone.
- **PLEASE DO NOT GET THE MONITOR WET** (sweat is okay).
- You should **wear** the monitor **while you are awake** for 7 days, removing the device only for sleep and water-based activities (e.g. bathing, showering, or swimming).
- The monitor will flash intermittently when it is **NOT** recording. If the monitor stops flashing, it indicates that the monitor **IS** recording.
- Please return the monitor and this log to the UMass Muscle Physiology Laboratory, Totman Bldg., Room 22.

INSTRUCTIONS FOR COMPLETING THIS ACTIVITY LOG

We want to know:

- When you woke up and when you went to bed
- When the monitor was put on and taken off
- Any activities you completed that day (e.g., long walks, yard work, etc.).
- If there was anything out of the ordinary about your activity pattern

If you went on a long walk from 11:00 am to 11:30 am, write walking in the activity column, 11:00 am to 11:30 am in the time column, and 30 minutes in the duration column.

If you have any questions please contact:

UMass Muscle Physiology Lab

Phone: (413) 545 – 5305

Email: umassmplab@umass.edu

Day 1

Date: _____ Day of the week _____

Wake up Time: _____ Bed Time: _____

Monitor on Time: _____ Monitor off Time: _____

List any physical activities (e.g., long walks, fitness club, etc), or naps during the day:

Activity: Time of day: Duration:

_____

_____

_____

Did you wear the monitor during all waking hours (except for showering)?

☐ Yes ☐ No, Times not worn:

_____

Was there anything out of the ordinary about your activity pattern this day?

☐ Yes, Explain Below ☐ No

_____

_____

Day 2

Date: _____ Day of the week _____

Wake up Time: _____ Bed Time: _____

Monitor on Time: _____ Monitor off Time: _____

List any physical activities (e.g., long walks, fitness club, etc), or naps during the day:

Activity: Time of day: Duration:

_____

_____

_____

Did you wear the monitor during all waking hours (except for showering)?

☐ Yes ☐ No, Times not worn:

_____

Was there anything out of the ordinary about your activity pattern this day?

☐ Yes, Explain Below ☐ No

_____

_____

_____

Day 3

Date: _____ Day of the week _____

Wake up Time: _____ Bed Time: _____

Monitor on Time: _____ Monitor off Time: _____

List any physical activities (e.g., long walks, fitness club, etc), or naps during the day:

Activity: Time of day: Duration:

_____

_____

_____

Did you wear the monitor during all waking hours (except for showering)?

☐ Yes ☐ No, Times not worn:

_____

Was there anything out of the ordinary about your activity pattern this day?

☐ Yes, Explain Below ☐ No

_____

_____

Day 4

Date: _____ Day of the week _____

Wake up Time: _____ Bed Time: _____

Monitor on Time: _____ Monitor off Time: _____

List any physical activities (e.g., long walks, fitness club, etc), or naps during the day:

Activity: Time of day: Duration:

_____

_____

_____

Did you wear the monitor during all waking hours (except for showering)?

☐ Yes ☐ No, Times not worn:

_____

Was there anything out of the ordinary about your activity pattern this day?

☐ Yes, Explain Below ☐ No

_____

_____

_____

Day 5

Date: _____ Day of the week _____

Wake up Time: _____ Bed Time: _____

Monitor on Time: _____ Monitor off Time: _____

List any physical activities (e.g., long walks, fitness club, etc), or naps during the day:

Activity: Time of day: Duration:

_____

_____

_____

Did you wear the monitor during all waking hours (except for showering)?

☐ Yes ☐ No, Times not worn:

_____

Was there anything out of the ordinary about your activity pattern this day?

☐ Yes, Explain Below ☐ No

_____

_____

Day 6

Date: _____ Day of the week _____

Wake up Time: _____ Bed Time: _____

Monitor on Time: _____ Monitor off Time: _____

List any physical activities (e.g., long walks, fitness club, etc), or naps during the day:

Activity: Time of day: Duration:

_____

_____

_____

Did you wear the monitor during all waking hours (except for showering)?

☐ Yes ☐ No, Times not worn:

_____

Was there anything out of the ordinary about your activity pattern this day?

☐ Yes, Explain Below ☐ No

_____

_____

_____

Day 7

Date: _____ Day of the week

_____

Wake up Time: _____ Bed Time: _____

Monitor on Time: _____ Monitor off Time: _____

List any physical activities (e.g., long walks, fitness club, etc), or naps during the day:

Activity: Time of day: Duration:

_____

_____

_____

Did you wear the monitor during all waking hours (except for showering)?

☐ Yes ☐ No, Times not worn:

_____

Was there anything out of the ordinary about your activity pattern this day?

☐ Yes, Explain Below ☐ No

_____

_____

Day 8

Date: _____ Day of the week _____

Wake up Time: _____ Bed Time: _____

Monitor on Time: _____ Monitor off Time: _____

List any physical activities (e.g., long walks, fitness club, etc), or naps during the day:

Activity: Time of day: Duration:

_____

_____

_____

Did you wear the monitor during all waking hours (except for showering)?

☐ Yes ☐ No, Times not worn:

_____

Was there anything out of the ordinary about your activity pattern this day?

☐ Yes, Explain Below ☐ No

_____

_____

_____

REFERENCES

1. Aagaard P, Andersen JL, Dyhre-Poulsen P, Leffers A-M, Wagner A, et al. 2001. A mechanism for increased contractile strength of human pennate muscle in response to strength training: changes in muscle architecture. *J Physiol*. 534(2):613–23

2. Addison O, Marcus RL, Lastayo PC, Ryan AS. 2014. Intermuscular fat: A review of the consequences and causes. *Int J Endocrinol*. 2014:

3. Aeles J, Bolsterlee B, Kelp NY, Dick TJM, Hug F. 2022. Regional variation in lateral and medial gastrocnemius muscle fibre lengths obtained from diffusion tensor imaging. *J Anat.* 240(1):131–44

4. Akagi R, Kanehisa H, Kawakami Y, Fukunaga T. 2008. Establishing a new index of muscle cross-sectional area and its relationship with isometric muscle strength. *J Strength Cond Res.* 22(1):82–87

5. Akazawa N, Kishi M, Hino T, Tsuji R, Tamura K, Moriyama H. 2021. Increased intramuscular adipose tissue of the quadriceps is more strongly related to declines in ADL than is loss of muscle mass in older inpatients. *Clinical Nutrition*. 40(3):1381–87

6. Andersen JL. 2003. Muscle fibre type adaptation in the elderly human muscle. *Scand J Med Sci Sports.* 13(1):40–47

7. Andrich DE, Ou Y, Melbouci L, Leduc-Gaudet JP, Auclair N, et al. 2018. Altered lipid metabolism impairs skeletal muscle force in young rats submitted to a short-term high-fat diet. *Front Physiol*. 9(SEP):1327

8. Arroyo E, Stout JR, Beyer KS, Church DD, Varanoske AN, et al. 2018. Effects of supine rest duration on ultrasound measures of the vastus lateralis. *Clin Physiol Funct Imaging*. 38(1):155–57

9. Bamman MM, Newcomer BR, Larson-Meyer DE, Weinsier RL, Hunter GR. 2000. Evaluation of the strength-size relationship in vivo using various muscle size indices. *Med Sci Sports Exerc*. 32(7):1307–13

10. Bartolomei S, Rovai C, Lanzoni IM, di Michele R. 2022. Relationships between muscle architecture, deadlift performance, and maximal isometric force produced at the midthigh and midshin pull in resistance-trained individuals. *J Strength Cond Res.* 36(2):299–303

11. Basser PJ, Mattiello J, LeBihan D. 1994. MR diffusion tensor spectroscopy and imaging. *Biophys J*. 66(1):259–67

12. Basser PJ, Pierpaoli C. 2011. Microstructural and physiological features of tissues elucidated by quantitative-diffusion-tensor MRI. *Journal of Magnetic Resonance*. 213:560–70

13. Baum T, Inhuber S, Dieckmeyer M, Cordes C, Ruschke S, et al. 2016. Association of quadriceps muscle fat with isometric strength measurements in healthy males using chemical shift encoding-based water-fat magnetic resonance imaging. *J Comput Assist Tomogr*. 40(3):447–51

14. Berry DB, Regner B, Galinsky V, Ward SR, Frank LR. 2018. Relationships between tissue microstructure and the diffusion tensor in simulated skeletal muscle. *Magn Reson Med*. 80(1):317–29

15. Bigland Ritchie B, Jones DA, Hosking GP, Edwards RHT. 1978. Central and peripheral fatigue in sustained maximum voluntary contractions of human quadriceps muscle. *Clin Sci Mol Med*. 54(6):609–14

16. Biltz NK, Collins KH, Shen KC, Schwartz K, Harris CA, Meyer GA. 2020. Infiltration of intramuscular adipose tissue impairs skeletal muscle contraction. *Journal of Physiology*. 598(13):2669–83

17. Blazevich AJ, Gill ND, Zhou S. 2006. Intra- and intermuscular variation in human quadriceps femoris architecture assessed in vivo. *J Anat*. 209(3):289–310

18. Boesch C. 2007. Musculoskeletal spectroscopy. *Journal of Magnetic Resonance Imaging*. 25(2):321–38

19. Boesch C, Slotboom J, Hoppeler H, Kreis R. 1997. In vivo determination of intra-myocellular lipids in human muscle by means of localized 1H-MR-spectroscopy. *Magn Reson Med*. 37(4):484–93

20. Bolsterlee B, D'Souza A, Herbert RD. 2019. Reliability and robustness of muscle architecture measurements obtained using diffusion tensor imaging with anatomically constrained tractography. *J Biomech*. 86:71–78

21. Bolsterlee B, Finni T, D'Souza A, Eguchi J, Clarke EC, Herbert RD. 2018. Three-dimensional architecture of the whole human soleus muscle in vivo. *PeerJ*. 2018(4):

22. Bolsterlee B, Veeger HEJ, van der Helm FCT, Gandevia SC, Herbert RD. 2015. Comparison of measurements of medial gastrocnemius architectural parameters from ultrasound and diffusion tensor images. *J Biomech*. 48(6):1133–40

23. Bonnard C, Durand A, Peyrol S, Chanseaume E, Chauvin M-A, et al. 2008. Mitochondrial dysfunction results from oxidative stress in the skeletal muscle of diet-induced insulin-resistant mice. *Journal of Clinical Investigation*

24. Borga M. 2018. The role of imaging in obesity special feature: review article mri adipose tissue and muscle composition analysis-a review of automation techniques

25. Brix G, Heiland S, Bellemann ME, Koch T, Lorenz WJ. 1993. MR imaging of fat-containing tissues: Valuation of two quantitative imaging techniques in comparison with localized proton spectroscopy. *Magn Reson Imaging*. 11(7):977–91

26. Bruce CR, Dyck DJ. 2004. Cytokine regulation of skeletal muscle fatty acid metabolism: effect of interleukin-6 and tumor necrosis factor-α. *American Journal of Physiology-Endocrinology and Metabolism*. 287(4):E616–21

27. Buck FM, Grehn H, Hilbe M, Pfirrmann CWA, Manzanell S, Hodler J. 2009. Degeneration of the long biceps tendon: comparison of mri with gross anatomy and histology. *American Journal of Roentgenology*. 193(5):1367–75

28. Burakiewicz J, Sinclair CDJ, Fischer D, Walter GA, Kan HE, Hollingsworth KG. 2017. Quantifying fat replacement of muscle by quantitative MRI in muscular dystrophy

29. Cahill GF. 1976. Starvation in man. *Clin Endocrinol Metab*. 5(2):397–415

30. Callahan DM, Kent-Braun JA. 2011. Effect of old age on human skeletal muscle force-velocity and fatigue properties. *J Appl Physiol*. 111:1345–52

31. Chance B. 1992. Noninvasive approaches to oxygen delivery and cell bioenergetics in functioning muscle. *Clinical Journal of Sport Medicine*. 2(2):132–38

32. Charles JP, Suntaxi F, Anderst WJ. 2019. In vivo human lower limb muscle architecture dataset obtained using diffusion tensor imaging. *PLoS One*. 14(10):

33. Chen X, Sanchez GN, Schnitzer MJ, Delp SL. 2016. Changes in sarcomere lengths of the human vastus lateralis muscle with knee flexion measured using in vivo microendoscopy. *J Biomech*. 49(13):2989–94

34. Chen X, Xun K, Chen L, Wang Y. 2009. TNF-α, a potent lipid metabolism regulator. *Cell Biochem Funct*. 27(7):407–16

35. Choi L, Liu Z, Matthews CE, Buchowski MS. 2011. Validation of accelerometer wear and nonwear time classification algorithm. *Med Sci Sports Exerc*. 43(2):357–64

36. Choi SJ, Files DC, Zhang T, Wang ZM, Messi ML, et al. 2016. Intramyocellular lipid and impaired myofiber contraction in normal weight and obese older adults. *Journals of Gerontology - Series A Biological Sciences and Medical Sciences*. 71(4):557–64

37. Coen PM, Dubé JJ, Amati F, Stefanovic-Racic M, Ferrell RE, et al. 2010. Insulin resistance Is associated with higher intramyocellular triglycerides in type I but not type II myocytes concomitant with higher ceramide content. *Diabetes*. 59(1):80–88

38. Coppack SW. 2001. Pro-inflammatory cytokines and adipose tissue. *Proceedings of the Nutrition Society*. 60(3):349–56

39. Csapo R, Malis V, Sinha U, Du J, Sinha S. 2014. Age-associated differences in triceps surae muscle composition and strength – an MRI-based cross-sectional comparison of contractile, adipose and connective tissue. *BMC Musculoskelet Disord*. 15(1):209

40. Cutts A. 1988. The range of sarcomere lengths in the muscles of the human lower limb. *J Anat*. 160:79–88

41. Damon BM, Ding Z, Anderson AW, Freyer AS, Gore JC. 2002. Validation of diffusion tensor MRI-based muscle fiber tracking. *Magn Reson Med*. 48(1):97–104

42. Damon BM, Ding Z, Hooijmans MT, Anderson AW, Zhou X, et al. 2021. A MATLAB toolbox for muscle diffusion-tensor MRI tractography. *J Biomech*. 124:

43. Damon BM, Froeling M, Buck AKW, Oudeman J, Ding Z, et al. 2017. Skeletal muscle diffusion tensor-MRI fiber tracking: rationale, data acquisition and analysis methods, applications and future directions

44. Damon BM, Heemskerk AM, Ding Z. 2012. Polynomial fitting of DT-MRI fiber tracts allows accurate estimation of muscle architectural parameters. *Magn Reson Imaging*. 30(5):589–600

45. D'Antona G, Lanfranconi F, Pellegrino MA, Brocca L, Adami R, et al. 2006. Skeletal muscle hypertrophy and structure and function of skeletal muscle fibres in male body builders. *Journal of Physiology*. 570(3):611–27

46. de Bock K, Dresselaers T, Kiens B, Richter EA, van Hecke P, Hespel P. 2007. Evaluation of intramyocellular lipid breakdown during exercise by biochemical assay, NMR spectroscopy, and Oil Red O staining. *American Journal of Physiology-Endocrinology and Metabolism*. 293(1):E428–34

47. de Sousa LGO, Marshall AG, Norman JE, Fuqua JD, Lira VA, et al. 2021. The effects of diet composition and chronic obesity on muscle growth and function. *J Appl Physiol*. 130(1):124–38

48. Delmonico MJ, Harris TB, Visser M, Park SW, Conroy MB, et al. 2009. Longitudinal study of muscle strength, quality, and adipose tissue infiltration. *Am J Clin Nutr*. 90(6):1579–85

49. Dieckmeyer M, Zoffl F, Grundl L, Inhuber S, Schlaeger S, et al. 2020. Association of quadriceps muscle, gluteal muscle, and femoral bone marrow composition using chemical shift encoding-based water-fat MRI: a preliminary study in healthy young volunteers. *Eur Radiol Exp*. 4(1):

50. Dixon WT. 1984. Simple proton spectroscopic imaging. *Radiology*. 153(1):189–94

51. El-Badry AM, Breitenstein S, Jochum W, Washington K, Paradis V, et al. 2009. Assessment of hepatic steatosis by expert pathologists: The end of a gold standard. *Ann Surg*. 250(5):691–96

52. Englund DA, Sharp RL, Selsby JT, Ganesan SS, Franke WD. 2017. Resistance training performed at distinct angular velocities elicits velocity-specific alterations in muscle strength and mobility status in older adults. *Exp Gerontol*. 91:51–56

53. Englund EK, Elder CP, Xu Q, Ding Z, Damon BM. 2011. Combined diffusion and strain tensor MRI reveals a heterogeneous, planar pattern of strain development during isometric muscle contraction. *J Physiol Regul Integr Comp Physiol*. 300:1079–90

54. Engstrom CM, Loeb GE, Reid JG, Forrest WJ, Avruch L. 1991. Morphometry of the human thigh muscles. A comparison between anatomical sections and computer tomographic and magnetic resonance images. *J Anat*. 176:139–56

55. Erlandson MC, Lorbergs AL, Mathur S, Cheung AM. 2016. Muscle analysis using pQCT, DXA and MRI. *Eur J Radiol*. 85(8):1505–11

56. Eshima H, Tamura Y, Kakehi S, Kurebayashi N, Murayama T, et al. 2017. Long-term, but not short-term high-fat diet induces fiber composition changes and impaired contractile force in mouse fast-twitch skeletal muscle. *Physiol Rep*. 5(7):e13250

57. Faron A, Sprinkart AM, Kuetting DLR, Feisst A, Isaak A, et al. 2020. Body composition analysis using CT and MRI: intra-individual intermodal comparison of muscle mass and myosteatosis. *Sci Rep*. 10(1):11765

58. Finni T. 2006. Structural and functional features of human muscle-tendon unit. *Scand J Med Sci Sports*. 16(3):147–58

59. Forsting J, Rohm M, Froeling M, Güttsches AK, Vorgerd M, et al. 2021. High inter-rater reliability of manual segmentation and volume-based tractography in healthy and dystrophic human calf muscle. *Diagnostics*. 11(9):

60. Fragala MS, Kenny AM, Kuchel GA. 2015. Muscle quality in aging: a multi-dimensional approach to muscle functioning with applications for treatment. *Sports Medicine*. 45(5):641–58

61. Franchi M v., Raiteri BJ, Longo S, Sinha S, Narici M v., Csapo R. 2018. Muscle architecture assessment: strengths, shortcomings and new frontiers of in vivo imaging techniques. *Ultrasound Med Biol*. 44(12):2492–2504

62. Frank-Wilson AW, Chalhoub D, Figueiredo P, Jónsson P v., Siggeirsdóttir K, et al. 2018. Associations of quadriceps torque properties with muscle size, attenuation, and intramuscular adipose tissue in older adults. *Journals of Gerontology - Series A Biological Sciences and Medical Sciences*. 73(7):931–38

63. Froeling M, Nederveen AJ, Nicolay K, Strijkers GJ. 2013. DTI of human skeletal muscle: The effects of diffusion encoding parameters, signal-to-noise ratio and T2 on tensor indices and fiber tracts. *NMR Biomed*. 26(11):1339–52

64. Froeling M, Oudeman J, Strijkers GJ, Maas M, Drost MR, et al. 2015. Muscle changes detected with diffusion-tensor imaging after long-distance running. *Radiology*. 274(2):548–62

65. Frontera WR, Reid KF, Phillips EM, Krivickas LS, Hughes VA, et al. 2008. Muscle fiber size and function in elderly humans: a longitudinal study. *J Appl Physiol*. 105:637–42

66. Frontera WR, Suh D, Krivickas LS, Hughes VA, Goldstein R, Roubenoff R. 2000. Skeletal muscle fiber quality in older men and women. *Am J Physiol Cell Physiol*. 279(3 48-3):

67. Fukunaga T, Ichinose Y, Ito M, Kawakami Y, Fukashiro S. 1997. Determination of fascicle length and pennation in a contracting human muscle in vivo. *J Appl Physiol*. 82(1):354–58

68. Fukunaga T, Roy RR, Shellock FG, Hodgson JA, Day MK, et al. 1992. Physiological cross-sectional area of human leg muscles based on magnetic resonance imaging. *Journal of Orthopaedic Research.* 10(6):926–34

69. Gaeta M, Messina S, Mileto A, Vita GL, Ascenti G, et al. 2012. Muscle fat-fraction and mapping in Duchenne Muscular Dystrophy: evaluation of disease distribution and correlation with clinical assessments. *Skeletal Radiol*. 41(8):955–61

70. Galbán CJ, Maderwald S, Stock F, Ladd ME. 2007. Age-related changes in skeletal muscle as detected by diffusion tensor magnetic resonance imaging

71. Galbán CJ, Maderwald S, Uffmann K, Ladd ME. 2005. A diffusion tensor imaging analysis of gender differences in water diffusivity within human skeletal muscle. *NMR Biomed*. 18(8):489–98

72. Gallagher D, Visser M, Sepulveda D, Pierson RN, Harris T, Heymsfield SB. 1996. How useful is body mass index for comparison of body fatness across age, sex, and ethnic groups? *Am J Epidemiol*. 143(3):228–39

73. Glover GH. 1991. Multipoint dixon technique for water and fat proton and susceptibility imaging. *Journal of Magnetic Resonance Imaging*. 1(5):521–30

74. Goodpaster BH, Carlson CL, Visser M, Kelley DE, Scherzinger A, et al. 2001. Attenuation of skeletal muscle and strength in the elderly: The health ABC study. *J Appl Physiol*. 90(6):2157–65

75. Goodpaster BH, Chomentowski P, Ward BK, Rossi A, Glynn NW, et al. 2008. Effects of physical activity on strength and skeletal muscle fat infiltration in older adults: a randomized controlled trial. *J Appl Physiol*. 105(5):1498–1503

76. Goodpaster BH, He J, Watkins S, Kelley DE. 2001. Skeletal muscle lipid content and insulin resistance: evidence for a paradox in endurance-trained athletes. *J Clin Endocrinol Metab*. 86(12):5755–61

77. Goodpaster BH, Kelley DE, Thaete FL, He J, Ross R. 2000. Skeletal muscle attenuation determined by computed tomography is associated with skeletal muscle lipid content. *J Appl Physiol.* 89(1):104–10

78. Goodpaster BH, Park SW, Harris TB, Kritchevsky SB, Nevitt M, et al. 2006. The loss of skeletal muscle strength, mass, and quality in older adults: the health, aging and body composition study

79. Goodpaster BH, Thaete FL, Simoneau JA, Kelley DE. 1997. Subcutaneous abdominal fat and thigh muscle composition predict insulin sensitivity independently of visceral fat. *Diabetes.* 46(10):1579–85

80. Goodpaster BH, Theriault R, Watkins SC, Kelley DE. 2000. Intramuscular lipid content is increased in obesity and decreased by weight loss. *Metabolism*. 49(4):467–72

81. Goodpaster BH, Wolf D. 2004. Skeletal muscle lipid accumulation in obesity, insulin resistance, and type 2 diabetes. *Pediatr Diabetes*. 5:219–26

82. Gordon JA, Hoffman JR, Arroyo E, Varanoske AN, Coker NA, et al. 2017. Comparisons in the recovery response from resistance exercise between young and middle-aged men. *J Strength Cond Res*. 31(12):3454–62

83. Greco A v., Mingrone G, Giancaterini A, Manco M, Morroni M, et al. 2002. Insulin resistance in morbid obesity. *Diabetes*. 51(1):144–51

84. Greenberg MJ, Mealy TR, Watt JD, Jones M, Szczesna-Cordary D, Moore JR. 2009. The molecular effects of skeletal muscle myosin regulatory light chain phosphorylation. *American Journal of Physiology-Regulatory, Integrative and Comparative Physiology*. 297(2):R265–74

85. Grimm A, Meyer H, Nickel MD, Nittka M, Raithel E, et al. 2018. Evaluation of 2-point, 3-point, and 6-point Dixon magnetic resonance imaging with flexible echo timing for muscle fat quantification. *Eur J Radiol*. 103:57–64

86. Grimm A, Meyer H, Nickel MD, Nittka M, Raithel E, et al. 2018. Repeatability of Dixon magnetic resonance imaging and magnetic resonance spectroscopy for quantitative muscle fat assessments in the thigh. *J Cachexia Sarcopenia Muscle*. 9(6):1093–1100

87. Grimm A, Nickel MD, Chaudry O, Uder M, Jakob F, et al. 2019. Feasibility of Dixon magnetic resonance imaging to quantify effects of physical training on muscle composition—A pilot study in young and healthy men. *Eur J Radiol*. 114:160–66

88. Guerini H, Omoumi P, Guichoux F, Vuillemin V, Morvan G, et al. 2015. Fat suppression with dixon techniques in musculoskeletal magnetic resonance imaging: A pictorial review. *Semin Musculoskelet Radiol*. 19(4):335–47

89. Gür H, Gransberg L, vanDyke D, Knutsson E, Larsson L. 2003. Relationship between in vivo muscle force at different speeds of isokinetic movements and myosin isoform expression in men and women. *Eur J Appl Physiol*. 88(6):487–96

90. Hakkinen K, Hakkinen A. 1991. Muscle cross-sectional area, force production and relaxation characteristics in women at different ages. *Eur J Appl Physiol Occup Physiol*. 62(6):410–14

91. Hakkinen K, Newton RU, Gordon SE, McCormick M, Volek JS, et al. 1998. Changes in muscle morphology, electromyographic activity, and force production characteristics during progressive strength training in young and older Men. *J Gerontol A Biol Sci Med Sci*. 53A(6):B415–23

92. Hanson ED, Srivatsan SR, Agrawal S, Menon KS, Delmonico MJ, et al. 2009. Effects of strength training on physical function: influence of power, strength, and body composition. *Journal of strength and conditioning research / National Strength & Conditioning Association*. 23(9):2627–37

93. Hausman GJ, Basu U, Du M, Fernyhough-Culver M, Dodson M v. 2014. Intermuscular and intramuscular adipose tissues: Bad vs. good adipose tissues

94. Hill TL, Eisenberg E, Greene L. 1980. Theoretical model for the cooperative equilibrium binding of myosin subfragment 1 to the actin-troponin-tropomyosin complex. *Proceedings of the National Academy of Sciences*. 77(6):3186–90

95. Hilton TN, Tuttle LJ, Bohnert KL, Mueller MJ, Sinacore DR. 2008. Excessive adipose tissue infiltration in skeletal muscle in individuals with obesity, Diabetes Mellitus, and Peripheral Neuropathy: association with performance and function background and purpose

96. Hioki M, Kanehira N, Koike T, Saito A, Takahashi H, et al. 2016. Associations of intramyocellular lipid in vastus lateralis and biceps femoris with blood free fatty acid and muscle strength differ between young and elderly adults. *Clin Physiol Funct Imaging*. 36(6):457–63

97. Hogrel JY, Barnouin Y, Azzabou N, Butler-Browne G, Voit T, et al. 2015. NMR imaging estimates of muscle volume and intramuscular fat infiltration in the thigh: variations with muscle, gender, and age. *Age (Omaha)*. 37(3):1–11

98. Hooijmans MT, Damon BM, Froeling M, Versluis MJ, Burakiewicz J, et al. 2015. Evaluation of skeletal muscle DTI in patients with duchenne muscular dystrophy. *NMR Biomed*. 28(11):1589–97

99. Hooijmans MT, Niks EH, Burakiewicz J, Anastasopoulos C, van den Berg SI, et al. 2017. Non-uniform muscle fat replacement along the proximodistal axis in Duchenne muscular dystrophy. *Neuromuscular Disorders*. 27(5):458–64

100. Horowits R, Dalakas MC, Podolsky RJ. 1990. Single skinned muscle fibers in duchenne muscular dystrophy generate normal force. *Ann Neurol*. 27(6):636–41

101. Hoult DI, Busby SJW, Gadian DG, Radda GK, Richards RE, Seeley PJ. 1974. Observation of tissue metabolites using 31P nuclear magnetic resonance. *Nature*. 252(5481):285–87

102. Howald H, Boesch C, Kreis R, Matter S, Billeter R, et al. 2002. Content of intramyocellular lipids derived by electron microscopy, biochemical assays, and 1H-MR spectroscopy. *J Appl Physiol*. 92(6):2264–72

103. Hu HH, Chen J, Shen W. 2016. Segmentation and quantification of adipose tissue by magnetic resonance imaging

104. Hughes VA, Frontera WR, Wood M, Evans WJ, Dallal GE, et al. 2001. Longitudinal muscle strength changes in older adults: influence of muscle mass, physical activity, and health. *J Gerontol A Biol Sci Med Sci*. 56(5):B209–17

105. Hulens M, Vansant G, Lysens R, Claessens A, Muls E, Brumagne S. 2001. Study of differences in peripheral muscle strength of lean versus obese women: an allometric approach. *Int J Obes*. 25(5):676–81

106. Hulver MW, Berggren JR, Cortright RN, Dudek RW, Thompson RP, et al. 2003. Skeletal muscle lipid metabolism with obesity. *American Journal of Physiology-Endocrinology and Metabolism*. 284(4):E741–47

107. Hvid LG, Suetta C, Aagaard P, Kjaer M, Frandsen U, Ørtenblad N. 2013. Four days of muscle disuse impairs single fiber contractile function in young and old healthy men. *Exp Gerontol*. 48(2):154–61

108. Hwang J-H, Pan JW, Heydari S, Hetherington HP, Stein DT. 2001. Regional differences in intramyocellular lipids in humans observed by in vivo 1H-MR spectroscopic imaging. *J Appl Physiol*. 90(4):1267–74

109. Inhuber S, Sollmann N, Schlaeger S, Dieckmeyer M, Burian E, et al. 2019. Associations of thigh muscle fat infiltration with isometric strength measurements based on chemical shift encoding-based water-fat magnetic resonance imaging. *Eur Radiol Exp*. 3(1):

110. Ishizaka K, Oyama N, Mito S, Sugimori H, Nakanishi M, et al. 2011. Comparison of 1H-MR Spectroscopy, 3-point DIXON, and Multi-echo gradient echo for measuring hepatic fat fraction. *Magn Reson Med Sci*. 10(1):41–48

111. Izquierdo, Ibañez, Gorostiaga, Garrues, Zúñiga, et al. 1999. Maximal strength and power characteristics in isometric and dynamic actions of the upper and lower extremities in middle-aged and older men. *Acta Physiol Scand*. 167(1):57–68

112. Jacques MF, Onambele-Pearson GL, Reeves ND, Stebbings GK, Smith J, Morse CI. 2018. Relationships between muscle size, strength, and physical activity in adults with muscular dystrophy. *J Cachexia Sarcopenia Muscle*. 9(6):1042–52

113. Janssen I, Heymsfield SB, Wang Z, Ross R. 2000. Skeletal muscle mass and distribution in 468 men and women aged 18–88 yr. *J Appl Physiol*. 89(1):81–88

114. Jiang Z, Marriott K, Maly MR. 2019. Impact of inter- and intramuscular fat on muscle architecture and capacity. *Crit Rev Biomed Eng*. 47(6):515–33

115. Jones DK, Cercignani M. 2010. Twenty-five pitfalls in the analysis of diffusion MRI data. *NMR Biomed*. 23(7):803–20

116. Jubrias SA, Odderson IR, Esselman PC, Conley KE. 1997. Decline in isokinetic force with age: muscle cross-sectional area and specific force. *Archiv European Journal of Physiology*. 434(3):246–53

117. Kang B, Kim M, Song S, Jun D won, Jang K. 2017. Feasibility of modified Dixon MRI techniques for hepatic fat quantification in hepatic disorders: validation with MRS and histology. *Br J Radiol*, p. 20170378

118. Kemp G, Radda G. 1994. Quantitative interpretation of bioenergetic data from 31P and 1H magnetic resonance spectroscopic studies of skeletal muscle: an analytical review. *Magn Reson Q*. 10(1):43–63

119. Kent-Braun J, Miller RG, Weiner MW. 1994. Magnetic resonance spectroscopy studies of human muscle. *Radiol Clin North Am*. 32(2):313–35

120. Kent-Braun JA. 1999. Central and peripheral contributions to muscle fatigue in humans during sustained maximal effort. *Eur J Appl Physiol Occup Physiol*. 80(1):57–63

121. Kent-Braun JA, Ng A v. 1999. Specific strength and voluntary muscle activation in young and elderly women and men. *J Appl Physiol*. 87(1):22–29

122. Kent-Braun JA, Ng A v., Doyle JW, Towse TF. 2002. Human skeletal muscle responses vary with age and gender during fatigue due to incremental isometric exercise. *J Appl Physiol*. 93(5):1813–23

123. Kent-Braun JA, Ng A v., Young K. 2000. Skeletal muscle contractile and noncontractile components in young and older women and men. *J Appl Physiol*. 88(2):662–68

124. Kermarrec E, Budzik JF, Khalil C, le Thuc V, Hancart-Destee C, Cotten A. 2010. In vivo diffusion tensor imaging and tractography of human thigh muscles in healthy subjects. *American Journal of Roentgenology*. 195(5):

125. Kim J, Hickner RC, Cortright RL, Lynis Dohm G, Houmard JA. 2000. Lipid oxidation is reduced in obese human skeletal muscle. *American Journal of Physiology-Endocrinology And Metabolism*. 279(5):E1039–44

126. Klass M, Baudry S, Duchateau J. 2007. Voluntary activation during maximal contraction with advancing age: a brief review. *Eur J Appl Physiol*. 100(5):543–51

127. Klupp E, Cervantes B, Schlaeger S, Inhuber S, Kreuzpointer F, et al. 2019. Paraspinal muscle DTI metrics predict muscle strength. *Journal of Magnetic Resonance Imaging*. 50(3):816–23

128. Koopman R, Schaart G, Hesselink MK. 2001. Optimisation of oil red O staining permits combination with immunofluorescence and automated quantification of lipids. *Histochem Cell Biol*. 116(1):63–68

129. Koster A, Ding J, Stenholm S, Caserotti P, Houston DK, et al. 2011. Does the amount of fat mass predict age-related loss of lean mass, muscle strength, and muscle quality in older adults? *Journals of Gerontology - Series A Biological Sciences and Medical Sciences*. 66 A(8):888–95

130. Kovanlikaya A, Guclu C, Desai C, Becerra R, Gilsanz V. 2005. Fat quantification using three-point dixon technique. *Acad Radiol*. 12(5):636–39

131. Krivickas LS, Amato AA, Krishnan G, Murray A v., Frontera WR. 2005. Preservation of in vitro muscle fiber function in dermatomyositis and inclusion body myositis: A single fiber study. *Neuromuscular Disorders*. 15(5):349–54

132. Krivickas LS, Yang JI, Kim SK, Frontera WR. 2002. Skeletal muscle fiber function and rate of disease progression in amyotrophic lateral sclerosis. *Muscle Nerve*. 26(5):636–43

133. Krššák M, Lindeboom L, Schrauwen-Hinderling V, Szczepaniak LS, Derave W, et al. 2021. Proton magnetic resonance spectroscopy in skeletal muscle: Experts' consensus recommendations. *NMR Biomed*. 34(5):

134. Kubo K, Kanehisa H, Azuma K, Ishizu M, Kuno S-Y, et al. 2003. Muscle architectural characteristics in young and elderly men and women. *Int J Sports Med*. 24(2):125–30

135. Kukuk GM, Hittatiya K, Sprinkart AM, Eggers H, Gieseke J, et al. 2015. Comparison between modified Dixon MRI techniques, MR spectroscopic relaxometry, and different histologic quantification methods in the assessment of hepatic steatosis. *Eur Radiol*. 25(10):2869–79

136. Kumar D, Karampinos DC, MacLeod TD, Lin W, Nardo L, et al. 2014. Quadriceps intramuscular fat fraction rather than muscle size is associated with knee osteoarthritis. *Osteoarthritis Cartilage*. 22(2):226–34

137. Lafortuna CL, Maffiuletti NA, Agosti F, Sartorio A. 2005. Gender variations of body composition, muscle strength and power output in morbid obesity. *Int J Obes*. 29(7):833–41

138. Lanza IR, Russ DW, Kent-Braun JA. 2004. Age-related enhancement of fatigue resistance is evident in men during both isometric and dynamic tasks. *J Appl Physiol*. 97(3):967–75

139. Larsson L, Degens H, Li M, Salviati L, Lee Y il, et al. 2019. Sarcopenia: aging-related loss of muscle mass and function. *Physiol Rev*. 99(1):427–511

140. le Bihan D. 1991. Molecular diffusion nuclear magnetic resonance imaging. *Magn Reson Q*. 7(1):1–30

141. le Bihan D, Mangin J-F, Poupon C, Clark CA, Pappata S, et al. 2001. Diffusion tensor imaging: concepts and applications. *Journal of Magnetic Resonance Imaging*. 13(4):534–46

142. Lexell J, Taylor CC. 1991. Variability in muscle fibre areas in whole human quadriceps muscle: effects of increasing age. *J. Anat*. 174:239–49

143. Li GD, Liang YY, Xu P, Ling J, Chen YM. 2016. Diffusion-tensor imaging of thigh muscles in Duchenne Muscular Dystrophy: correlation of apparent diffusion coefficient and fractional anisotropy values with fatty infiltration. *American Journal of Roentgenology*. 206(4):867–70

144. Li M, Larsson L. 2010. Force-generating capacity of human myosin isoforms extracted from single muscle fibre segments. *Journal of Physiology*. 588(24):5105–14

145. Lieber RL. 2002. *Skeletal muscle structure, function, and plasticity*. Baltimore: Lippincott Williams & Wilkins

146. Lieber RL. 2022. Can we just forget about pennation angle?

147. Lieber RL, Fridén J. 2000. Functional and Clinical Significance of Skeletal Muscle Architecture. *Muscle Nerve*. 23:1647–66

148. Lindle RS, Metter EJ, Lynch NA, Fleg JL, Fozard JL, et al. 1997. Age and gender comparisons of muscle strength in 654 women and men aged 20–93 yr. *J Appl Physiol*. 83(5):1581–87

149. Lynch NA, Metter EJ, Lindle RS, Fozard JL, Tobin JD, et al. 1999. Muscle quality. I. Age-associated differences between arm and leg muscle groups. *J Appl Physiol*. 86(1):188–94

150. Ma J. 2008. Dixon techniques for water and fat imaging

151. MacIntosh BR, Gardiner PF, McComas AJ. 2006. *Skeletal Muscle: Form and Function.* Human Kinetics

152. Maden-Wilkinson TM, Degens H, Jones DA, McPhee JS. 2013. Comparison of MRI and DXA to measure muscle size and age-related atrophy in thigh muscles. *J Musculoskelet Neuronal Interact.* 13(3):320–28

153. Maffiuletti NA, Jubeau M, Agosti F, Col A, Sartorio A. 2008. Quadriceps muscle function characteristics in severely obese and nonobese adolescents. *Eur J Appl Physiol*. 103(4):481–84

154. Maffiuletti NA, Jubeau M, Munzinger U, Bizzini M, Agosti F, et al. 2007. Differences in quadriceps muscle strength and fatigue between lean and obese subjects. *Eur J Appl Physiol*. 101(1):51–59

155. Manini TM, Clark BC, Nalls MA, Goodpaster BH, Ploutz-Snyder LL, Harris TB. 2007. Reduced physical activity increases intermuscular adipose tissue in healthy young adults. *American Journal of Clinical Nutrition*. 85(2):377–84

156. Marcus RL, Addison O, Dibble LE, Foreman KB, Morrell G, Lastayo P. 2012. Intramuscular adipose tissue, sarcopenia, and mobility function in older individuals. *J Aging Res*. 2012:

157. Marcus RL, Addison O, Kidde JP, Dibble LE, Lastayo PC. 2010. Skeletal muscle fat infiltration: Impact of age, inactivity, and exercise. *The journal of nutrition, health & aging 2010 14:5*. 14(5):362–66

158. Martin DC, Medri MK, Chow RS, Oxorn V, Leekam RN, et al. 2001. Comparing human skeletal muscle architectural parameters of cadavers with in vivo ultrasonographic measurements. *J. Anat.* 199:429–34

159. Martin ML, Travouillon KJ, Fleming PA, Warburton NM. 2020. Review of the methods used for calculating physiological cross-sectional area (PCSA) for ecological questions. *J Morphol*. 281(7):778–89

160. Martins AR, Nachbar RT, Gorjao R, Vinolo MA, Festuccia WT, et al. 2012. Mechanisms underlying skeletal muscle insulin resistance induced by fatty acids: Importance of the mitochondrial function. *Lipids Health Dis.* 11:

161. Maughan RJ, Watson JS, Weir J. 1983. Strength and cross-sectional area of human skeletal muscle. *J Physiol.* 338(1):37–49

162. McKillop DF, Geeves MA. 1993. Regulation of the interaction between actin and myosin subfragment 1: evidence for three states of the thin filament. *Biophys J*. 65(2):693–701

163. McPhee JS, Cameron J, Maden-Wilkinson T, Piasecki M, Yap MH, et al. 2018. The contributions of fiber atrophy, fiber loss, in situ specific force, and voluntary activation to weakness in sarcopenia. *Journals of Gerontology - Series A Biological Sciences and Medical Sciences*. 73(10):1287–94

164. Mehlem A, Hagberg CE, Muhl L, Eriksson U, Falkevall A. 2013. Imaging of neutral lipids by oil red O for analyzing the metabolic status in health and disease. *Nat Protoc*. 8(6):1149–54

165. Messa GAM, Piasecki M, Hurst J, Hill C, Tallis J, Degens H. 2020. The impact of a high-fat diet in mice is dependent on duration and age, and differs between muscles. *Journal of Experimental Biology*

166. Miller MS, Bedrin NG, Ades PA, Palmer BM, Toth MJ. 2015. Molecular determinants of force production in human skeletal muscle fibers: effects of myosin isoform expression and cross-sectional area. *Am J Physiol Cell Physiol*. 308:473–84

167. Miller MS, Bedrin NG, Callahan DM, Previs MJ, Ii MEJ, et al. 2013. Age-related slowing of myosin actin cross-bridge kinetics is sex specific and predicts decrements in whole skeletal muscle performance in humans. *J Appl Physiol*. 115:1004–14

168. Miller MS, Callahan DM, Toth MJ. 2014. Skeletal muscle myofilament adaptations to aging, disease and disuse and their effects on whole muscle performance in older adult humans. *Front Physiol.* 5(SEP):

169. Miller MS, Toth MJ. 2013. Myofilament protein alterations promote physical disability in aging and disease. *Exerc Sport Sci Rev*. 41(2):93–99

170. Miller MS, VanBuren P, LeWinter MM, Braddock JM, Ades PA, et al. 2010. Chronic heart failure decreases cross-bridge kinetics in single skeletal muscle fibres from humans. *Journal of Physiology.* 588(20):4039–53

171. Minati L, Węglarz WP. 2007. Physical foundations, models, and methods of diffusion magnetic resonance imaging of the brain: A review. *Concepts in Magnetic Resonance Part A*. 30A(5):278–307

172. Mitsiopoulos N, Baumgartner RN, Heymsfield SB, Lyons W, Gallagher D, Ross R. 1998. Cadaver validation of skeletal muscle measurement by magnetic resonance imaging and computerized tomography. *J Appl Physiol*. 85(1):115–22

173. Miura H, McCully K, Nioka S, Chance B. 2004. Relationship between muscle architectural features and oxygenation status determined by near infrared device. *Eur J Appl Physiol*. 91(2–3):273–78

174. Moritani T, deVries HA. 1979. Neural factors versus hypertrophy in the time course of muscle strength gain. *Am J Phys Med*. 58(3):115–30

175. Morse CI, Degens H, Jones DA. 2007. The validity of estimating quadriceps volume from single MRI cross-sections in young men. *Eur J Appl Physiol*. 100(3):267–74

176. Mukherjee P, Berman JI, Chung SW, Hess CP, Henry RG. 2008. Diffusion tensor MR imaging and fiber tractography: theoretic underpinnings. *American Journal of Neuroradiology*. 29(4):632–41

177. Murach KA, Dungan CM, Kosmac K, Voigt TB, Tourville TW, et al. 2019. Fiber typing human skeletal muscle with fluorescent immunohistochemistry. *J Appl Physiol*. 127(6):1632–39

178. Naarding KJ, Reyngoudt H, Van Zwet EW, Hooijmans MT, Tian C, et al. 2020. MRI vastus lateralis fat fraction predicts loss of ambulation in Duchenne muscular dystrophy. *Neurology*. 94(13):E1386–94

179. Naressi A, Couturier C, Devos JM, Janssen M, Mangeat C, et al. 2001. Java-based graphical user interface for the MRUI quantitation package. *Magma: Magnetic Resonance Materials in Physics, Biology, and Medicine*. 12(2–3):141–52

180. Narici M. 1999. Human skeletal muscle architecture studied in vivo by non-invasive imaging techniques: functional significance and applications. *Journal of Electromyography and Kinesiology*. 9(2):97–103

181. Nicklas TA, Baranowski T, Cullen KW, Berenson G. 2001. Eating patterns, dietary quality and obesity. *J Am Coll Nutr*. 20(6):599–608

182. Noble JJ, Keevil SF, Totman J, Charles-Edwards GD. 2014. In vitro and in vivo comparison of two-, three- and four-point Dixon techniques for clinical intramuscular fat quantification at 3T. *British Journal of Radiology*. 87(1036):

183. Noureddin M, Lam J, Peterson MR, Middleton M, Hamilton G, et al. 2013. Utility of magnetic resonance imaging versus histology for quantifying changes in liver fat in nonalcoholic fatty liver disease trials. *Hepatology*. 58(6):1930–40

184. Nunes PM, van de Weijer T, Veltien A, Arnts H, Hesselink MKC, et al. 2012. Increased intramyocellular lipids but unaltered in vivo mitochondrial oxidative phosphorylation in skeletal muscle of adipose triglyceride lipase-deficient mice Downloaded from. *Am J Physiol Endocrinol Metab*. 303:71–81

185. Ogawa M, Yoshiko A, Tanaka N, Koike T, Oshida Y, Akima H. 2020. Comparing intramuscular adipose tissue on T1-weighted and two-point Dixon images. *PLoS One*. 15(4):

186. Ogden CL, Fryar CD, Martin CB, Freedman DS, Carroll MD, et al. 2020. Trends in obesity prevalence by race and Hispanic origin—1999-2000 to 2017-2018. *JAMA*. 324(12):1208

187. Okamoto Y, Kunimatsu A, Kono T, Kujiraoka Y, Sonobe J, Minami M. 2010. Gender differences in MR muscle tractography. *Magn Reson Med Sci*. 9(3):111–18

188. Oudeman J, Nederveen AJ, Strijkers GJ, Maas M, Luijten PR, Froeling M. 2016. Techniques and applications of skeletal muscle diffusion tensor imaging: A review

189. Palmer TB, Thompson BJ. 2017. Influence of age on passive stiffness and size, quality, and strength characteristics. *Muscle Nerve*. 55(3):305–15

190. Pathare N, Walter GA, Stevens JE, Yang Z, Okerke E, et al. 2005. Changes in inorganic phosphate and force production in human skeletal muscle after cast immobilization. *J Appl Physiol*. 98(1):307–14

191. Pette D, Staron RS. 2000. Myosin isoforms, muscle fiber types, and transitions. *Microsc. Res. Tech*. 50:500–509

192. Pillen S, Tak RO, Zwarts MJ, Lammens MMY, Verrijp KN, et al. 2009. Skeletal muscle ultrasound: correlation between fibrous tissue and echo intensity. *Ultrasound Med Biol*. 35(3):443–46

193. Ponrartana S, Ramos-Platt L, Wren TAL, Hu HH, Perkins TG, et al. 2015. Effectiveness of diffusion tensor imaging in assessing disease severity in Duchenne muscular dystrophy: preliminary study. *Pediatr Radiol*. 45(4):582–89

194. Pons C, Borotikar B, Garetier M, Burdin V, Salem D ben, et al. 2018. Quantifying skeletal muscle volume and shape in humans using MRI: A systematic review of validity and reliability. *PLoS One*. 13(11):

195. Powell PL, Roy RR, Kanim P, Bello MA, Edgerton VR. 1984. Predictability of skeletal muscle tension from architectural determinations in guinea pig hindlimbs. *J Appl Physiol*. 57(6):1715–21

196. Rastelli F, Capodaglio P, Orgiu S, Santovito C, Caramenti M, et al. 2015. Effects of muscle composition and architecture on specific strength in obese older women. *Exp Physiol*. 100(10):1159–67

197. Reed RL, Pearlmutter L, Yochum K, Meredith KE, Mooradian AD. 1991. The relationship between muscle mass and muscle strength in the elderly. *J Am Geriatr Soc*. 39(6):555–61

198. Reeder SB, Pineda AR, Wen Z, Shimakawa A, Yu H, et al. 2005. Iterative decomposition of water and fat with echo asymmetry and least-squares estimation (IDEAL): Application with fast spin-echo imaging. *Magn Reson Med*. 54(3):636–44

199. Reid KF, Doros G, Clark DJ, Patten C, Carabello RJ, et al. 2012. Muscle power failure in mobility-limited older adults: Preserved single fiber function despite lower whole muscle size, quality and rate of neuromuscular activation. *Eur J Appl Physiol*. 112(6):2289–2301

200. Reid KF, Fielding RA. 2012. Skeletal muscle power: a critical determinant of physical functioning in older adults. *Exerc Sport Sci Rev*. 40(1):4–12

201. Reid KF, Pasha E, Doros G, Clark DJ, Patten C, et al. 2014. Longitudinal decline of lower extremity muscle power in healthy and mobility-limited older adults: influence of muscle mass, strength, composition, neuromuscular activation and single fiber contractile properties. *Eur J Appl Physiol*. 114(1):29–39

202. Reyngoudt H, Marty B, Boisserie J-M, le Louër J, Koumako C, et al. 2021. Global versus individual muscle segmentation to assess quantitative MRI-based fat fraction changes in neuromuscular diseases. *Eur Radiol*. 31(6):4264–76

203. Ross R, Goodpaster B, Kelley D, Boada F. 2006. Magnetic resonance imaging in human body composition research: from quantitative to qualitative tissue measurement. *Ann N Y Acad Sci*. 904(1):12–17

204. Rossi A, Zoico E, Goodpaster BH, Sepe A, di Francesco V, et al. 2010. Quantification of intermuscular adipose tissue in the erector spinae muscle by MRI: agreement with histological evaluation. *Obesity*. 18(12):2379–84

205. Ryushi T, Fukunaga T. 1986. Influence of subtypes of fast-twitch fibers on isokinetic strength in untrained men. *Int J Sports Med*. 07(05):250–53

206. Sadeghi S, Wallace FA, Calder PC. 1999. Dietary lipids modify the cytokine response to bacterial lipopolysaccharide in mice. *Immunology*. 96(3):404–10

207. Schaap LA, Koster A, Visser M. 2013. Adiposity, muscle mass, and muscle strength in relation to functional decline in older persons. *Epidemiol Rev*. 35(1):51–65

208. Scheel M, von Roth P, Winkler T, Arampatzis A, Prokscha T, et al. 2013. Fiber type characterization in skeletal muscle by diffusion tensor imaging. *NMR Biomed*. 26(10):1220–24

209. Schlaffke L, Rehmann R, Froeling M, Kley R, Tegenthoff M, et al. 2017. Diffusion tensor imaging of the human calf: Variation of inter- and intramuscle-specific diffusion parameters. *Journal of Magnetic Resonance Imaging*. 46(4):1137–48

210. Schrauwen-Hinderling VB, Hesselink MKC, Schrauwen P, Kooi ME. 2006. Intramyocellular lipid content in human skeletal muscle. *Obesity*. 14(3):357–67

211. Sepe A, Tchkonia T, Thomou T, Zamboni M, Kirkland JL. 2011. Aging and regional differences in fat cell progenitors – A mini-review. *Gerontology*. 57(1):66–75

212. Shaw CS, Jones DA, Wagenmakers AJM. 2008. Network distribution of mitochondria and lipid droplets in human muscle fibres. *Histochem Cell Biol*. 129(1):65–72

213. Shin DD, Hodgson JA, Reggie Edgerton V, Sinha S. 2009. In vivo intramuscular fascicle-aponeuroses dynamics of the human medial gastrocnemius during plantarflexion and dorsiflexion of the foot. *J Appl Physiol*. 107:1276–84

214. Simoneau J-A, Bouchard C. 1989. Human variation in skeletal muscle fiber-type proportion and enzyme activities. *American Journal of Physiology*. 257(4):E567–72

215. Simoneau J-A, Kelley DE. 1997. Altered glycolytic and oxidative capacities of skeletal muscle contribute to insulin resistance in NIDDM. *J Appl Physiol*. 83(1):166–71

216. Sinha S, Sinha U, Edgerton VR. 2006. In vivo diffusion tensor imaging of the human calf muscle. *Journal of Magnetic Resonance Imaging*. 24(1):182–90

217. Sinha U, Csapo R, Malis V, Xue Y, Sinha S. 2015. Age-related differences in diffusion tensor indices and fiber architecture in the medial and lateral gastrocnemius. *Journal of Magnetic Resonance Imaging*. 41(4):941–53

218. Smith AC, Parrish TB, Abbott R, Hoggarth MA, Mendoza K, et al. 2014. Muscle-fat MRI: 1.5 Tesla and 3.0 Tesla versus histology. *Muscle Nerve*. 50(2):170–76

219. Smith DS, Berglund J, Kullberg J, Ahlström H, Avison MJ, Welch EB. 2010. Optimization of Fat-Water Separation Algorithm Selection and Options Using Image-based Metrics with Validation by ISMRM Fat-Water Challenge Datasets

220. Soares JM, Marques P, Alves V, Sousa N. 2013. A hitchhiker's guide to diffusion tensor imaging. *Front Neurosci*. 7:

221. Staron RS, Hagerman FC, Hikida RS, Murray TF, Hostler DP, et al. 2000. Fiber type composition of the vastus lateralis muscle of young men and women. *The Journal of Histochemistry & Cytochemistry*. 48(5):623–29

222. Stouge A, Khan KS, Kristensen AG, Tankisi H, Schlaffke L, et al. 2020. MRI of skeletal muscles in participants with Type 2 Diabetes with or without Diabetic Polyneuropathy. *Radiology*. 297(3):608–19

223. Straight CR, Toth MJ, Miller MS. 2021. Current perspectives on obesity and skeletal muscle contractile function in older adults. *J Appl Physiol*. 130(1):10–16

224. Straight CR, Voigt TB, Jala A V., Chase JD, Ringham OR, et al. 2019. Quadriceps lipid content has sex-specific associations with whole-muscle, cellular, and molecular contractile function in older adults. *Journals of Gerontology - Series A Biological Sciences and Medical Sciences*. 74(12):1879–86

225. Sturm R, Hattori A. 2013. Morbid obesity rates continue to rise rapidly in the United States. *Int J Obes*. 37(6):889–91

226. Suetta C, Hvid LG, Justesen L, Christensen U, Neergaard K, et al. 2009. Effects of aging on human skeletal muscle after immobilization and retraining. *J Appl Physiol*. 107(4):1172–80

227. Sundberg CW, Kuplic A, Hassanlouei H, Hunter SK. 2018. Mechanisms for the age-related increase in fatigability of the knee extensors in old and very old adults. *J Appl Physiol*. 125(1):146–58

228. Tarnopolsky MA, Rennie CD, Robertshaw HA, Fedak-Tarnopolsky SN, Devries MC, Hamadeh MJ. 2007. Influence of endurance exercise training and sex on intramyocellular lipid and mitochondrial ultrastructure, substrate use, and mitochondrial enzyme activity. *Am J Physiol Regul Integr Comp Physiol*. 292(9):1271–78

229. Tomlinson DJ, Erskine RM, Morse CI, Winwood K, Onambélé-Pearson G. 2016. The impact of obesity on skeletal muscle strength and structure through adolescence to old age

230. Tomlinson DJ, Erskine RM, Winwood K, Morse CI, Onambélé GL. 2014. The impact of obesity on skeletal muscle architecture in untrained young vs. old women. *J Anat.* 225(6):675–84

231. Triplett WT, Baligand C, Forbes SC, Willcocks RJ, Lott DJ, et al. 2014. Chemical shift-based MRI to measure fat fractions in dystrophic skeletal muscle. *Magn Reson Med*. 72(1):8–19

232. Troiano RP, Berrigan D, Dodd KW, Masse LC, Tilert T, McDowell M. 2008. Physical activity in the United States measured by accelerometer. *Med Sci Sports Exerc*. 40(1):181–88

233. Tuttle LJ, Sinacore DR, Mueller MJ. 2012. Intermuscular adipose tissue is muscle specific and associated with poor functional performance. *J Aging Res.* 2012:

234. van Donkelaar CC, Kretzers LJG, Bovendeerd PHM, Lataster LMA, Nicolay K, et al. 1999. Diffusion tensor imaging in biomechanical studies of skeletal muscle function. *J Anat.* 194(1):79–88

235. Van Hooren B, Teratsias P, Hodson-Tole EF. 2020. Ultrasound imaging to assess skeletal muscle architecture during movements: a systematic review of methods, reliability, and challenges. *J Appl Physiol*. 128(4):978–99

236. van Loon LJC, Koopman R, Stegen JHCH, Wagenmakers AJM, Keizer HA, Saris WHM. 2003. Intramyocellular lipids form an important substrate source during moderate intensity exercise in endurance-trained males in a fasted state. *J Physiol*. 553(2):611–25

237. van Loon LJC, Schrauwen-Hinderling VB, Koopman R, Wagenmakers AJM, Hesselink MKC, et al. 2003. Influence of prolonged endurance cycling and recovery diet on intramuscular triglyceride content in trained males

238. Vanderthommen M, Duteil S, Wary C, Raynaud JS, Leroy-Willig A, et al. 2003. A comparison of voluntary and electrically induced contractions by interleaved 1H and 31P-NMRS in humans. *J Appl Physiol*. 94(3):1012–24

239. Vega GL, Adams-Huet B, Peshock R, Willett D, Shah B, Grundy SM. 2006. Influence of body fat content and distribution on variation in metabolic risk. *J Clin Endocrinol Metab*. 91(11):4459–66

240. Visser M, Goodpaster BH, Kritchevsky SB, Newman AB, Nevitt M, et al. 2005. Muscle mass, muscle strength, and muscle fat infiltration as predictors of incident mobility limitations in well-functioning older persons. *J Gerontol A Biol Sci Med Sci*. 60(3):324–33

241. Visser M, Langlois J, Guralnik JM, Cauley JA, Kronmal RA, et al. 1998. High body fatness, but not low fat-free mass, predicts disability in older men and women: the Cardiovascular Health Study. *Am J Clin Nutr*. 68(3):584–90

242. Walcott S, Warshaw DM, Debold EP. 2012. Mechanical Coupling between Myosin Molecules Causes Differences between Ensemble and Single-Molecule Measurements. *Biophys J*. 103(3):501–10

243. Walton JM, Roberts N, Whitehouse GH. 1997. Measurement of the quadriceps femoris muscle using magnetic resonance and ultrasound imaging. *Br J Sports Med*. 31(1):59–64

244. Watanabe Y, Yamada Y, Fukumoto Y, Ishihara T, Yokoyama K, et al. 2013. Echo intensity obtained from ultrasonography images reflecting muscle strength in elderly men. *Clin Interv Aging*. 8:993–98

245. Weis J, Johansson L, Ortiz-Nieto F, Ahlström H. 2009. Assessment of lipids in skeletal muscle by LCModel and AMARES. *Journal of Magnetic Resonance Imaging*. 30(5):1124–29

246. Whipple RH, Wolfson LI, Amerman PM. 1987. The relationship of knee and ankle weakness to falls in nursing home residents: an isokinetic study. *J Am Geriatr Soc*. 35(1):13–20

247. Wickiewicz TL, Roy RR, Edgerton VR. 1983. Muscle architecture of the human lower limb. *Clin Orthop Relat Res*. 179:275–83

248. Williams SE, Heemskerk AM, Welch EB, Li K, Damon BM, Park JH. 2013. Quantitative effects of inclusion of fat on muscle diffusion tensor MRI measurements. *Journal of Magnetic Resonance Imaging*. 38(5):1292–97

249. Wokke BH, Bos C, Reijnierse M, van Rijswijk CS, Eggers H, et al. 2013. Comparison of dixon and T1-weighted MR methods to assess the degree of fat infiltration in duchenne muscular dystrophy patients. *Journal of Magnetic Resonance Imaging*. 38(3):619–24

250. Wren TAL, Bluml S, Tseng-Ong L, Gilsanz V. 2008. Three-point technique of fat quantification of muscle tissue as a marker of disease progression in Duchenne muscular dystrophy: preliminary study. *AJR Am J Roentgenol*. 190(1):

251. Yanagisawa O, Shimao D, Maruyama K, Nielsen M, Irie T, Niitsu M. 2009. Diffusion-weighted magnetic resonance imaging of human skeletal muscles: gender-, age- and muscle-related differences in apparent diffusion coefficient. *Magn Reson Imaging*. 27(1):69–78

252. Zaraiskaya T, Kumbhare D, Noseworthy MD. 2006. Diffusion tensor imaging in evaluation of human skeletal muscle injury. *Journal of Magnetic Resonance Imaging*. 24(2):402–8

253. Zhan C, Olsen S, Zhang HC, Kannengiesser S, Chandarana H, Shanbhogue KP. 2019. Detection of hepatic steatosis and iron content at 3 Tesla: comparison of two-point Dixon, quantitative multi-echo Dixon, and MR spectroscopy. *Abdominal Radiology*. 44(9):3040–48